A FRAMEWORK FOR CHARACTERIZING REGIONAL ALTERATIONS IN DOPAMINE NEUROTRANSMISSION IN THE CONTEXT OF DRUGS AND DISEASE USING FAST-SCAN CYCLIC VOLTAMMETRY

by

Rashed Harun

B.S. University of Pittsburgh, 2008

Submitted to the Graduate Faculty of

the School of Medicine in partial fulfillment

of the requirements for the degree of

Doctor of Philosophy

University of Pittsburgh

2015

UNIVERSITY OF PITTSBURGH

SCHOOL OF MEDICINE

This dissertation was presented

by

Rashed Harun

It was defended on

August 27, 2015

and approved by

Dr. Anthony A. Grace, PhD, Departments of Neuroscience, Psychiatry, and Psychology

Dr. Charles W. Bradberry, PhD, Department of Psychiatry

Dr. C. Edward Dixon, PhD, Department of Neurology

Dr. Gonzalo E. Torres, PhD, Department of Neurobiology

Dr. Paul A. Garris, PhD, Department of Biological Sciences

Dissertation Advisor:

Dr. Amy K. Wagner, MD, Department of Physical Medicine & Rehabilitation

A FRAMEWORK FOR CHARACTERIZING REGIONAL ALTERATIONS IN DOPAMINE NEUROTRANSMISSION IN THE CONTEXT OF DRUGS AND DISEASE USING FAST-SCAN CYCLIC VOLTAMMETRY

Rashed Harun, PhD

University of Pittsburgh, 2015

ABSTRACT: Dopamine (DA) has become a sort of buzzword as the ‘pleasure’ neurotransmitter that signals for natural rewards, but is ‘hijacked’ by drugs of abuse and the instant gratification we derive from our phones, Facebook, and fast-food diets in the fast-paced world we live in. In reality, DA has much more nuanced and varied functions that include the regulation of attention, working memory, motivation, movement, and even endocrine functions, which largely depends upon the region DA is acting in the brain. Dysfunction of DA neurotransmission is implicated in conditions like Parkinson’s disease (PD), attention deficit/hyperactivity disorder (ADHD), drug addiction, and traumatic brain injury (TBI) to name just a few. As such, the DAergic system represents a rational pharmaceutical target that act as DA receptor agonists, antagonists, indirect agonists, and DA reuptake inhibitors. Understanding how region-specific DA neurotransmission is altered in pathological states and following both acute and chronic drug administration, requires multi-faceted research approaches but can be significantly driven by advancements in research methodologies. It is for this reason that we hope readers will find the work contained herein particularly timely and important. Although the work contained here represents research conducted using fast-scan cyclic voltammetry (FSCV), an electrochemical method to monitor *in vivo* electrically stimulated DA neurotransmission that has been around since the mid 1980s, we describe the development of a novel quantitative interpretive framework for FSCV data that enhances the ability to characterize the region-specific DA neurotransmission in the context of drugs and diseases. To illustrate the utility of our framework, we demonstrate how our approach has been used to resolve the mechanistic actions of the most commonly used Parkinsonian drug, L-DOPA, on regiospecific DA neurotransmission. Moreover, our framework was utilized to characterize the regiospecific DAergic dysfunction following an experimental model of TBI and the robust neurorestorative effects of chronic methylphenidate treatment in this model. To this end,

we not only describe a theoretical framework for characterizing regiospecific alterations in DA neurotransmission, but we also offer practical examples that may serve as a roadmap for studying DA neurotransmission kinetics in the context of drugs and other diseases.

TABLE OF CONTENTS

LIST OF TABLES

LIST OF FIGURES

PREFACE

When I decided to pursue my PhD, I did it purely for idealistic reasons-to fulfill my curiosity and more importantly because I thought this line of research was very important for advancing the understanding of the dopamine system and its essential role in various human conditions. When I began this journey, I thought I was at the edge of making a major breakthrough in how we study dopamine neurotransmission. I did not know that I would have to wrestle with theories for years, repeatedly proving myself wrong, until I finally actualized my goal. I am very proud of the essential feature of my doctoral research, the development of the quantitative neurobiological framework to interpret stimulated DA responses, as it reflects an eclectic synthesis of various lines of neuroscience research. I think it's a better outcome that I had even hoped for when I enthusiastically began this journey. Publishing this theory only in my final year of my PhD, I see this work as only the beginning of much progress that can stem from it. Now is a critical juncture where this line of research can take off with concerted effort, and I am excited for its future!

I've had my highest highs and my lowest lows in my PhD, and if it wasn't for a few compassionate souls, I'm not sure where I would be. It was my advisor, Amy who first encouraged my out-of-the-box thinking about stimulated DA neurotransmission that led me to pursue my PhD. Through her guidance, among other things, I was able to develop the framework that became the foundation of my thesis. Foremost, I am most humbled by the uplifting advice she gave me to remind me of my calling when I forgot and inspired me more when I remembered. I am fortunate to have the most amazing family that has supported me from the beginning to end, being genuinely happy for me after all my milestones and publications. Not to belittle the chapters to follow, but I

am most grateful for finding my wife Ouiam along the way. I hope that we will do great things together in the next chapters of our lives!

1.0 INTRODUCTION

The central dopaminergic (DAergic) systems principally arise from two midbrain structures- the nucleus accumbens and the substantia nigra pars compacta, which densely innervate subcortical regions of the striatum and diffusely project throughout the cortex. As a modulatory substance, DA regulates various functions attributed to all these regions like abstract reasoning and working memory in the prefrontal cortex, and reward and reinforcement-based learning in the nucleus accumbens. Perhaps most obvious is the role of DA in regulating voluntary movement, which becomes absent following the degeneration of DAergic projections to the dorsolateral striatum in late-stage PD. As a neurotransmitter system that is critically involved in various conditions like ADHD, PD, and TBI, the DAergic system is one of the most commonly targeted systems in neuropsychiatric conditions.

Techniques that can monitor *in vivo* DA dynamics are critical for understanding how the DAergic system is involved in regulating cognition/behavior and how drugs and diseases alter DA neurotransmission. Electrophysiology, PET imaging, and microdialysis methods offer complementary methods to assess neural firing, integrity of DAergic systems, and *in vivo* DA levels. In this body of work, we highlight the rich information of presynaptic DA neurotransmission that can be gained using fast-scan cyclic voltammetry (FSCV).

FSCV is a powerful technique that can monitor real-time *in vivo* kinetics of presynaptic DA neurotransmission with fine temporal and spatial resolution and unparalleled specificity. The development of the technique has a rich history whose origins nearly date back to the time when DAergic pathways were first identified in the brain (Dahlstroem & Fuxe 1964). Ralph Adams was the first person to insert electrodes in the brain to measure catecholamine levels (Kissinger *et al.* 1973), François Gonon introduced the use of carbon fiber microelectrodes (Gonon *et al.* 1978) for voltammetric measurements, and Armstrong-James et al. introduced the application of high speed voltage waveforms to electrodes to detect sub-micromolar catecholamine concentrations *in vitro* (Armstrong-James *et al.* 1980). It was the work of Millar, Stamford, Kruk, and Wightman who first demonstrated the feasibility of contemporary method of using FSCV to monitor *in vivo* striatal DA responses to electrical stimulations of ascending DAergic fibers contained within the median forebrain bundle (MFB) (Millar *et al.* 1985, Ewing *et al.* 1983).

Although much contemporary FSCV research is conducted on awake freely-behaving animals that can be useful for correlating *in vivo* DA dynamics to behavior (Robinson *et al.* 2002, Saddoris *et al.* 2015, Cameron *et al.* 2014), the MFB-stimulated DA neurotransmission paradigm in anesthetized rats has its own set of advantages by allowing investigators to control DA neural firing activity to generate robust high signal-to-noise ratio DA responses that are amenable for quantitative analysis. The MFB-stimulated DA response paradigm is very translational in its approach for assessing how pharmacological agents, disease, and various experimental contexts can affect presynaptic DA neurotransmission primarily because it can be performed *in vivo*. Stimulated striatal DA responses reflect a complex interplay between synaptically released DA and DA clearance that is predominantly mediated by reuptake through DA transporters (DAT). *The principal focus of this doctoral work has been to develop a framework to interpret FSCV data*

of stimulated DA neurotransmission and apply it to characterize drug pharmacodynamics and disease states as a validation for future FSCV research.

Our framework to interpret stimulated DA responses builds off of work by Wightman et al. who developed the Michaelis-Menten (M-M) model of stimulated DA neurotransmission (Wightman *et al.* 1988) to estimate the contributions of release and reuptake processes that underlie DA response shapes. Albeit a relatively simple framework, the M-M model has been instrumental for research demonstrating how various drugs, genetic manipulations, disease models, and experimental manipulations affect presynaptic DA neurotransmission kinetics over the past 25 years (Budygin *et al.* 2002, Wu *et al.* 2002, Wightman & Zimmerman 1990, Chadchankar *et al.* 2011). However, even when the M-M model was proposed, it was duly noted that some brain regions like the dorsal striatum do not adhere to the kinetics of the proposed model (May & Wightman 1989). Moreover, this seminal publication noted "the development of valid models for a description of chemical neurotransmission is, thus, an ongoing process with new experimental data providing the necessary information to refine and adjust the models." Although there have been advancements over the many years in the understanding of chemical neurotransmission, these contemporary principles have not been systematically incorporated to update the interpretive framework for stimulated DA responses. It was this void that we sought to fill in this body of work with our introduction of the quantitative neurobiological (QN) model of stimulated DA neurotransmission (Harun *et al.* 2015) (see Chapter 2), and it was by filling this void that allowed us to pave the way for future FSCV research and make important contributions in the DA research field.

The QN model incorporates contemporary principles of stimulated neurotransmission and incorporates the effects of stimulation on release and reuptake processes during stimulated DA

responses. We believe the QN model not only provides more realistic estimations of underlying DA release and reuptake processes that contribute to DA response shapes, but also, it offers the flexibility to interpret responses obtained from various brain regions. In fact, it was largely out of necessity that we created the QN model to study regional DAergic dysfunction in the context of experimental brain injury, which produces more severe DAergic dysfunction in dorsal striatal regions that cannot adequately be described by the M-M model (see *chapters 2&4*). As different brain regions serve vastly different DA-dependent functions (Macdonald & Monchi 2011), exhibit differential DAergic vulnerability in disease contexts (Macdonald & Monchi 2011, Janezic *et al.* 2013), and exhibit differential DA pharmacodynamics (Patel *et al.* 1992, Wu *et al.* 2001), the QN framework greatly extends the utility of the stimulated DA response paradigm by extending the regions that are amenable for characterization.

In this body of work, we provide a detailed description of the theoretical foundations of the QN model, the equations developed to simulate DA responses, and examples of the application of the QN model in *Chapter 2.* By way of practical example, this work features the application of the QN framework to demonstrate novel findings of the dose and region-specific effects of L-DOPA on DA release and reuptake kinetics in *Chapter 3*, regiospecific dysfunction of DA neurotransmission after experimental brain injury and the neurorestorative effects of chronic methylphenidate in *Chapter 4*, and sex- and hormonal influences on stimulated DA neurotransmission in the context of experimental brain injury in *Chapter 5*. This body of work demonstrates that the combination of the stimulated DA responses paradigm and the QN interpretive framework can serve as a powerful tool to understand how drugs and diseases alter DA neurotransmission.

As the DAergic system plays an important role in many functions, many diseases, and represents a major pharmaceutical target, we hope that this work is only the very beginning of much more research using the methodologies described herein. We have a vested interest in seeing that this work serves as a catalyst for future research along these lines. Already, we are working on an active collaboration to apply our methods to study how DA neurotransmission is altered in the context of a cardiac arrest, which has been proving to be very different from what we observe in our TBI model. To broaden the impact of this research, we are actively working to ease the adoption for others by making our in-house QNsim 1.0 software freely available to others interested in simulating MFB stimulated DA responses according to the QN model. Moreover, we are pursuing the publication of an instructional video through the *Journal of Visualized Experiments* to demonstrate how to simulate DA responses with the QNsim 1.0 software.

2.0 A NEUROBIOLOGICAL MODEL OF STIMULATED DOPAMINE NEUROTRANSMISSION TO INTERPRET FAST-SCAN CYCLIC VOLTAMMETRY DATA

Rashed Harun, BS; Christine M. Grassi; Miranda J. Munoz;

Gonzalo E. Torres, Amy K. Wagner, MD

2.1 SUMMARY

Fast-scan cyclic voltammetry (FSCV) is an electrochemical method that can assess real-time in vivo dopamine (DA) concentration changes to study the kinetics of DA neurotransmission. Electrical stimulation of dopaminergic (DAergic) pathways can elicit FSCV DA responses that largely reflect a balance of DA release and reuptake. Interpretation of these evoked DA responses requires a framework to discern the contribution of DA release and reuptake. The current, widely implemented interpretive framework for doing so is the Michaelis-Menten (M-M) model, which is grounded on two assumptions- 1) DA release rate is constant during stimulation, and 2) DA reuptake occurs through dopamine transporters (DAT) in a manner consistent with M-M enzyme kinetics. Though the M-M model can simulate evoked DA responses that rise convexly, response types that predominate in the ventral striatum, the M-M model cannot simulate dorsal striatal responses that rise concavely. Based on current neurotransmission principles and experimental FSCV data, we developed a novel, quantitative, neurobiological framework to interpret DA responses that assumes DA release decreases exponentially during stimulation and continues post-stimulation at a diminishing rate. Our model also incorporates dynamic M-M kinetics to describe

DA reuptake as a process of decreasing reuptake efficiency. We demonstrate that this quantitative, neurobiological model is an extension of the traditional M-M model that can simulate heterogeneous regional DA responses following manipulation of stimulation duration, frequency, and DA pharmacology. The proposed model can advance our interpretive framework for future in vivo FSCV studies examining regional DA kinetics and their alteration by disease and DA pharmacology.

2.2 INTRODUCTION

Midbrain dopaminergic neurons densely innervate the striatum, regulating motor, cognitive, and limbic functions. DAergic pathway dysfunction is implicated in conditions like Parkinson's Disease (PD), Attention Deficit Hyperactive Disorder (ADHD), and Traumatic Brain Injury (TBI). Agents that affect DA neurotransmission kinetics can be effective for some in managing the neurobehavioral symptoms associated with these conditions; however, little is known about how the kinetics of DA neurotransmission are altered in these conditions. A better understanding of DA neurotransmission kinetics in both physiological and pathological states, and in response to pharmacology, could lead to better characterization of DAergic dysfunction and mechanisms of drug action to guide clinical treatment approaches.

Fast-scan cyclic voltammetry (FSCV) is an electrochemical technique that is capable of measuring *in vivo* DA concentration changes in real time to study the kinetics of DA neurotransmission. Following electrical stimulation of DAergic projections, DA responses can be obtained using FSCV that reflect a balance of DA release and DA clearance. Interpreting DA

responses, therefore, requires a theoretical framework from which to delineate the contribution of DA release and DA clearance to the overall evoked DA responses observed.

As *in vivo* FSCV techniques began to gain popularity as a tool to study DA neurotransmission, the Michaelis-Menten (M-M) model was proposed as a useful framework to describe stimulated DA responses in terms of DA release and reuptake (Wightman & Zimmerman 1990). Application of the M-M model to FSCV derived data is grounded on two basic assumptions- 1) that each stimulation pulse releases a constant amount of DA, and 2) that DA clearance is primarily mediated by reuptake through DA transporters (DAT) which follow saturation-based Michaelis-Menten (M-M) enzyme kinetics (**Figure 1A**). These assumptions led to the formulation of **Equation 1** that has been used widely used with FSCV to interpret stimulated DA responses (Wightman et al. 1988). **Equation 1** predicts DA responses should rise linearly during stimulation in the absence of reuptake, but convexly when factoring in reuptake due to a progressively increasing contribution of DA reuptake during electrical stimulation (**Figure 1B**).

$$\frac{d[DA]}{dt} = \underbrace{f \cdot [DA]_p}_{\text{(DA release)}} - \underbrace{\frac{V_{max}}{\frac{K_m}{[DA]} + 1}}_{\text{(DA reuptake)}}$$

Equation 1

In this equation, $[DA]_p$ is the incremental increase in [DA] that would be evoked by one stimulation pulse in the absence of reuptake, V_{max} is the constant for maximal DA reuptake rate,

and K_m is the M-M constant which represents the extracellular DA concentration ($[DA]_{EC}$) that saturates 50% of DAT.

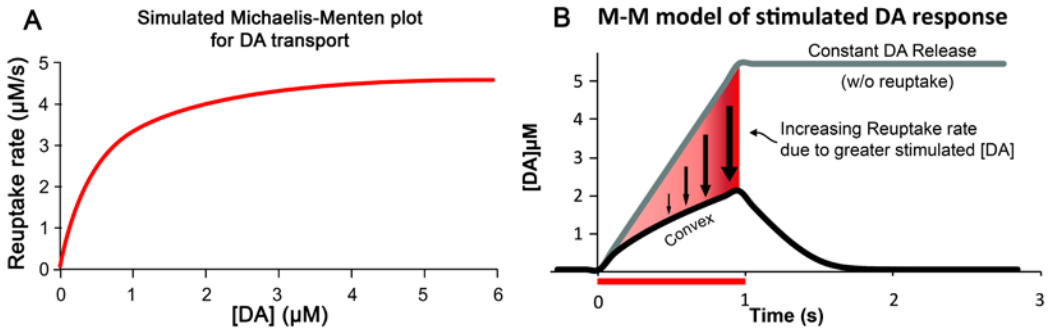

Figure 1: Predictions of the M-M model

A) A reuptake efficiency curve was simulated using Vmax=5µM/s and Km=0.5µM, which shows a plausible relationship between DA reuptake rate and $[DA]_{EC}$ based on M-M enzyme kinetics. B) The M-M model always predicts a convex response because, in the absence of reuptake, $[DA]_{EC}$ would increase linearly with time due to constant release (gray trace). By factoring in reuptake according to M-M enzyme kinetics, the progressively greater reuptake rate during stimulation (progressively increasing size of black arrows) results in a convex DA stimulus response shape (black trace).

Though the M-M model has been implemented commonly to interpret stimulated DA responses, several publications have demonstrated that some striatal evoked DA responses, such as concave DA responses, are often encountered in the dorsal striatum (May & Wightman 1989) and cannot be described by the M-M model (May & Wightman 1989, Moquin & Michael 2009, Wang *et al.* 2011, Taylor *et al.* 2012). Interestingly, these responses previously have been attributed to artifacts of diffusional distortion (May & Wightman 1989); however, more recent studies suggest that diffusion cannot explain the characteristics of these DA responses (Moquin & Michael 2009, Taylor et al. 2012). These findings suggest that the M-M model might not accurately describe the complex kinetics associated with the neurobiological mechanisms underlying stimulated DA neurotransmission. In their 1990 seminal publication that describes the M-M model, Wightman and Zimmerman acknowledged that the M-M model does not account for

neurobiological mechanisms that could contribute to DA stimulus response characteristics, such as frequency-dependent release modulation and modulation by D2 autoreceptors. Moreover, they asserted that “the development of valid models for a description of chemical neurotransmission is thus an ongoing process with new experimental data providing the necessary information to refine and adjust the models” (Wightman & Zimmerman 1990).

Relatively recent and rapid molecular and electrophysiological advancements in neuroscience have made it possible to understand additional components of pre-synaptic function that may contribute to the heterogeneity of DA stimulus responses observed with FSCV; however, the information provided through these advancements have not yet been integrated or applied to the foundational principles offered by Wightman and Zimmerman when introducing in vivo FSCV as a neurotransmission assessment tool. Thus, there is a need to generate a more contemporary and informative model for evaluating DA kinetics using FSCV. Here, we introduce a novel neurobiological framework from which to interpret stimulated DA responses in a manner that complements and further informs current M-M approaches used in characterizing neurotransmission. The model is built on assumptions grounded in contemporary principles derived from neurotransmission research and our own experimental data. In this framework we describe DA release during stimulation not as a constant or increasing, as previously suggested from other FSCV studies (Wightman & Zimmerman 1990, Wightman et al. 1988, Moquin & Michael 2009), but as exponentially decreasing over the course of stimulation, a phenomenon that has been demonstrated with other neurotransmitter systems (Neves & Lagnado 1999, Pyott & Rosenmund 2002, Zucker 1999) including DA (Pan & Ryan 2012). Moreover, following stimulation, rather than an immediate cessation of DA release, as has previously been suggested

(Wightman et al. 1988), this framework accounts for a post-stimulation DA release component, that continues for some time after the termination of the stimulus, which occurs commonly due to an accumulation of $[Ca^{2+}]_{in}$ as a result of stimulation (Barrett & Stevens 1972, Neves & Lagnado 1999, Goda & Stevens 1994, Dodge *et al.* 1969, Delaney & Tank 1994, Borges *et al.* 1995, Yao *et al.* 2011).

Based on observations from experimental data, we also do not describe DA clearance efficiency as a fixed relationship between reuptake rate and extracellular [DA] with constant V_{max} and K_m terms as the M-M model suggests. Rather, we describe clearance efficiency in the context of a stimulated release paradigm, and as one that decreases over the course of an evoked DA response due to stimulation-induced changes in transporter function. These fundamental assumptions provide a basis from which to mathematically model stimulated DA responses of various morphologies not previously possible.

In experimental designs that aim to characterize alterations in striatal DA neurotransmission in pathological states, a neurobiological framework is necessary that can interpret the various response-types collected using unbiased sampling methods. The flexibility of the model proposed in this report is such that it can capture and characterize innate heterogeneity in striatal DA responses as well as perturbations in stimulus response curves due to a spectrum of clinically relevant pathophysiological states or drug treatment paradigms. Though this neurobiological framework is more complex than the basic M-M model, it uses the M-M model as a frame of reference to incorporate principles of neurotransmission that provide a contemporary and realistic perspective from which to interpret and quantify FSCV data of DA neurotransmission.

2.3 NEUROBIOLOGICAL PRINCIPLES OF STIMULATED DA NEUROTRANSMISSION

2.3.1 Stimulated DA release

The M-M model, as it is currently applied to DA responses, makes the assumption that each pulse of stimulation releases a constant amount of DA. This assertion was supported with the quality of fit of the M-M model to experimental DA responses collected in the ventral striatum, although it was noted that prolonging 60Hz stimulations to more than 5s leads to a marked diminution of DA release (Wightman et al. 1988). However, not all stimulated DA responses of <5s can be simulated using the M-M model, especially DA responses that rise concavely during stimulation, which are often observed in the dorsal striatum (May & Wightman 1989, Moquin & Michael 2009). The poor model fit in cases where concavity characterizes the rising portion of the stimulus response curve suggests that the presynaptic kinetics of evoked DA responses is more complex than the release and/or reuptake processes assumed by the M-M model. Previous FSCV studies have suggested that DA release rate may follow a complex pattern that may even increase for a period during electrical stimulation (Moquin & Michael 2009, Wang et al. 2011). However, the supraphysiological stimulation frequencies typically implemented for *in vivo* FSCV studies on anesthetized rats (30Hz-80Hz) (Moquin & Michael 2009, Wang et al. 2011, Wightman et al. 1988, Wightman & Zimmerman 1990, Wu et al. 2001, Wagner *et al.* 2009a, Wagner *et al.* 2009b) should result in an attenuation of DA release during the course of stimulation due to a depletion of readily-releasable stores of synaptic vesicles, a phenomenon termed pulse train depression (PTD) that is widely supported in the neurotransmission literature (Dobrunz & Stevens 1997, Liley & North

1953, Pyott & Rosenmund 2002, Zucker 1999, Hagler & Goda 2001, Neves & Lagnado 1999, Hubbard 1963, Pan & Ryan 2012, Taschenberger & von Gersdorff 2000).

Because the mechanisms of synaptic transmission are largely conserved across different synapse types, PTD associated with synaptic vesicle release has been observed in many synapses including hippocampal glutamatergic synapses (Pyott & Rosenmund 2002, Hagler & Goda 2001), retinal bipolar synapses (Neves & Lagnado 1999), and neuromuscular junctions (Hubbard 1963, Liley & North 1953) using membrane capacitance measurements (Neves & Lagnado 1999), live fluorescent synaptic vesicle imaging (Pan & Ryan 2012), and electrophysiology (Pyott & Rosenmund 2002). PTD has even been demonstrated in the Calyx of Held, a synapse that is known for its high fidelity of synaptic transmission in response to sustained high frequency stimulations (Taschenberger & von Gersdorff 2000). In our overview of the neurotransmission literature, PTD of synaptic vesicle release was a ubiquitously observed phenomenon, making it unlikely that DAergic synapses are a unique example that would exhibit constant or increasing release during the course of sustained stimulation pulse trains (Dobrunz & Stevens 1997, Liley & North 1953, Pyott & Rosenmund 2002, Zucker 1999, Hagler & Goda 2001, Neves & Lagnado 1999, Hubbard 1963, Pan & Ryan 2012, Taschenberger & von Gersdorff 2000). In fact, PTD associated with DA release has been demonstrated recently in midbrain DAergic neuronal cultures (Pan & Ryan 2012).

The discrepancy between FSCV research, which suggests *constant*, *complex*, or *increasing* neurotransmitter release with on-going stimulation pulse trains, and other lines of neurobiological research, which have consistently demonstrated *decreasing* neurotransmitter release, may be due to the fact that FSCV measurements represent a balance of DA release *and reuptake*. We assert

that the paradoxical findings on DA release from FSCV studies can be reconciled using a novel clearance kinetics paradigm that includes temporally attenuating DA reuptake efficiency that we describe later in this report (see *DA reuptake*).

In our neurobiological model, we assume DA release decreases exponentially during a pulse train consistent with principles of neurotransmission supported in the literature noted above. PTD begins at the stimulation onset, and this phenomenon is often modeled as an exponential decay function that plateaus to a steady-state level (Taschenberger & von Gersdorff 2000, Pyott & Rosenmund 2002). Various studies have established a relationship between the kinetics of PTD and stimulation frequency, calcium influx, the size of the readily-releasable pool (RRP), and the kinetics of vesicle recruitment into the RRP during stimulation (Pyott & Rosenmund 2002, Zucker 1999, Hagler & Goda 2001). Adopting a paradigm of PTD from which to model stimulated DA release in FSCV studies would afford the flexibility needed to model frequency-dependent modulation of DA release, and DA release modulation by D2 autoreceptors, both of which are known to affect voltage-gated calcium currents (Cardozo & Bean 1995, Jomphe *et al.* 2006).

2.3.2 Post-stimulation DA release

The M-M model assumes that DA release ceases at the end of stimulation (Wightman et al. 1988), because DA neurons exhibit a period of inhibited neuronal firing activity following electrical stimulation (Kuhr *et al.* 1987). However, neurotransmitter release is not directly related to neuronal firing activity per se, but rather, it is related to the subsequent Ca^{2+} influx and intracellular Ca^{2+}accumulation that result from action potentials or supraphysiological electrical stimulations (Atluri & Regehr 1998, Fierro *et al.* 1998). As such, increased neurotransmitter release can persist

that is independent of neuronal firing, but is associated with the accumulation of intracellular Ca^{2+} ($[Ca^{2+}]_{in}$) induced by pulse trains, for seconds after stimulation pulse trains cease (Barrett & Stevens 1972, Neves & Lagnado 1999, Goda & Stevens 1994, Dodge et al. 1969). Post-stimulation neurotransmitter release is a common phenomenon observed in many synapses including retinal amacrine cells (Borges et al. 1995), hippocampal neurons (Goda & Stevens 1994, Yao et al. 2011), cerebellar granule cells (Geppert *et al.* 1994), and DAergic/GABAergic periglomerular cells (Borisovska *et al.* 2013).

The literature suggests that the post-stimulation neurotransmitter release that follows pulse trains has at least two distinct kinetic components, a *rapid* and a *prolonged* component, which are likely due to a continuation of two identified Ca^{2+}-dependent release mechanisms that occur during stimulation (Atluri & Regehr 1998). Following pulse trains, intracellular calcium is rapidly sequestered, buffered, or extruded; however, modest elevations of $[Ca^{2+}]_{in}$ can remain for many seconds following stimulation that are dependent on the duration of stimulation. (Fierro et al. 1998).

The rapid component post-stimulation DA release may be predominantly mediated by synaptotagmins. Neurons utilize the synaptotagmin family of Ca^{2+}-sensors to precisely synchronize neuronal firing to synaptic vesicle release. Synaptotagmins are low-affinity Ca^{2+} sensors that form part of the SNARE complex in synaptic vesicles that are docked and primed for release. Synaptotagmins are ideally localized to detect large increases in $[Ca^{2+}]_{in}$ by adjacent voltage-gated Ca^{2+} channels in response to action potentials. In response to Ca^{2+}-activation, synaptotagmins allow for rapid synaptic vesicle extrusion. Thus, the rapid actions of the low

affinity synaptotagmin may be limited to a short period immediately following stimulation because high concentrations of $[Ca^{2+}]_{in}$ are rapidly eliminated following stimulation (Fierro et al. 1998).

The prolonged component of post-stimulation DA release may be mediated by members of the Double C2-like containing protein (DOC2) family (Yao et al. 2011). DOC2 has a much higher affinity for Ca^{2+} than synaptotagmin, but remains mainly cytosolic in the absence of Ca^{2+} (Groffen *et al.* 2006). The cytosolic localization of DOC2 makes these Ca^{2+} sensors inadequate for rapid neurotransmission that is induced by the membrane-bound synpatotagmins. However, DOC2 is sensitive to generalized $[Ca^{2+}]_{in}$ changes that can persist for seconds following neuronal activity (Fierro et al. 1998), and thus, DOC2 can increase synaptic vesicle release for a protracted period following stimulation (Atluri & Regehr 1998). Interestingly, members of the DOC2 family are of central importance to spontaneous neurotransmitter release, whose roles in regulating stimulated or basal DA concentrations are unexplored (Groffen *et al.* 2010, Pang *et al.* 2011).

Quantifiable evidence of post-stimulation DA release may manifest itself in FSCV experiments by prolonging the decay phase of stimulated DA responses. Post-stimulation DA release may also cause DA signals to continue rising following stimulus termination if the post-stimulation release rate is greater than the reuptake rate, a phenomenon which has been documented previously in the FSCV literature (Taylor et al. 2012, Kawagoe & Wightman 1994, Kuhr et al. 1987). Without properly accounting for post-stimulation DA release, FSCV analysis that uses the traditional M-M model would systematically underestimate the true reuptake kinetics extracted from the post-stimulation phase of DA responses.

2.3.3 DA reuptake

FSCV experiments on DAT knock-out mice have demonstrated that DA reuptake via DAT is the predominant mechanism for striatal DA clearance (Jones *et al.* 1999a). To describe striatal DA reuptake, the M-M model assumes DA reuptake is solely dependent upon DAT saturation that can be described using M-M enzyme kinetics according to **Equation 1**. However, there are several potential neurobiological factors that need to be considered when modeling DA reuptake, including DAT trafficking to and away from presynaptic plasma membranes and the effects of electrically stimulated DA release and reuptake on electrochemical gradients that drive DA reuptake.

DA reuptake through DAT is coupled to electrochemical gradients produced by Na^+, Cl^-, and DA itself. Since the electrochemical gradients for these ions are altered during electrically stimulated DA responses, this disruption could potentially confound the M-M model assumption that DA reuptake is solely dependent upon DAT saturation by $[DA]_{EC}$. For instance, if Na^+, Cl^-, or DA accumulates in the intracellular space, then the driving force for further DA reuptake through DAT could diminish with continued stimulation (Gu *et al.* 1994, Jones *et al.* 1999b). In physiological conditions, ionic gradients may not be altered substantially to effect DA reuptake; however, with the application of supraphysiological stimulations in FSCV studies, these ionic gradients become more important when interpreting DA clearance associated with electrically evoked stimulus responses.

DAergic neurons are exceptionally large unmyelinated neurons with very extensive terminal arborizations, making action potential propagation, the subsequent calcium influx, DA

release, and DA reuptake, and the restoration of electrochemical gradients energetically exhaustive processes (Pissadaki & Bolam 2013, Matsuda *et al.* 2009). Supraphysiological MFB stimulations in FSCV studies result in the rapid synchronous firing activity of a collection of DAergic neurons (Kuhr et al. 1987), which may deplete the energy required to sustain DA neurotransmission. In fact, in response to MFB stimulation, voltammetric responses demonstrate striatal changes in DA concentrations and also changes in pH, O_2, and adenosine concentrations consistent with increased cellular activity and ATP utilization (Kennedy *et al.* 1992, Takmakov *et al.* 2010, Phillips *et al.* 2003, Cechova & Venton 2008). The increased metabolic demand following MFB stimulations results in energy depletion, by ATP depletion and/or by depletion of energy stored in electrochemical gradients, which are expected to attenuate reuptake processes (**Figure 2**), just as blocking Na^+-K^+-ATPase with ouabain has been shown to alter stimulated DA responses, in part, by attenuating DA reuptake kinetics (Jones et al. 1999b).

Following stimulated DA release and reuptake into the intracellular space, DA is either sequestered into synaptic vesicles or degraded by intracellular enzymes like monoamine oxidase –B (MAO-B). If the kinetics of these processes are not rapid enough, then DA would necessarily accumulate in the intracellular space, which could significantly diminish the electrochemical driving force for further DA reuptake (**Figure 2**).

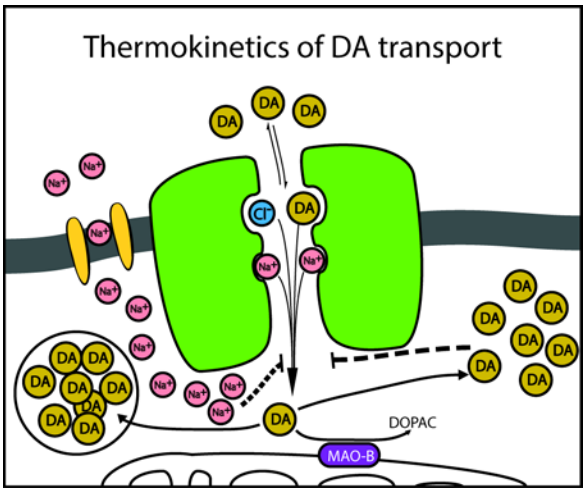

Figure 2: Thermodynamic inhibition of DAT can occur during stimulated DA responses

Thermodynamic inhibition of DAT can occur during stimulated DA responses. Following DA reuptake, DA molecules may get sequestered by synaptic vesicles, degraded, or transiently accumulate in the intracellular space to inhibit reuptake. The accumulation of intracellular DA may be predicted to increase Km. Electrical stimulation may also transiently diminish the electrochemical gradient of Na+ that is required for DA reuptake. The diminished Na+ electrochemical gradient may also decrease DA transport efficiency.

In FSCV studies, intracellular DA accumulation during stimulated DA responses and/or energy depletion may manifest itself by progressively decreasing DA reuptake efficiency (i.e. the function of individual transporters) over the duration of a stimulated DA response (**Figure 2**). Consistent with a stimulation-induced attenuation of reuptake efficiency, Wang et al. (2011) recently reported that increasing stimulation duration attenuates the apparent V_{max} in stimulated DA responses. This finding corresponds well with our empirical data demonstrating that the decay kinetics of stimulated DA responses are attenuated by increasing stimulation duration. **Figure 3** depicts mean DA responses collected in the dorsal (n=7) and ventral (n=6) neostriatal regions (**Figure 3A and D,** respectively) using different durations of 60Hz stimulations. Decay efficiency plots were generated for these responses (**Figure 3B,E)**, graphically representing the DA decay rate as the dependent variable and the extracellular DA concentration load as the independent variable. These plots are similar to M-M plots like **Figure 1A**, which represent the relationship

between reuptake rate and $[DA]_{EC}$. As DA concentration increases, reuptake *rate* does not increase *ad infinitum*, and reuptake rate approaches Vmax as DAT becomes saturated. Whereas, the M-M model predicts Vmax and Km to be constants, producing a singular relationship between reuptake rate vs. $[DA]_{EC}$, we found that increasing the stimulation duration significantly altered the slope of decay efficiency curves as measured by the decay efficiency slopes at the half-maximal decay rate ($Decay_{1/2mx}$) (repeated-measures ANOVA $F(4,24)=5.330$, $p<0.005$, $F(4,20)=12.187$, $p<0.001$, for dorsal and ventral responses, respectively). Pairwise comparison of 1s vs. 10s stimulations demonstrate that longer stimulation durations attenuate DA decay efficiency ($t=2.551$, $p<0.05$, $t=3.738$, $p<0.05$ for dorsal and ventral responses, respectively) (**Figure 3C,E**), suggesting that DA reuptake efficiency likely decreases with increasing stimulation duration; however, as DA decay rates reflect the difference between DA reuptake rate and post-stimulation DA release rate, post-stimulation DA release may also contribute to observed changes in decay efficiency.

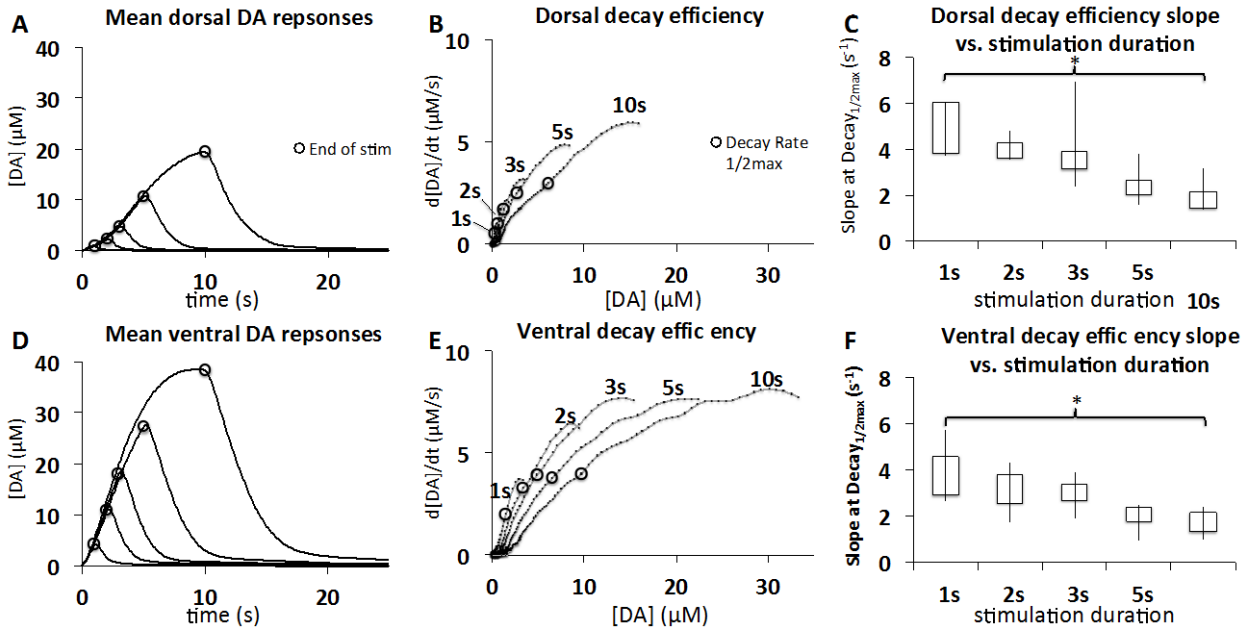

Figure 3: Increasing stimulation duration decreases DA decay kinetics

Mean stimulated DA responses using 1,2,3,5, and 10s stimulations were collected from the dorsal (n=6) (A) and ventral (n=7) (D) striatum. The circles mark the end of the stimulations stimulation. Decay efficiency curves were plotted for the different stimulation durations (B,E), with circles indicating Decay Rate1/2max. The slope of the decay efficiency plot at Decay Rate1/2max is significantly affected by stimulation duration in the dorsal and ventral striatum

(repeated-measures ANOVA $F(4,24)=5.330$, $p<0.005$, $F(4,20)=12.187$, $p<0.001$, respectively). C&D) Box and whisker plots showing the range (vertical lines) and the interquartile range (boxes) of the decay efficiency slopes, demonstrate that the decay efficiency slope is significantly attenuated by longer stimulation durations (1s vs. 10s, $t=2.551$, $p<0.05$, $t=3.738$, $p<0.05$, respectively), suggestive of attenuating reuptake kinetics with increasing stimulation duration.

The concept of attenuating reuptake efficiency during a stimulated DA response is also supported by the existence of concave DA responses that are, as aforementioned, inconsistent with the M-M model. In the context of an attenuating release rate described in the *Stimulated Dopamine Release* section, modeling DA responses with constant reuptake efficiency (i.e. constant Vmax and Km) predicts solely convex responses (**Figure 4A**) similar to the M-M model as demonstrated in **Figure 1B**. A constant reuptake efficiency model predicts that reuptake rate increases during the rising phase of DA responses; whereas, a concave stimulated DA response shape emerges only when the rate of reuptake decreases faster than the rate of release decreases, which can only occur in an attenuating reuptake efficiency model (**Figure 4B**). These theoretical and experimental results emphasize the need to account for the concept of attenuating reuptake efficiency when interpreting *in vivo* stimulated DA responses, even though the precise mechanism that causes reuptake rate to decrease during a stimulated DA response remains to be elucidated. In our model, we incorporated the concept of attenuating reuptake efficiency by allowing for an increasing Km, and this method can simulate DA responses that exhibit diverse concave and convex morphologies as demonstrated in **Figure 4B**- morphologies that are characteristic of experimental DA responses.

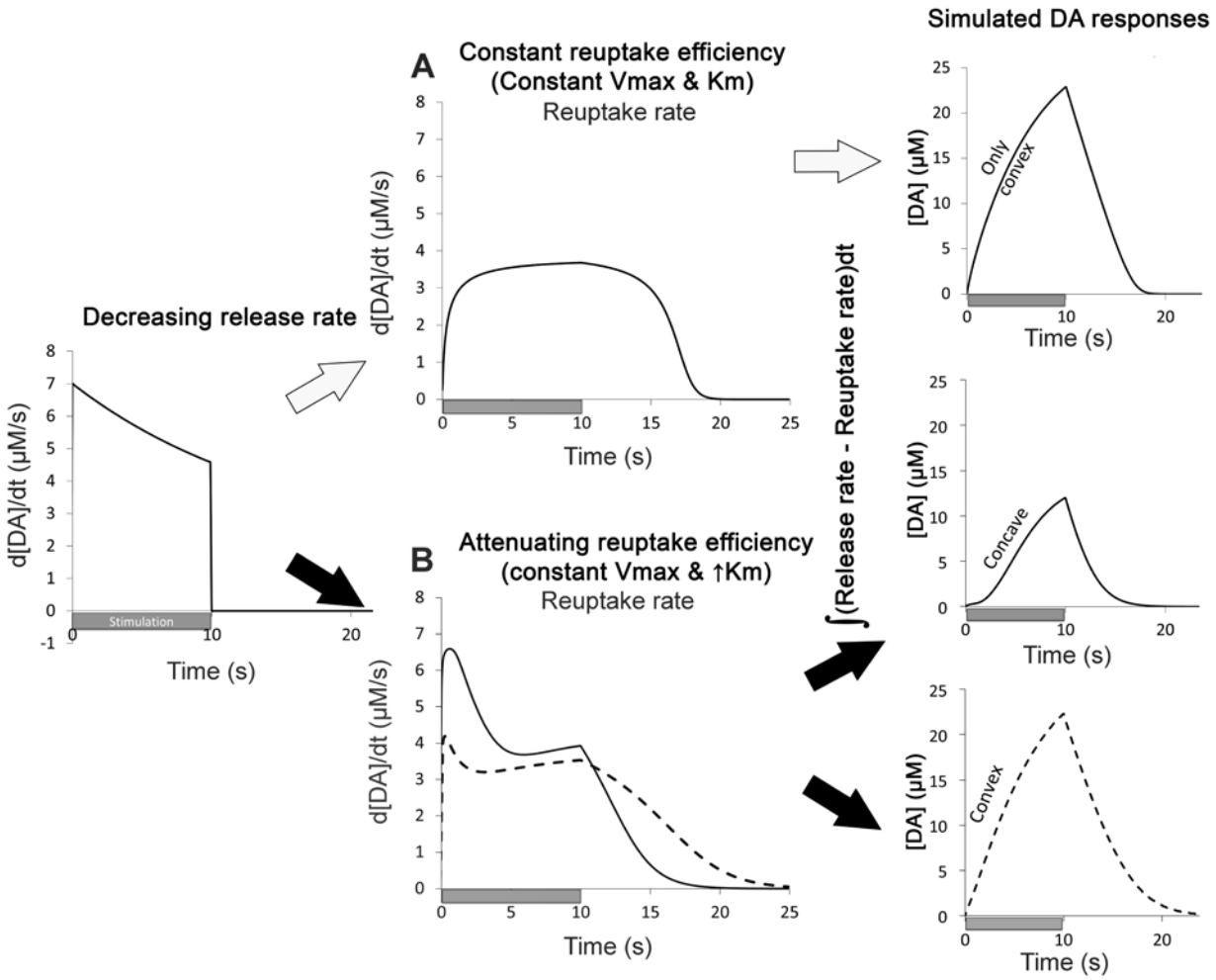

Figure 4: Heterogeneity of DA response patterns requires attenuating reuptake efficiency

A) Responses simulated with constant reuptake efficiency always yields convex DA responses. B) However, responses simulated with an attenuating reuptake efficiency concept can yield either concave or convex DA responses depending on the balance between reuptake and release dynamics. Concavity of DA responses emerges when reuptake rate decreases faster than release rate decreases.

2.4 MATHEMATICAL MODELING OF THE PRINCIPLES OF STIMULATED DA NEUROTRANSMISSION

Above, we qualitatively described the principles of PTD associated with neurotransmitter release, post-stimulation neurotransmitter release, and progressively attenuating reuptake efficiency as

components that need to be considered when defining and interpreting kinetic parameters associated with stimulated DA responses. In this section, we describe how we have chosen to mathematically represent these components of DA neurotransmission in order to simulate DA responses across a range of experimental DA response types. In turn, the simulations presented demonstrate how these neurobiological principles map onto the characteristic behaviors of experimental DA responses obtained using in vivo FSCV with an evoked release paradigm, with the goal of providing a realistic quantitative kinetic parameterization reflective of DA release and reuptake processes observed with stimulated DA responses.

To mathematically represent the dynamic neurobiological components of DA release and reuptake that contribute to variable components of stimulated DA responses, we developed equations to describe DA release and reuptake rates as a function of time. These rates were then integrated over time in Matlab to simulate DA vs. time graphs. The equations described below are modifiable so that they may be used to simulate a variety of DA response types observed experimentally.

2.4.1 DA release (during stimulation)

To describe DA release rate, we used a monoexponential decay function with an added constant (**Equation 2**), similar to what has previously been described for glutamatergic synapses (Taschenberger & von Gersdorff 2000).

$$DAR(t_{stim}) = \Delta DAR * e^{-t_{stim}/\Delta DAR\tau} + DAR_{SS}$$

Equation 2

In **Equation 2**, DAR(t_{stim}) describes DA release rate as a function of time into the stimulation (t_{stim}), with ΔDAR, ΔDARτ, and DAR_{SS} being parameters to be estimated in the simulation. ΔDAR represents a theoretical change in DA release rate at infinite time, ΔDARτ is the exponential decay constant, and DAR_{SS} is the steady-state DA release rate that maybe representative of a DA release rate when depletion of the RRP by the pulse-trains is offset by Ca^{2+}-induced recruitment vesicles into the RRP (Neher & Sakaba 2008) (**Figure 5A**).

2.4.2 Post-stimulation DA release

Stimulated neurotransmitter release occurs through at least two kinetically distinct Ca^{2+}-mediated processes, while post-stimulation DA release can be expected due to intracellular Ca^{2+} accumulation that varies based on stimulation duration (Pan & Ryan 2012, Fierro et al. 1998). We, thus, represented post-stimulation DA release as a function that was continuous with stimulated DA release (i.e. the rate of DA release at the end of stimulation (DAR_{ES}) = the initial rate of post-stimulation DA release). We implemented a function that accounts for both a rapid and prolonged component of post-stimulation release, similar to previous description by Atluri and Regehr (1998).

Equation 3 describes post-stimulation DA release rate in terms of a rapid exponential decay phase and a prolonged linear decay phase to represent both rapid and slow components of post-stimulation release that are hypothesized to occur as a result of raised $[Ca^{2+}]_{in}$ via

synaptotagmin and DOC2 relevant processes (**Figure 5A)**. Because of the differential kinetics of rapid and prolonged post-stimulation components, the relative contribution of the rapid post-stimulation DA release component decreases over the time course of the post-stimulation period (**Figure 5A**).

$$DAR_{post}(t_{post}) = \underbrace{X_r * DAR_{ES} * e^{-\frac{t_{post}}{\tau_r}}}_{\text{(Rapid)}} + \underbrace{(1 - X_r) * DAR_{ES} - m * t_{post}}_{\text{(Prolonged)}}$$

Equation 3

In **Equation 3**, X_R describes the fractional component of post-stimulation DA release undergoing rapid decay. Neurobiologically, X_R may represent the fractional component of post-stimulation DA release that is predominantly synaptotagmin-mediated. This fractional component may decrease during pulse train stimulations due to a gradual recruitment of DOC2-mediated release (Pyott & Rosenmund 2002). *m* describes the linear decay slope of the prolonged DA release component. Experimentally, we observe sustained elevated DA concentrations that decay with a time course that is related to stimulation duration (e.g. DA concentrations do not return to baseline even 10s post-stimulation of 60Hz, 10s responses in **Figure 3A**). Neurobiologically, the prolongations of DA release by stimulation duration, could be due to prolongations of elevated $[Ca^{2+}]_{in}$ that are also stimulation duration-dependent (Fierro et al. 1998).

2.4.3 DA reuptake

Similar to the M-M model, our framework assumes that DA reuptake is determined by saturation of DAT, but our framework also accounts for decreasing DA reuptake efficiency as suggested by our experimental data (**Figure 3**). Therefore, to describe DA reuptake rate, we utilize the same equation to describe DA reuptake as the M-M model (**Equation 1**), except we describe K_m as a time dependent function rather than a constant (**Equation 4**).

$$ReuptakeRate(t) = \frac{V_{max}}{\frac{K_m(t)}{[DA]} + 1}$$

Equation 4

Our empirical data suggests that DAT efficiency decreases over the course of a stimulated DA response (**Figure 3**), which may be due to a rapid accumulation of $[DA]_{in}$ or the diminution of Na^+ electrochemical gradients during stimulation. In our model, we assume that DAT act as pumps with reuptake rate not only determined by DAT saturation as M-M enzyme kinetics suggests, but also dependent upon the electrochemical driving force for reuptake, where the maximal rate of reuptake (Vmax) is a constant that can theoretically be attained when DAT is saturated and electrochemical gradients are large enough. However, with a diminution of electrochemical gradients that may occur during stimulated DA responses, the $[DA]_{EC}$ required to attain half-maximal reuptake rate (K_m) would progressively increase during a stimulated DA response. In this neurobiological context, the half-maximal reuptake rate occurs not simply when the $[DA]_{EC}$

saturates 50% of transporters, but it can highly depend upon the thermodynamic forces mediating reuptake, which is different from standard definitions of K_m, and so the term should be considered as an apparent K_m. To describe the attenuation of DAT efficiency, our model assumes a variable K_m that monotonically increases throughout the duration of a stimulated DA response, which we describe with a logistic function in **Equation 5**.

$$K_m(t) = K_{m_i} + \Delta K_m \left(1 - \frac{1}{1 + \frac{t}{K_{m_{inf}}}^{k}} \right)$$

Equation 5

Equation 5 describes how K_m increases during stimulation using K_{m_i}, $K_{m_{inf}}$, ΔK_m, and *k* parameters that can be estimated in simulations. Here, K_{m_i} represents the initial K_m value, ΔK_m is the amplitude of the K_m change, $K_{m_{inf}}$ is the inflection point in the $K_m(t)$ curve, and *k* is the Hill-Coefficient, representing the steepness of the function about the inflection point. These parameters allow for representation $K_m(t)$ and how it may increase monotonically with a single inflection point over the course of a DA response (**Figure 5B**).

The time-dependent changes K_m described in **Equation 5** may continue to increase in the post-stimulation phase while DAT continues to clear $[DA]_{EC}$. However, logically, K_m would not progressively increase far after stimulation cessation. Therefore, we held K_m constant after the rapid component of the post-stimulation DA release rate ≈ 0. Future work may help modify the post-stimulation K_m kinetics.

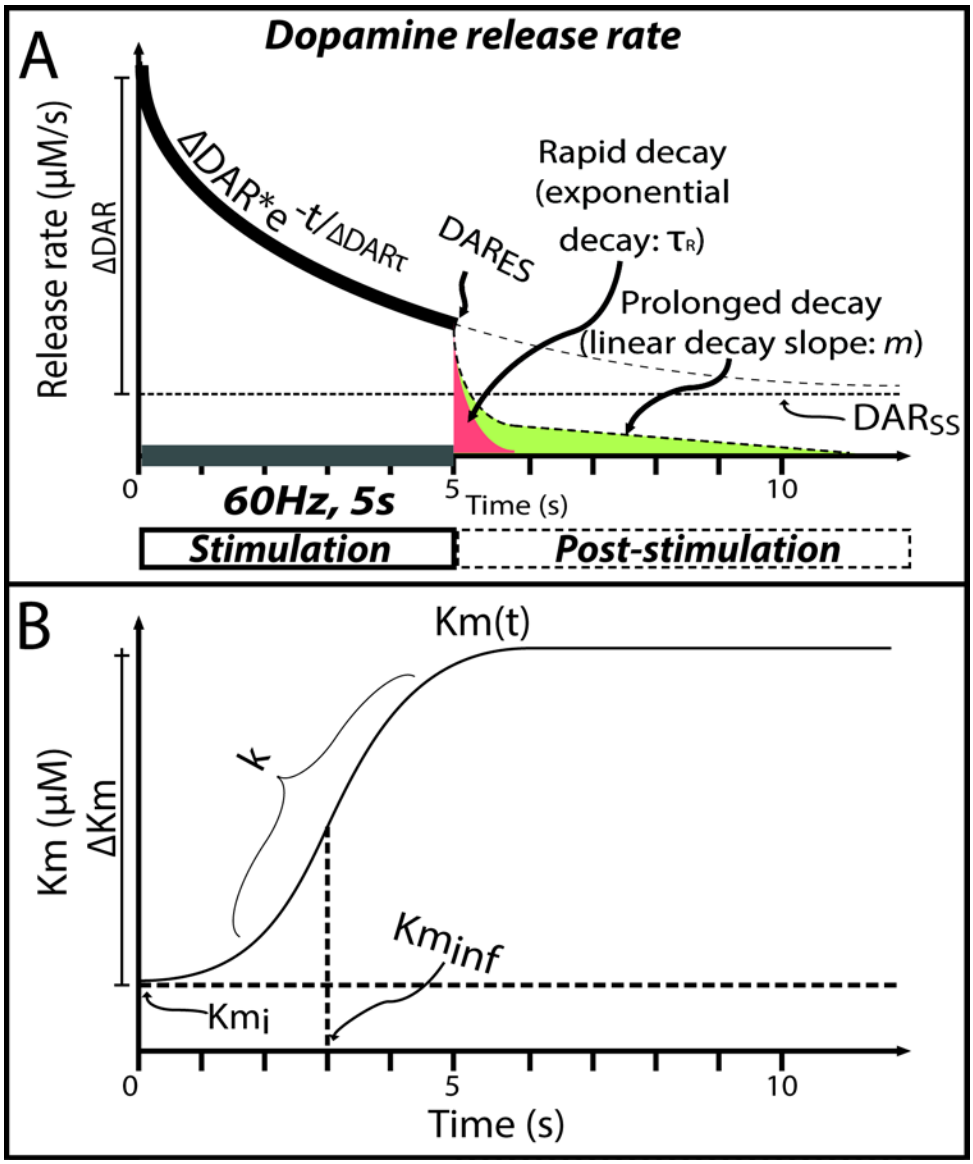

Figure 5: Mathematical representations of DA release and reuptake kinetics utilized to perform simulations of experimental DA responses

A) DA release rate during stimulation is described by **Equation 3** as a mono-exponential function and an additional steady-state DA release rate (DAR_{ss}). Post-stimulation DA release rate continues after stimulation as described by **Equation 4**, with post-stimulation DA release consisting of a rapid exponential decay and a prolonged linear decay component. B) A logistic function was used to describe Km as increasing during the stimulated DA responses according to **Equation 5**. This figure illustrates how the parameters ΔK_m, k, and K_{m_i} determine how K_m changes in a simulation.

Table 1. Equations and parameters utilized in simulations

***DA release rate (during stimulation)*:**		
$\boldsymbol{\Delta DAR * e^{-t_{stim}/\Delta DAR\tau} + DAR_{SS}}$	ΔDAR	DA release rate undergoing decay
	$\Delta DAR\tau$	Time constant relating to decay of stimulated DA release rate
	DAR_{ss}	Steady-state DA release rate
***DA release rate (post-stimulation)*:**		
$\boldsymbol{DAR_{post}(t_{post}) = X_R * DAR_{ES} * e^{-\frac{t_{post}}{\tau_r}} + (1 - X_R) * DAR_{ES} - m * t_{post}}$	X_R	Rapid release fractional component
	DAR_{ES}	DA release rate at end of stimulation
	τ_r	Time constant of rapid release component
	m	Linear decay slope of prolonged release component
DA reuptake rate:		
$\boldsymbol{ReuptakeRate(t) = \frac{V_{max}}{\frac{K_m(t)}{[DA]} + 1}}$ where, $\boldsymbol{K_m(t) = K_{m_i} + \Delta K_m \left(1 - \frac{1}{1 + \frac{t}{K_{m_{inf}}}^{k}} \right)}$	V_{max}	Maximal reuptake rate
	$K_m(t)$	M-M constant (An inverse measure of efficiency)
	K_{m_i}	Initial K_m
	ΔK	Magnitude of change in K_m dynamics
	$K_{m_{inf}}$	Time of inflection of K_m dynamics
	k	Measure of the steepness of the inflection in K_m dynamics

2.5 APPLICATION OF MODELING METHODS TO EXPERIMENTAL DA RESPONSES

Equations 2, 3 and 5 were utilized to simulate DA vs. T responses according to **Equation 6** using MATLAB (The MathWorks Inc, Natick, MA).

$$[DA](t) = \int \left(DAR(t) + DAR_{delay}\left(t_{ps}\right) \right) dt - \int \frac{V_{max}}{\frac{K_m(t)}{[DA]} + 1} dt$$

Equation 6

The simulations were initiated using the DA release rate at t=0 for the [DA] in the reuptake term. Thereafter, [DA](t) was substituted for [DA] and DA(t) was calculated iteratively for all time points in the simulation. We found using time increments of .005s was adequate to run simulations as it generated expected smooth traces of DA responses and is also shorter than the inter-scan intervals of DA measurements in typical FSCV studies (Wagner et al. 2009b, May & Wightman 1989, Jones *et al.* 1995b).

Multiple sets of parameters for **Equations 2, 3, and 5,** representing differential release and reuptake kinetics can yield a good qualitative fit of experimental data. Because stimulated DA responses largely represent a balance between DA release and reuptake, the less efficient reuptake kinetics are in a simulation, the less robust release kinetics need to be to in order to model the same DA response. It is informative to obtain conservative estimates of release and reuptake kinetics; whereas, there is no upper limit to how robust release kinetics could be- reuptake kinetics would have to be similarly robust to counterbalance it. In order to obtain conservative estimates of reuptake and release kinetics, simulations using **Equation 6** were fit to experimental data by first minimizing V_{max} and subsequently adjusting the simulation parameters to minimize the total DA released in the simulations. In doing so, this method yielded simulations with conservative estimates of reuptake, and therefore, DA release as well.

2.5.1 Regiospecific stimulated DA responses

It was previously demonstrated that stimulated DA response morphology in the ventral striatum have a more convex rising pattern than responses collected in the dorsal striatum (May & Wightman 1989), and this has been a general finding in our lab as well. In order to demonstrate applicability of our modeling methods on the wide-ranging DA response shapes observed in the striatum, we obtained stimulated DA responses from the anterior dorsal (n=7) and middle ventral neostriatum (n=6) to collect DA responses that rise concavely and convexly during 60Hz stimulations, respectively, as reported previously (May & Wightman 1989) (see methods section for details).

We demonstrate that both dorsal and ventral striatal responses can be modeled according to the quantitative model described in this report (**Figure 6**). Without accounting for post-stimulation DA release, the modeled DA responses (black dashed lines in **Figure 6A&B**) undershoot the decay phase of experimental DA responses, but with the addition of estimated post-stimulation DA release components responses could be simulated well (gray dashed lines **Figure 6A&B**). Responses from both striatal regions were modeled with similar dopamine release dynamics, but differences were observed with uptake kinetics (**Figure 6C & D**). Notably, there was a difference in the $K_{m_{inf}}$, where the inflection point occurs later in dorsal responses compared to ventral responses (5.4s vs. 2.4s, respectively) (**Table 2**). These differences in the Km dynamics may be due to regional differences in bioenergetics or DAT function, causing dorsal striatal responses to exhibit a more prolonged attenuation of DA reuptake efficiency compared to the ventral striatum (Ciliax *et al.* 1995). These simulations allow us to estimate the amount of DA released and cleared over the time course of DA responses (**Table 3**). These simulations suggest that a greater

proportion of DA released in the first 1s of stimulation is cleared by reuptake in the dorsal striatum compared to the ventral striatum (93.3% vs. 73.6%, respectively) (**Table 3**), indicative of more robust clearance mechanisms in the dorsal striatum compared to the ventral striatum as established before (Jones *et al.* 1995a).

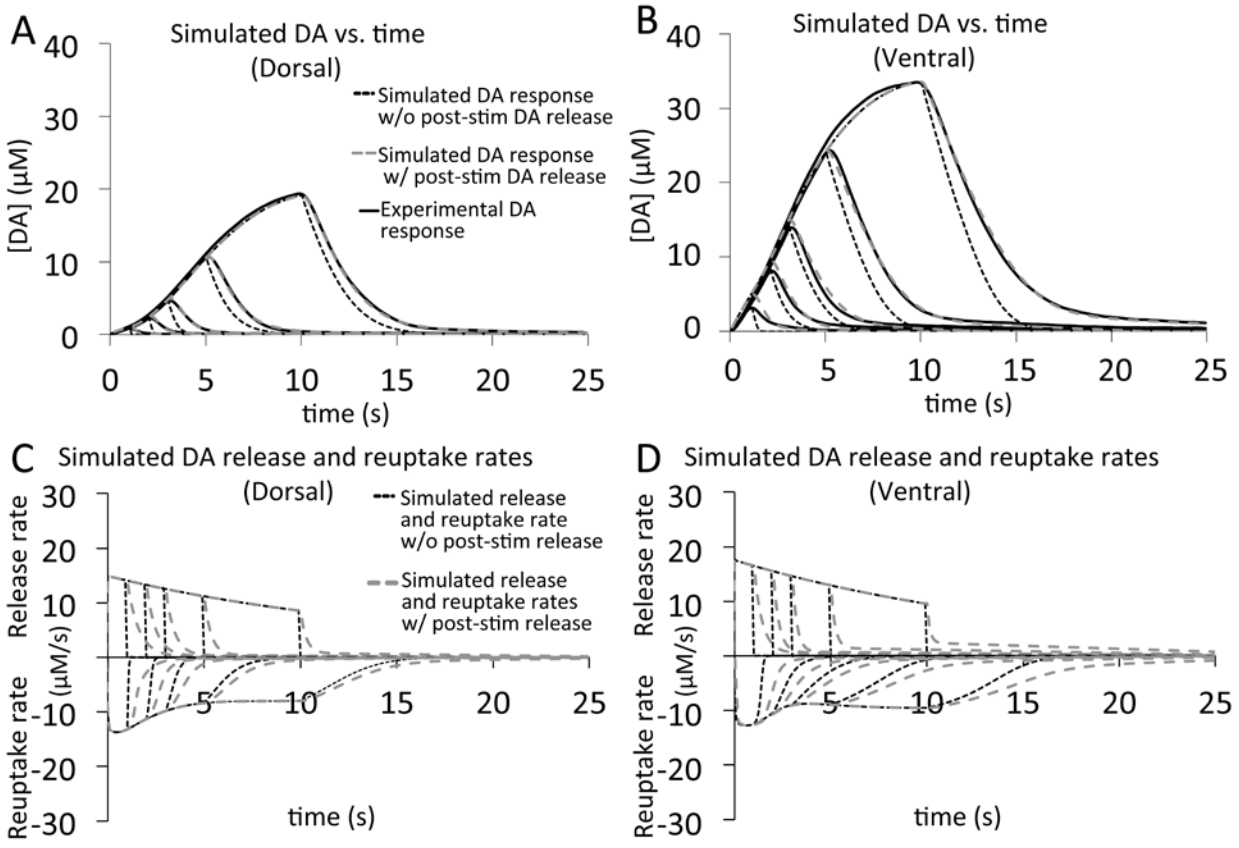

Figure 6: Simulations of regiospecific stimulated DA responses

A/B) Experimental DA responses (solid black lines) were simulated using the described methods (gray dashed lines). Simulations of experimental data without accounting for a post-stimulation DA release component are also depicted (black dashed lines). C/D) Simulated DA release and reuptake rates during the response time course according to the neurobiological model are depicted (gray dashed lines). Moreover, simulated release and reuptake rates without accounting for a post-stimulation DA release component are also depicted (black dashed lines).

Table 2: Simulation parameters of dorsal and ventral neostriatl DA responses

Dorsal						τ_R *(s)*	*m (s)*	X_R
ΔDAR (μM/s)	13.1	Vmax (μM/s)	14.4		1s	0.6	0.005	0.97
ΔDARτ (s)	15	Km_i *(μM)*	0.03	Post-stimulation DA release	2s	0.5	0.01	0.965
DARss (μM/s)	1.8	ΔKm (μM)	17.5		3s	0.45	0.025	0.962
		Km_{inf}	5.4		5s	0.35	0.03	0.96
		k	3.25		10s	0.3	0.04	0.92
Ventral								
ΔDAR (μM/s)	17.2	Vmax (μM/s)	13.2		1s	0.43	0.02	0.97
ΔDARτ (s)	16	Km_i *(μM)*	0.08	Post-stimulation DA release	2s	0.3	0.03	0.96
DARss (μM/s)	0.3	ΔKm (μM)	12.5		3s	0.24	0.03	0.95
		Km_{inf}	2.9		5s	0.22	0.06	0.89
		k	4		10s	0.15	0.11	0.75

Table 3: Metrics derived from simulations of regiospecific DA responses

Metrics	***Dorsal***	***Ventral***
Total DA released by 10s stimulation:	**121.74μM**	**155.29μM**
DA released during 10s of stimulation:	113.63μM	130.91μM
DA cleared during 10s of stimulation:	**94.51μM**	**98.28μM**
% of DA cleared during 10s of stimulation:	83.2%	75.1%
DA released during 1s of stimulation:	**14.47μM**	**16.98μM**
DA cleared during 1s of stimulation:	13.49μM	12.50μM
% of DA cleared during 1s of stimulation:	**93.3%**	**73.6%**

2.5.2 Varying frequency of stimulated DA responses

To further test the validity and utility of the quantitative neurobiological model proposed, we simulated DA responses that were collected in the dorsal striatum (n=3), in which we varied the frequency of 10s stimulations between 35-60Hz (**Figure 7**). In simulating these DA responses, we held V_{max} constant because the local DAT concentration should be relatively constant between stimulations. The model was able to simulate the different frequency responses as shown in **Figure**

7A. The frequency of the stimulation determined the initial DA release rate, wherein higher frequencies were associated with stronger initial release rates (**Figure 7B**). Moreover, with higher stimulation frequencies, there was a faster decay in DA release kinetics (DARτ) (**Table 4**). These simulation parameters are consistent with the demonstrated effects of stimulation frequency on glutamate release in glutamatergic synapses (Pyott & Rosenmund 2002). Interestingly, DA reuptake rate does not vary greatly across the different frequencies of stimulation (**Figure 7B**), but the $K_m(t)$ function has a strong relationship with the frequency of stimulation, such that the greater the stimulation frequency, the more leftward the inflection in the Km(t) function (**Figure 7C** and **Table 4**). Thus, these simulations suggest that the attenuation of reuptake efficiency occurs faster with higher frequency of stimulations, as would be expected if energy depletion and perturbations in electrochemical gradients by electrical stimulations underlie the major mechanism of reuptake efficiency attenuation during DA responses. Because the simulations suggest DA reuptake rate does not greatly change across different frequencies of stimulation but that the $K_m(t)$ function does, our data suggests that the $[DA]_{in}$ that accumulates during stimulated DA responses may play a relatively minor role compared to energy depletion in attenuating DA reuptake kinetics during a stimulated DA response.

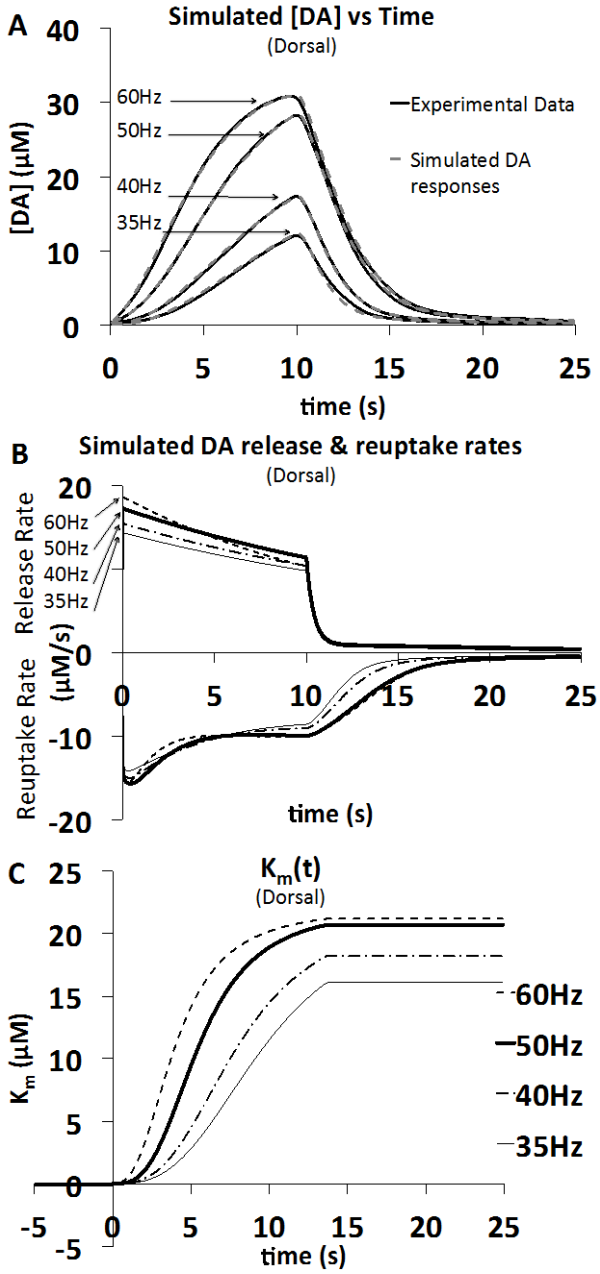

Figure 7: Simulations of DA responses by varying frequency

A) Experimental DA responses (solid black lines) were simulated using the quantitative neurobiological method (gray dashed lines). B) Simulated DA release and reuptake rates depicted for the various frequencies of stimulation. C) The Km(t) functions that were used to simulate each DA response reveals a left-ward shift in the Km(t) function with increasing stimulation frequency, suggesting faster attenuation of reuptake kinetics.

Table 4: Simulations of responses while varying stim frequency

Parameters	*60Hz*	*50Hz*	*40Hz*	*35Hz*
ΔDAR (μM/s)	15.7	14.4	12.7	11.7
ΔDARτ (s)	13.2	19	19.5	20
DARss (μM/s)	3	2.9	2.8	2.7
τ_R *(s)*	0.4	0.4	0.4	0.4
m (s)	0.04	0.04	0.04	0.04
X_R	0.91	0.91	0.92	0.92
Vmax (μM/s)	16.5	16.5	16.5	16.5
Km_i *(μM)*	0.04	0.04	0.04	0.04
ΔKm (μM)	22	22	22	22
Km_{inf}	4	5.5	8	9.7
k	2.6	3	2.9	2.9

2.5.3 Regiospecific pharmacological response to methylphenidate

The quantitative neurobiological framework may also be applied to study regiospecific effects of pharmacological agents that affect DAergic systems. We examined how mean dorsal (n=4) and ventral (n=4) striatal responses are altered 15min. post-administration of the competitive DAT inhibitor MPH (10mg/kg i.p.). Though, primarily a DAT inhibitor, MPH can have indirect effects on enhancing DA release (Sandoval *et al.* 2002, Volz *et al.* 2008), which may be similar to the effects of cocaine, a similar DAT inhibitor (Venton *et al.* 2006). MPH may also increase DAT surface expression as has been demonstrated by other DAT inhibitors (Little *et al.* 2002, Daws *et al.* 2002).

In **Figure 8A,B**, we demonstrate how our simulations are capable of approximating post-MPH changes in 60Hz, 5s stimulated DA responses from baseline. Pre- and post-MPH DA responses were simulated by holding constant the parameterization of post-stimulation DA release

kinetics (**Table 5**). This assumption was made because pre- and post-drug responses were recorded from the same site with the same duration of stimulation, which should yield similar dynamics of $[Ca^{2+}]$ accumulation and therefore post-stimulation DA release dynamics. By assuming post-stimulation DA release kinetics are constant, MPH-induced changes could be modeled as changes in stimulated DA release and reuptake kinetics. Pre- and post-MPH responses were successfully modeled as an increase in $K_{mi,}$ as expected for a DAT inhibitor, but also by increases in DA release rates and V_{max} (**Figure 8C,D, & Table 5**), consistent with others' reports (Daws et al. 2002, Little et al. 2002, Venton et al. 2006, Volz et al. 2008). Similar pattern of changes in V_{max}, DA release kinetics, and K_m kinetics were observed in the dorsal and ventral striatal regions.

Interestingly, our simulations indicate that the % of DA released that was cleared during 5s of stimulation did not greatly change, and even slightly increased with the MPH challenge (**Table 6**). This is because MPH enhances DA release, and although MPH inhibits DAT, this effect is partially masked by the stimulation-dependent attenuation of reuptake efficiency. However, MPH did attenuate the % of DA cleared during 1s of stimulation because the stimulation-dependent attenuation of reuptake efficiency has a less pronounced role in the initial phase of the DA response, allowing for the observation of the DAT-inhibiting effect of MPH.

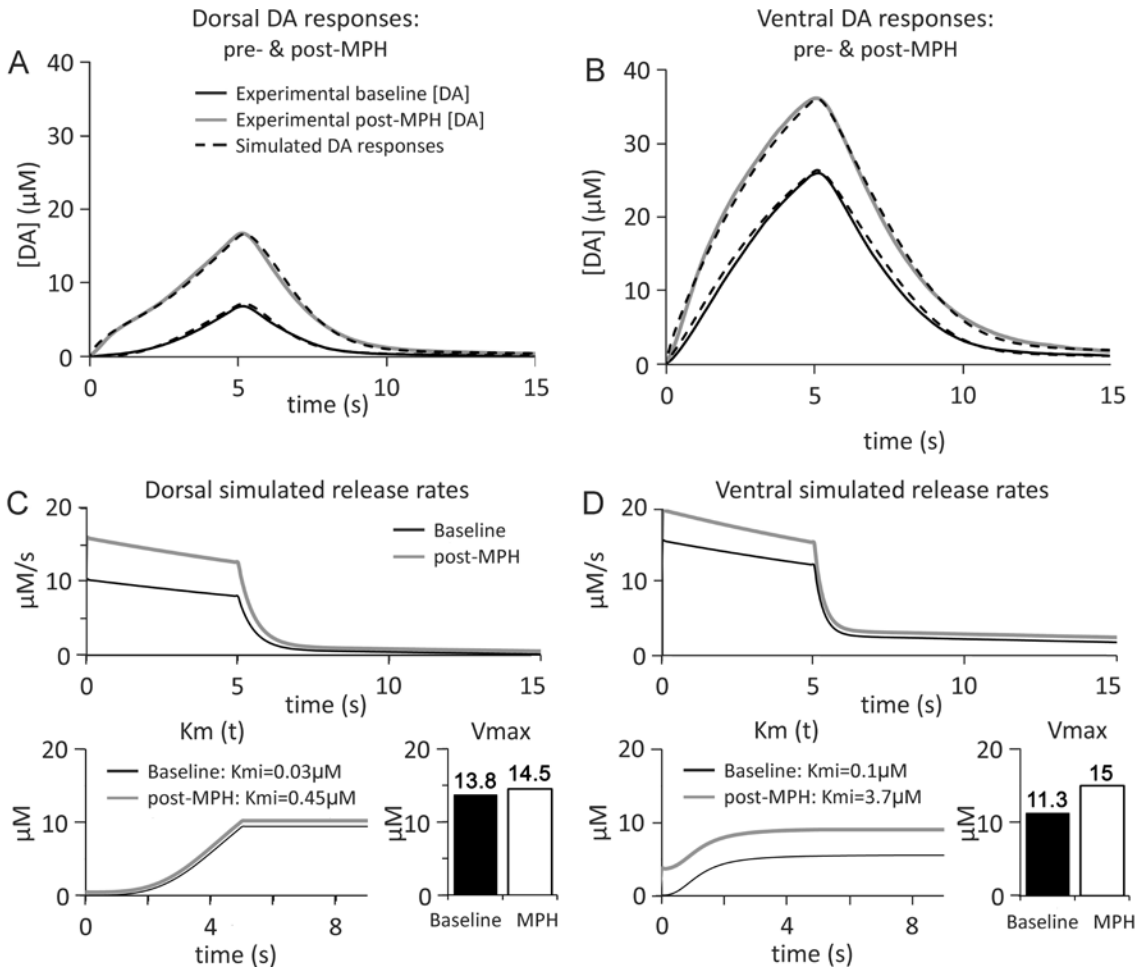

Figure 8: Regiospecific DA responses following methylphenidate administration

Dorsal (n=4) (A) and ventral (n=4) (B) striatum before and 15 min. after administration of MPH (10mg/kg, i.p.). C&D) Simulated DA release rates were plotted for baseline and post-MPH responses, revealing a post-MPH increase in release rate. The Km(t) functions used in the simulations are also plotted, revealing the expected increase in Kmi post-MPH administration but similar pattern of Km increasing pre- and post-MPH. Moreover, the Vmax increases post-MPH administration in both the dorsal (C) and ventral (D) striatum.

Table 5: Simulation parameters in pre- and post-MPH responses

	Dorsal		*Ventral*	
Parameters	***Baseline***	***MPH***	***Baseline***	***MPH***
ΔDAR (μM/s)	9.8	14.5	13	16.8
ΔDARτ (s)	19	19	17	16
DARss (μM/s)	0.5	1.5	2.7	3.1
τ_R *(s)*	0.53	0.53	0.3	0.3
m (s)	0.06	0.06	0.09	0.09
X_R	0.91	0.91	0.78	0.78
Vmax (μM/s)	13.8	14.5	11.3	15
Km_i *(μM)*	0.03	0.45	0.1	3.7
ΔKm (μM)	19.5	19.5	5.5	5.5
Km_{inf}	5.1	5	1.2	1.2
k	3.5	3.5	2.5	2.5

Table 6: Metrics derived from simulations of MPH responses

	Dorsal		*Ventral*	
Metrics	***Baseline***	***MPH***	***Baseline***	***MPH***
Total DA released by 5s stimulation:	65.60μM	77.39μM	97.12μM	118.84μM
DA released during 5s of stimulation:	54.52μM	65.32μM	70.56μM	87.05μM
DA cleared during 5s of stimulation:	48.01μM	48.82μM	45.33μM	51.62μM
% of DA cleared during 5s of stimulation:	36.7%	37.3%	34.6%	39.4%
DA released during 1s of stimulation:	12.02μM	14.65μM	15.51μM	20.30μM
DA cleared during 1s of stimulation:	11.62μM	10.44μM	10.12μM	8.46μM
% of DA cleared during 1s of stimulation:	96.7%	71.2%	65.2%	41.7%

2.6 DISCUSSION

FSCV DA responses obtained using electrical stimulation paradigms reflect a balance between DA release and reuptake. Albeit, stimulated DA responses are supra-physiological, the high signal-to-noise ratio of stimulated DA responses is amenable for kinetic analyses that are otherwise difficult in physiological non-stimulated conditions.

This work highlights some of the dynamics of stimulated DA release and reuptake that may be predicted based on contemporary research and initially validated using our experimental data. Rather than DA reuptake following simple M-M enzyme kinetics described by constant V_{max} and K_m parameters, we suggest reuptake follows a dynamic M-M model described by a constant V_{max} and a variable K_m term associated with a decreasing efficiency of reuptake during stimulated DA responses. Rather than DA release described by a constant amount of DA released-per-pulse in the M-M model, we suggest that release decreases exponentially during a stimulation pulse train. Moreover, we suggest that this release continues into the post-stimulation period following a biphasic decay pattern.

Though the concept of release occurring in the post-stimulation phase has been demonstrated and studied since the late 1960s (Katz & Miledi 1968, Barrett & Stevens 1972), many of the specific molecular mechanisms of post-stimulation release have only recently been discovered and currently are being investigated (Groffen et al. 2006, Groffen et al. 2010, Pang et al. 2011). The elevated $[Ca]_{in}$ that can result from sustained stimulations may lead to post-stimulation DA release using the Ca^{2+}-sensor synaptotagmin, while the prolonged phase of post-stimulation DA release may be mediated by more sensitive Ca^{2+}-sensors like DOC2. Since DOC2 proteins have been demonstrated as contributors to post-stimulation release and spontaneous neurotransmitter release in other brain regions, (Groffen et al. 2006, Groffen et al. 2010, Pang et al. 2011, Yao et al. 2011) a demonstration of their expression in striatal DAergic terminals would be important in supporting the concept of post-stimulation DA release.

By taking a mathematical modeling approach, we demonstrate how the kinetics of DA release and reuptake may realistically contribute to the overall shape, and thus properties, of stimulated DA responses. A major strength of this approach is that it quantitatively describes a wide variety of stimulated DA response patterns exhibited throughout striatum, an exercise that has previously not been possible with the M-M model. In particular, dorsal striatal responses that predominantly rise concavely during 60Hz stimulation pulse-trains can be simulated using this proposed neurobiological model, without compromising the fundamental assumptions of the model.

Stimulated DA responses that exhibit concave shapes during electrical stimulations have previously been attributed to diffusional delays in electrode response to nearby DA concentration changes (Kawagoe 1993, Wu et al. 2001) or have been attributed to possible cytoarchitectural diffusional barriers in the striatum (May & Wightman 1989, Taylor et al. 2012). Signal deconvolution methods have often been implemented to remove artifacts attributed to diffusional distortion on stimulated DA responses (Kawagoe & Wightman 1994, Wightman et al. 1988, Wu et al. 2001). These methods were originally developed to remove the signal delays caused by Nafion electrode coatings, but have since been applied to bare electrodes, rationalized by the development of a biological layer that may form around the electrode to cause signal delays (Wu et al. 2001). However, recent work has demonstrated that DA responses collected on bare electrodes do not exhibit characteristics of responses expected for signals convoluted by diffusional distortion (Moquin & Michael 2009, Taylor et al. 2012). Moreover, electron microscopy analysis revealed the existence of intact synapses less than 1μm from explanted electrode tracts, suggesting that the use of signal deconvolution procedures maybe unnecessary for

data collected on bare electrodes (Taylor et al. 2012). In this report, we attribute DA response morphology primarily to represent underlying neurobiological processes and, therefore, we have not applied signal deconvolution algorithms to our dataset.

Concave responses have also been attributed to complex DA release kinetics, where release is initially inhibited and then gradually increases during stimulation (Moquin & Michael 2009). However, the theory of complex release kinetics described is at odds with the predicted exponential decay of release seen ubiquitously for neurotransmitter systems (Dobrunz & Stevens 1997, Liley & North 1953, Pyott & Rosenmund 2002, Zucker 1999, Hagler & Goda 2001, Neves & Lagnado 1999, Hubbard 1963, Pan & Ryan 2012, Taschenberger & von Gersdorff 2000). We suggest that apparent complex release patterns actually be attributable to a dynamic reuptake model that we described in this report. Taylor (2012) et al have reported that blocking DA reuptake with nomifensine administration elicits robust DA responses immediately following stimulation onset, suggesting that DA release is not inhibited at stimulus onset, but that efficient reuptake mechanisms limit the observable increases in $[DA]_{EC}$. The D2 antagonist raclopride, often considered a DA release enhancer, has similar effects to nomifensine on altering the morphology of concave responses (Moquin & Michael 2009). This may be due to the known effects of D2 antagonists on reuptake inhibition, especially at higher frequencies of stimulation (>50Hz) (Wu et al. 2002).

The concept that reuptake efficiency decreases during stimulated DA responses is a novel concept in the voltammetry field, but support for this finding has also been suggested by Wang et al. (Wang et al. 2011). Our experimental data recapitulate the previous findings by showing that

stimulation duration attenuated the efficiency of DA reuptake (**Figure 3**), but we also expound on how attenuating reuptake efficiency is necessary to explain the existence of the variety of experimental DA responses morphologies, particularly concave-shaped responses (**Figure 4**). We suggest that electrical stimulations may deplete ATP and/or the energy stored in electrochemical gradients- particularly, the Na^+ gradients- that are necessary for DA reuptake. Though **Figure 7** suggests intracellular DA accumulation may not predominantly contribute to the attenuation of reuptake efficiency during a stimulated DA response, DA reuptake kinetics may be altered by pharmacological manipulations that increase cytosolic DA levels as with the DA precursor L-Dopa or vesicle depleting agents like reserpine or amphetamine.

In contrast to the hypothesis that DA reuptake efficiency decreases during a stimulated DA response, work by Rodriguez et al. have used amperometric methods to suggest that electrical stimulation enhances DA reuptake (2007) and that MFB stimulation occasionally causes DA concentrations to transiently decrease in discrete striatal sites (2006). Our lab has never observed an MFB stimulated decrease in DA response voltammetrically, despite collecting stimulated responses in various striatal locations, using different electrode fabrication methods, and different frequencies and durations of stimulation presented in this report and elsewhere (Wagner et al. 2009a). Alternatively then, we suggest that pH changes associated with MFB stimulation, which are known to interact with endogenous catechol molecules to yield complex shifts in electrochemical recordings could be misinterpreted as DA decreases in amperometric recordings (Takmakov et al. 2010, Phillips et al. 2003). Though pH changes can be distinguished using FSCV, they cannot with amperometry. This distinguishing difference with *in vivo* electrochemistry techniques then suggests that the findings by Rodriguez should consider pH change and how it

interacts with basal DOPAC as an apparent contributor to stimulus response patterns observed in amperometric recordings (Rodriguez *et al.* 2007a, Rodriguez *et al.* 2006).

The neurobiological framework described in this paper suggests that stimulated DA responses vary greatly across striatal regions. This variation can be largely affected by local DA clearance mechanisms, with dorsal striatal regions having more efficient clearance kinetics leading to concave responses, while ventral striatum have less efficient clearance kinetics leading to convex responses using 60Hz stimulations. These observations are congruent with the dorso-ventral gradient of decreasing DAT density (Ciliax et al. 1995). The striatum is known to have a topographical organization, and thus the regiospecific differences in DA clearance can have important functional implications. The efficient DA clearance kinetics in the dorsal striatum can serve to limit DA diffusion and the time course of signaling in order to mediate the precise neural communication required for cognitive and motor functions ascribed to the dorsal striatum. In contrast, less efficient reuptake mechanisms of the ventral striatum may prolong DA signaling and diffusion to mediate limbic functions that may not require such rapid and precise neural communication as cognitive and motor functions. This regiospecific model of DA neurotransmission kinetics is consistent with findings in awake freely-behaving rats which show that there is a relative paucity of observable spontaneous transient DA fluctuations in the dorsal striatum compared to the ventral striatum (Robinson et al. 2002).

A caveat of the modeling approach described in this paper is that multiple sets of parameters can adequately model a single experimental stimulated DA response. In the experimental stimulated DA responses modeled in this paper, we performed the simulations by

minimizing the total amount of stimulated DA released. In doing so, this yielded conservative estimates of reuptake and post-stimulation DA release that are consistent with the equations incorporated into the model. Although the simulations can demonstrate how DA release and reuptake kinetics may contribute to the overall shape of experimental evoked DA responses, estimations of the true DA neurotransmission kinetics, in part, depend upon the ability to properly constrain parameters of the simulation. Increasing the boundary conditions for simulating the DA responses by collecting various durations of stimulated DA responses, particularly long 10s stimulations can greatly aid simulating responses that may provide a more realistic estimation of DA release and reuptake kinetics in a DA response. Further identification of techniques that will aid in realistically simulating DA responses is an on-going endeavor.

Though the equations that describe the processes of DA neurotransmission here are much more complex than the originally proposed M-M model, they are likely still oversimplifications of true neurobiological processes underlying the kinetics of stimulated DA neurotransmission. For example, though stimulated neurotransmitter release may be adequately modeled as an exponential decay function, it may be more appropriately modeled as a bi-exponential decay function, with a rapid and prolonged decay components as shown previously (Pyott & Rosenmund 2002). Moreover, DA reuptake may be affected by rapid DAT phosphorylation events that could alter the kinetics of DA transport (Miller 2011). DAT is also known to rapidly traffic to and away from the membrane in response to DAT substrates like DA itself (Furman *et al.* 2009a), and DAT may even be trafficked rapidly by stimulation-induced depolarization as has been demonstrated for the glycine transporter-2 (Geerlings *et al.* 2001). However, the mechanisms of DAT trafficking and its kinetics are unknown *in vivo*. Thus, the equations described in this paper should be regarded as

an initial set of equations and parameterization that can demonstrate how the neurobiological principles described in this paper may contribute to the morphology of stimulated DA responses. Continued advancements in the field of neurotransmission will be invaluable for further modification of these equations to mathematically represent DA release and reuptake kinetics and for developing better ways to constrain simulation parameters to reflect the true kinetics of stimulated DA neurotransmission.

The quantitative modeling approach described here endeavors to dissect experimental DA responses into the realistic estimations of DA release and reuptake kinetics. Our main impetus behind generating this novel framework was to develop a method to characterize DAergic dysfunction in our experimental model of TBI, which required a framework that could first quantify and characterize the diverse response-types exhibited in control animals; we have demonstrated how this model is able to simulate DA responses in **Figures 6,7, & 8**. Modeling DA responses following administration of D2 agonists, antagonists, L-Dopa, and other agents that may affect DA neurotransmission could further assess the utility of this framework and its validity. We anticipate this quantitative method will be utilized to understand better how different experimental conditions like sex, aging, and chronic drug treatment paradigms, TBI, and other disease conditions alter presynaptic DA neurotransmission, especially in the dorsal striatum.

2.7 METHODS

Animal Housing

Young-adult Sprague Dawley rats were used for all studies (Hilltop Laboratories, PA). Rats were housed 2 animals per cage with standard bedding and a 12:12h light/dark cycle (on 7:00a.m. to 7:00pm). All housing and procedures were in compliance with the Animal Care and Use Committee at the University of Pittsburgh and in accordance to recommendations outlined in the *Guide for the Care and Use of Laboratory Animals (1996).*

Voltammetric Electrode

Voltammetric electrodes were assembled as previously described in our work (Wagner et al. 2009a, Wagner et al. 2009b). 7μm diameter carbon fiber (T-300, Union Carbide, Danbury, CT) were threaded through borosilicate glass capillary tubes (1.0mm outer diameter, .75mm inner diameter). Capillary tubes were then pulled to a tip using the micropipette puller (Narishige, East Meadow). The carbon fibers were secured with epoxy (Spurr Polysciences, Warrington PA) and cured for 12 hours in 80°C. The exposed carbon fibers were cut to approximately 400μm. Electrical contact was established by filling capillary tubes with mercury and inserting a ni-chrome wire and sealed using epoxy.

Surgical Procedures for Fast-Scan Cyclic Voltammetry

For FSCV experiments, animals were deeply anesthetized with urethane (1.3g/kg, i.p.) in accordance to the Institutional Animal Care and Use guidelines of the University of Pittsburgh. Core body temperature will be maintained at 37°C with a homeothermic blanket (Harvard Apparatus, Hollison MA). Midline incisions were made, and the soft tissues were reflected to expose the skull and relevant landmarks for stereotactic electrode placement. Small burr holes were drilled for the placement of stimulating, the working carbon fiber electrodes. The dura was

removed from each area prior to electrode placement. An Ag/AgCl reference electrode was placed in contact with the dura mater to create a salt bridge. The voltammetric working electrode(s) were then lowered into the striatum using flat-skull coordinates from bregma (Anterior dorsolateral electrode: +1.7mm anterior-posterior (AP), -2.7mm medial-lateral (ML), and -4.6mm dorsal-ventral (DV), Middle ventromedial electrode: +1.0 AP, 2.0 ML, and -6.6 DV) (Paxinos & Watson 2007). Bipolar stimulating electrodes (MS301-1, Plastics One, Roanoke VA.) were placed just above the medial forebrain bundle (MFB) [-4.0 AP, 1.6 ML, -7.2 DV] (Paxinos & Watson 2007).

Voltammetric Data Collection

The potential applied to the carbon fiber microelectrode was controlled the LabView software, TarHeel CV (ESA, Chelmsford, Ma). Just prior to use in FSCV experiments, electrodes were electrochemically treated to increase sensitivity by applying a 70Hz biphasic potential waveform to the electrodes using linear ramp from 0 to 2 to 0V for 4s. A triphasic potential waveform was applied to the electrodes with linear ramp from 0 to 1V, 1 to -.5V, and back to 0V vs. the Ag/AgCl reference electrode, where it was held for 100ms between scans. Electrodes equilibrated for at least another 30 minutes *in vivo* before collecting experimental data. Scan rates were set to 300V/s. Amplifier outputs were digitized during potential scans by a 12-bit analog-to-digital converter operating at a 40KHz sampling frequency. A change in evoked [DA] concentration creates a signature waveform (cyclic voltammogram) with oxidation and reduction peaks occurring between 600-800mV and 100-300mV, respectively. The current associated with the DA oxidation peak was used for analysis, and the currents were converted to DA concentrations by *ex vivo* calibration of the electrode in a flow cell with different concentrations of DA in ACSF following the experiments.

Stimulation of the Medial Forebrain Bundle

In order to evoke DA release in the striatum for measurement with FSCV, DAergic projections contained within the MFB were stimulated. Following stereotaxic placement of the bipolar stimulating electrode just above the MFB, 5s, 60Hz electrical stimulations with a bipolar square waveform (280μA in amplitude, with a pulse width of 2ms) were used to elicit stimulated DA responses recorded by the working electrode. The stimulating electrode was lowered 200μm every 5 minutes until a clear DA signal was observed using the TarHeel CV software. The stimulating electrode was then lowered 100μm every 10 minutes until the summed signal amplitude of the two electrodes began to decrease, at which point experimental data was collected for the FSCV studies.

Studies of varying durations of stimulation & MPH studies:

Because prolonged stimulation durations affect the refractory time interval necessary to reproduce a stimulated DA response (Justice *et al.* 1988), our studies utilized a conservative interval period between stimulations to facilitate attainment of reproducible signals. Thus, for stimulations of 1s, 2s, 3s, 5s, 10s durations we waited 5, 10, 15, 15, and 20 minutes until the next stimulation, respectively. Following the collection of the stimulations of various durations, a subset of rats was used for assessing the response to a pharmacological MPH challenge. First, a 60Hz, 5s stimulation was collected for a baseline. 10mg/kg of MPH in .1M PBS was then administered via intraperitoneal injection. Another 60Hz, 5s stimulation was collected 15 min. post-MPH administration.

Studies of varying frequency of stimulation

A similar protocol was followed for obtaining DA responses of varying frequencies as varying duration, except only one working electrode in the dorsal striatum was utilized. 10s stimulations were used to collect data with 60, 50, 40, and 35Hz frequencies, with 20, 20, 15, and 10 min. wait intervals between stimulations, respectively, to allow for restoration of DA responses.

Data analysis

All experimental stimulated DA responses were temporally filtered using a low-pass 2-pole Butterworth filter with a 1Hz cutoff frequency in MATLAB.

Decay efficiency plots:

Decay efficiency plots were generated from the post-stimulation phase of experimental DA vs. t data. Linear regressions were iteratively performed on 5 consecutive data points, with the negative of the slopes plotted vs. the corresponding $\Delta[DA]_{EC}$ measured using FSCV. Maximal decay rates were determined from the decay efficiency plots.

Statistical analyses were performed in SPSS 22.0 for Mac (SPSS Inc., Chicago, IL) Min, median, max, and $1^{st}/3^{rd}$ quartile are graphically reported for decay efficiency slopes at Decay $Rate_{1/2max}$ for each stimulation duration tested. Repeated measures ANOVA was used to assess the main effects of stimulation duration on decay efficiency slope at Decay $Rate_{1/2max}$. Pair-wise comparison of 1s vs. 10s stimulations was performed using a pair-wise T-test. A $p\text{-}value \leq 0.05$ was considered significant for all analyses.

3.0 FAST-SCAN CYCLIC VOLTAMMTERY DEMONSTRATES THAT L-DOPA PRODUCES REGIONALLY-SELECTIVE, BIMODAL EFFECTS ON STRIATAL DOPAMINE KINETICS

Rashed Harun, BS; Kristin M. Hare; M. Elizabeth Brough; Miranda J. Munoz; Christine M. Grassi; Gonzalo E. Torres; Anthony A. Grace; Amy K. Wagner, MD

3.1 SUMMARY

Parkinson's disease (PD) is a debilitating condition that is caused by a relatively specific degeneration of dopaminergic (DAergic) neurons of the substantia nigra pars compacta. Levodopa (L-DOPA) was introduced as a viable treatment option for PD over 40 years ago and still remains the most common and effective therapy for PD. Though the effects of L-DOPA to augment striatal DA production are well known, little is actually known about how L-DOPA alters the kinetics of DA neurotransmission that contribute to its beneficial and adverse effects. In this study, we examined the effects of L-DOPA administration (50mg/kg carbidopa + 0, 100, and 250mg/kg L-DOPA) on regional electrically stimulated DA response kinetics using fast-scan cyclic voltammetry (FSCV) in anesthetized rats. We demonstrate that L-DOPA enhances DA release in both the dorsal striatum (D-STR) and nucleus accumbens (NAc), but surprisingly causes a delayed inhibition of release in the D-STR. In both regions, L-DOPA progressively attenuated reuptake kinetics, predominantly through a decrease in Vmax. These findings have important implications

on understanding the pharmacodynamics of L-DOPA, which can be informative for understand its therapeutic effects and also common side effects like L-DOPA induced dyskinesias (LID).

3.2 INTRODUCTION

Parkinson's Disease (PD) is the second most common neurodegenerative disease, and much research has been focused upon its pathophysiology and symptomology, yet there is still neither a cure nor an effective strategy to slow disease progression. PD associated pathology is linked to selective dopamine (DA) system neuronal fiber loss from projections originating in the substantia nigra *pars compacta* (SNpc) whose terminals innervate the dorsal striatum (D-STR) (McRitchie *et al.* 1997). Although several DAergic agents have been introduced (Camicioli *et al.* 2001, Guttman 1997), and have beneficial effects in PD, L-DOPA still remains the most common and effective therapy. Nevertheless, this drug has limitations, primarily motor complications that follow long-term use, which may be related to chronic dysregulation of the DA transporter (DAT) (Thanvi & Lo 2004, Troiano *et al.* 2009).

L-DOPA is the synthetic precursor to DA, but the specifics of how L-DOPA administration affects presynaptic DA neurotransmission is not fully understood. Many DAergic agents like DAT inhibitors not only have a primary specific target (e.g. DAT) but also have secondary effects on DA release, DA receptor sensitivity, and DAT trafficking (Harun *et al.* 2014, Saunders *et al.* 2000, Volz et al. 2008, Venton et al. 2006, Wagner et al. 2009a). Due to DAT density and neurochemical differences across striatal regions, DAergic agents can have markedly different actions on striatal sub-regions (Stamford *et al.* 1991, Harun et al. 2014, Ciliax et al. 1995, Jones et al. 1995b). In midbrain neuronal cultures, L-DOPA selectively increases intracellular DA 2-3X higher in SNc

vs. ventral tegmental area neurons (Mosharov *et al.* 2009). Also, L-DOPA can alter the kinetics of vesicle fusion events *in vitro* (Amatore *et al.* 2005, Sombers *et al.* 2004), but how these findings influence regional *in vivo* DA kinetics is not understood. Recent work using amperometry demonstrated that, in addition to the known effects of L-DOPA on enhancing release, L-DOPA could also inhibit DA reuptake (Rodriguez *et al.* 2007b), which has not been demonstrated in previous characterizations of the effects of L-DOPA on striatal DA neurotransmission using fast-scan cyclic voltammetry (FSCV) (Peters & Michael 2000, Wightman et al. 1988).

In this report, we examined how two doses of L-DOPA administration (100mg/kg and 250mg/kg) affects electrically stimulated DA neurotransmission kinetics using FSCV in rats, where FSCV DA signals represent a balance of DA release/reuptake that are amenable to kinetic analysis (Wightman & Zimmerman 1990). Recently, we have incorporated neurobiological components of attenuating release, attenuating reuptake efficiency, and post-stimulation DA release into a quantitative neurobiological (QN) framework that can be used for kinetic analysis of stimulated DA responses. We have shown initial evidence that this analytic approach effectively characterizes regional differences and pharmacologically induced changes in stimulated DA responses (Harun *et al.* 2014). Using this framework, we demonstrated regiospecific and dose-dependent effects of L-DOPA on stimulated DA release in the D-STR and NAc. As the synthetic precursor to DA, L-DOPA dose-dependently enhanced stimulated release, but importantly, L-DOPA also paradoxically inhibited release, especially in the context of the high 250mg/kg L-DOPA challenge in the D-STR. These release inhibitory effects of L-DOPA maybe due to an attenuation of the effective size of the readily releasable pool (RRP) of DA synaptic vesicles by the high dose of L-DOPA, as suggested by the faster stimulation-induced decay of DA release rate. Most importantly, we demonstrated that L-DOPA administration caused a progressive, dose-

dependent attenuation of reuptake efficiency in both the NAc and D-STR, primarily by a decrease in the maximal reuptake rate (Vmax) and also by an increase in the Michaelis-Menten constant (Km) with the high-dose L-DOPA challenge. These reuptake inhibitory effects of L-DOPA may represent a major mechanism by which the agent enhances DA neurotransmission clinically. These dose and time-dependent changes in DA neurotransmission kinetics may be important to consider when using L-DOPA for PD treatment, for which dose titration and optimization is crucial to managing symptoms and side-effects effectively.

3.3 METHODS

Animals and surgical procedure:

The animal experiments were approved by the Institutional Animal Care and Use Committee of the University of Pittsburgh. Fifteen young-adult male Sprague-Dawley rats (Hilltop Laboratories, Scottsdale, PA, USA) weighing between 350-375g were used for this study. Prior to study procedures, all animals had access to rat chow and water ad libitum. Animals were transported to our surgical laboratory, anesthetized with urethane (1.3g/kg, i.p.) for consistent long-term anesthesia, and mounted onto a stereotactic frame. Core body temperatures were maintained at 37°C with a homeothermic blanket. For stereotaxic placement of electrodes in the brain, a midline incision was made, soft-tissues reflected, and burr holes were drilled into the right parietal and frontal bones, after which dura was removed. Three groups of animals were used to demonstrate the dose-dependent regiospecific effects of L-DOPA that differed in acute pharmacological manipulation. All drugs were freshly prepared in .1M phosphate buffer solution (pH=7.2). The control group (n=4) was administered 50mg/kg of carbidopa (Matrix Scientific,

Columbia, SC) intraperitoneally (i.p.) followed by PBS (3mL/kg i.p.). The two experimental groups received 50mg/kg administrations of carbidopa, but also were administered a 100mg/kg (n=5) or a 250mg/kg (n=6) dose of L-3-(3,4-dihydroxyphenyl)alanine (L-DOPA) (Acros Organics, NJ).

Fast-scan cyclic voltammetry:

Carbon fiber microelectrodes (7µm in diameter and 250µm long) were fabricated as previously described (Wagner *et al.* 2005b, Harun et al. 2014). Prior to use, electrodes were electrochemically pretreated by applying a 70Hz biphasic potential waveform to the electrodes for 2s from 0 to 2 to 0 V vs. an Ag/AgCl reference electrode to enhance electrode sensitivity. Two recording microelectrodes were simultaneously inserted using flat skull coordinates (in mm) into the D-STR [anterioposterior (AP) +1.7, mediolateral (ML): 1.4, and dorsoventral (DV): -3.4] and into the NAc [AP: 1.0, ML: 2.1, and DV:-6.6] (Paxinos & Watson 2007). A reference electrode was placed in contact with proximal soft muscle tissue to create a salt bridge. A bipolar stimulating electrode (MS301-1, Plastics One, Roanoke, VA) was inserted over the median forebrain bundle (MFB) [AP: -4.0, ML: 1.6, DV: -7.2].

Biphasic 60Hz, 5s (280µA amplitude and 2ms pulse width) electrical stimulations were used to evoke DA overflow in the striatum. Regional DA responses were detected using carbon fiber microelectrodes to which a triphasic cyclic voltage waveform (0→1→-0.5→0V) was applied a rate of 300V/s every 100ms using the TarHeel CV software (ESA, Chelmsford, MA). The stimulating electrode was lowered 200µm every 5 min until a clear DA signal was observed, and then lowered 100µm every 10 min, until the signal amplitudes of the two electrodes peaked. Experimental DA responses were then collected using alternating 60Hz, 5s and 2s stimulations, waiting 15 and 10 minutes after stimulations, respectively (**Fig 9**). Carbidopa (Matrix Scientific,

Columbia, SC) and L-3-(3,4-dihydroxyphenyl)alanine (L-DOPA) (Acros Organics, NJ) solutions in 0.1M phosphate buffered solutions were freshly prepared. Carbidopa was administered (50mg/kg i.p.) immediately following the first two stable baseline responses, and L-DOPA (100 or 250mg/kg) or PBS (3mL/kg) was administered following the collection of the two post-carbidopa responses. DA response collection resumed until 75min post-L-DOPA administration (**Fig 1**). Responses were converted from currents to DA concentrations ([DA]) following electrode explantation and *in vitro* microelectrode calibration using seven standard DA concentration solutions in artificial cerebrospinal fluid (pH=7.2) composed of (in mM): 1.2 $CaCl_2$, 2.0 Na_2HPO_4, 1.0 $MgCl_2$, 2.7 KCl, 145 NaCl.

Interpretation of DA responses

DA response shape analysis

DA response shape analysis was performed using two morphometric methods: decay behavior and response amplitudes. Response amplitude is simply the peak [DA] of a response. Decay behavior was examined similar to previous studies (Moquin & Michael 2009, Jones et al. 1995b), where responses were time-shifted to match similar amplitudes in the decay phase to directly evaluate differences in decay behavior (see **Fig 10A** insert). The decay behavior was quantified by fitting an exponential regression to the 3s following the time point where curves were aligned. This approach yields a decay constant (k) that corresponds to the decay behavior, with larger k-values corresponding to faster decay kinetics.

Quantitative neurobiological model

To estimate how L-DOPA administration affected release and reuptake kinetics, 60Hz, 5s DA responses were modeled using our quantitative neurobiological (QN) model (Harun et al. 2014). Traditionally, stimulated DA responses can be interpreted using the Michaelis-Menten (M-

M) model (Wightman & Zimmerman 1990), which assumes a constant DA release rate, and DA reuptake rate through DAT that is modeled using M-M enzyme kinetics defined by constant Vmax and Km terms. The QN model is a refinement of the M-M model that accounts for stimulation effects on DA responses by including equations to describe stimulation-induced attenuated DA release, attenuated DA reuptake efficiency (increasing Km), and incorporation of a biphasic post-stimulation DA release component.

Table 7: Equations and parameters utilized in L-DOPA simulations

DA release rate (during stimulation):		
$\boldsymbol{DAR_{stim}(t) = \Delta DAR * e^{-t_{stim}/\Delta DAR\tau} + DAR_{SS}}$ **(Equation 1)**	ΔDAR	DA release rate undergoing decay
	$\Delta DAR\tau$	Exponential decay constant of release
	DAR_{ss}	Steady-state DA release rate
DA release rate (post-stimulation):		
$\boldsymbol{DAR_{post}(t_{post}) = X_R * DAR_{ES} * e^{-\frac{t_{post}}{\tau_R}} + (1 - X_R) * DAR_{ES} - m * t_{post}}$ **(Equation 2)**	X_R	Rapid release fractional component
	DAR_{ES}	DA release rate at end of stimulation
	τ_R	Exponential decay time constant of rapid release component
	m	Linear decay slope of prolonged release component
DA reuptake rate:		
$\boldsymbol{ReuptakeRate(t) = \frac{V_{max}}{\frac{K_m(t)}{[DA]} + 1}}$	V_{max}	Maximal reuptake rate
	$K_m(t)$	M-M constant (an inverse measure of efficiency)
where, $\boldsymbol{K_m(t) = K_{m_i} + \Delta K_m \left(1 - \frac{1}{1 + \frac{t}{K_{m\,inf}}^{k}}\right)}$ **(Equation 3)**	K_{m_i}	Initial K_m
	ΔK	Magnitude of change in K_m dynamics
	$K_{m_{inf}}$	Time of inflection of K_m dynamics
	k	Measure of the steepness of the inflection in K_m dynamics

The equations and terms that the QN model utilizes to describe the release and reuptake components of stimulated DA responses are reproduced in **Table 7**. Briefly, DA release rate during stimulation (DAR_{stim}) is described by **equation 1** as an exponential decay function with a time constant of $\Delta DAR\tau$ and a steady-state release rate (DAR_{ss}). This parameterization of stimulated DA release rate is adopted from studies characterizing how stimulation trains exponentially decrease the rate of neurotransmitter release (i.e. pulse-train depression (PTD)) (Pyott & Rosenmund 2002). The PTD of neurotransmitter release is associated with stimulation frequency and ambient temperature. When these factors are held constant, they can reflect the effective size of the readily-releasable pool (RRP) of vesicles, with faster stimulation induced decay of release associated with a smaller size of the RRP (Pyott & Rosenmund 2002, Dobrunz & Stevens 1997). Post-stimulation DA release rate (DAR_{post}) is described in **equation 2** as release rate that decreases bi-phasically after stimulation ends, with rapid exponential and prolonged linear decay components. The biphasic nature of post-stimulation DA release has been described previously (Atluri & Regehr 1998) and is likely related to the biphasic kinetics of intracellular Ca^{2+} clearance after stimulation (Fierro et al. 1998), which mediates neurotransmitter release through different Ca^{2+}-sensitive proteins (Groffen et al. 2010, Yao et al. 2011). Lastly, reuptake kinetics was modeled similar to the M-M model, except Km here is defined as a dynamic term that increases during stimulation according to the logistic function in **equation 3.** We incorporated the concept of stimulation-induced increases in Km to account for how stimulation frequency and duration attenuate the apparent reuptake kinetics that others and we have observed (Wang et al. 2011, Harun et al. 2014). How stimulation attenuates reuptake efficiency is not clearly understood, but it could be due to stimulation-induced depletion of energy stored in Na^{+}-gradients that are necessary for DA reuptake through DAT. The effects of stimulation on energy depletion may be particularly relevant to the

stimulation-induced attenuation of reuptake efficiency concept because DAergic neurons are in a delicate energy balance state owing to their dense axonal arborizations and lack of myelination (Pissadaki & Bolam 2013).

The equations in **table 7** were combined into **equation 4**, which was used to model experimental DA responses in Matlab R2014a (The MathWorks, Inc, Natick, MA). Because multiple sets of parameterizations are able to simulate the same experimental DA response well, we performed simulations systematically across studies to minimize artifacts of simulation methods by constraining initial Km (Km_i) between 0.1-0.4μM, which is similar to the Km assumed in other voltammetry studies and to Km parameters extracted from *in vitro* studies (Wu et al. 2001, Povlock *et al.* 1996). Moreover, we included 60Hz, 2s stimulations into the experimental protocol for internal validation that parameterizations for 5s DA responses were consistent with DA decay behavior in 2s DA responses. Since our initial inception of the QN model, we have since updated the framework to assume the rapid post-stimulation has a time constant (τ_R) that increases with increasing stimulation duration, which may occur due to greater calcium accumulation by increased stimulation-duration to prolong post-stimulation DA release. Although these adaptations provide larger estimates of release and reuptake metrics than previously reported (Harun et al. 2015), in our experience, they have enhanced the fit of simulations to experimental data. Moreover, these adaptations furthers our goal of developing systematic rational means of constraining parameters to enhance the accuracy of the simulations to model underlying release and reuptake processes.

$$[DA](t) = \int \left(DAR_{stim}(t) + DAR_{post}\left(t_{post}\right) \right) dt - \int \frac{V_{max}}{\frac{K_m(t)}{[DA]} + 1} dt$$

Equation 4

The simulations provide estimates of DA release and reuptake rates over the time course of single DA responses that are consistent with the assumptions of the model (see **Fig 11B**). We examined four metrics that are particularly relevant to characterizing the effect of L-DOPA on DA neurotransmission- 1) the initial DA release rate (DAR_i), which may be related to the physiological effects of L-DOPA on DA release, 2) the $\Delta DAR\tau$, which, as described above, could have implications on changes in the effective size of the RRP, 3) V_{max}, which is often related to the local density of DAT and also their efficiency for DA reuptake, and 4) Km_i, which is the M-M constant that is inversely related to DAT efficiency.

Statistical analysis

All response metrics (e.g. amplitudes, Vmax, DAR_i and others) were analyzed statistically in similar ways using SPSS 2.0 for Mac (SPSS Inc., Chicago, IL). Baseline differences between regions were evaluated using an independent samples Student's T-Test. Time dependent changes in L-DOPA induced effects were evaluated using repeated measures analysis of variance (rmANOVA). Two-factor rmANOVA was used to separately probe for dose and regional differences in the time course of L-DOPA effects. Follow up independent samples descriptive comparisons were performed using Fisher's least significant difference, while post-hoc within group comparisons over time were assessed using paired-T-tests. P-values ≤ 0.05 were considered to be significant in all comparisons.

3.4 RESULTS

In this report, we aimed to elucidate the basic mechanisms by which L-DOPA affects presynaptic DA neurotransmission kinetics in the D-STR and NAc using the MFB stimulated DA response paradigm. As there may be differential effects of L-DOPA by dose, we assessed the effects of 100mg/kg and 250mg/kg L-DOPA challenges. We stimulated the MFB-containing DAergic pathways with 60Hz, 5s stimulations to elicit robust DA responses amenable for kinetic analysis, which was performed using response shape analysis methods and by modeling DA responses using the QN method (Harun et al. 2014). Since multiple stimulation durations aid in validating the accuracy of the QN simulations, 60Hz, 2s stimulations were performed between 5s stimulations to aid with simulations, but kinetic parameters from the 60Hz, 2s responses were not directly used in our analyses (**Fig 9**).

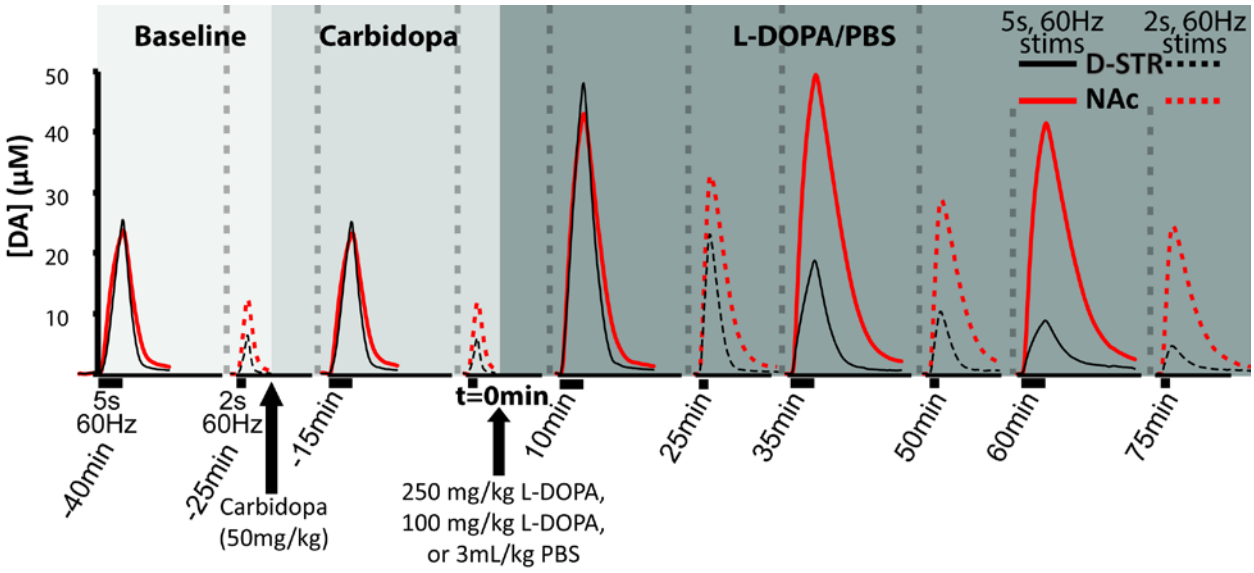

Figure 9: Timecourse of L-DOPA experiments

Mean regional DA responses obtained in the high dose L-DOPA challenge group are represented for demonstrative purposes. Responses were simultaneously detected in the D-STR (black traces) and the NAc (red traces). Only the 60Hz,5s responses (solid lines) were used for analysis, while the intermittent 60Hz, 2s responses (dashed lines) were used as internal validation of the accuracy of simulations performed on 60Hz,5s data.

3.4.1 L-DOPA-induced dose-dependent changes in stimulated DA response shapes

Prior to L-DOPA administration, rats were administered 50mg/kg (i.p.) of carbidopa to inhibit the peripheral metabolism of L-DOPA. However, Jonkers *et al.* (2001) demonstrated that carbidopa itself can act centrally as well to inhibit aromatic amino acid decarboxylase activity (AADC), which converts L-DOPA into DA in DAergic neurons (Jonkers *et al.* 2001). As such, we examined the effects of carbidopa over the experimental time course, where in lieu of L-DOPA, PBS vehicle (3mL/kg) was administered 25min following 50mg/kg carbidopa.

Both the high-dose (250mg/kg) and low dose (100mg/kg) of L-DOPA had clear effects on the decay phase of DA responses and response amplitudes in both regions, which were particularly apparent using the high dose of L-DOPA (**Fig 10 A/B**). First, we examined the decay phase of DA responses, which primarily reflects the clearance of DA that is mediated by reuptake through DAT (Budygin et al. 2002), but may also be confounded by post-stimulation DA release (Harun *et al.* 2014). We time shifted all 5s DA responses from individual recording sites to compare the exponential decay rates (k) of DA disappearance pre- and post-pharmacological manipulation (see inset in **Fig 10A/B**), where higher k values are indicative of faster DA clearance.

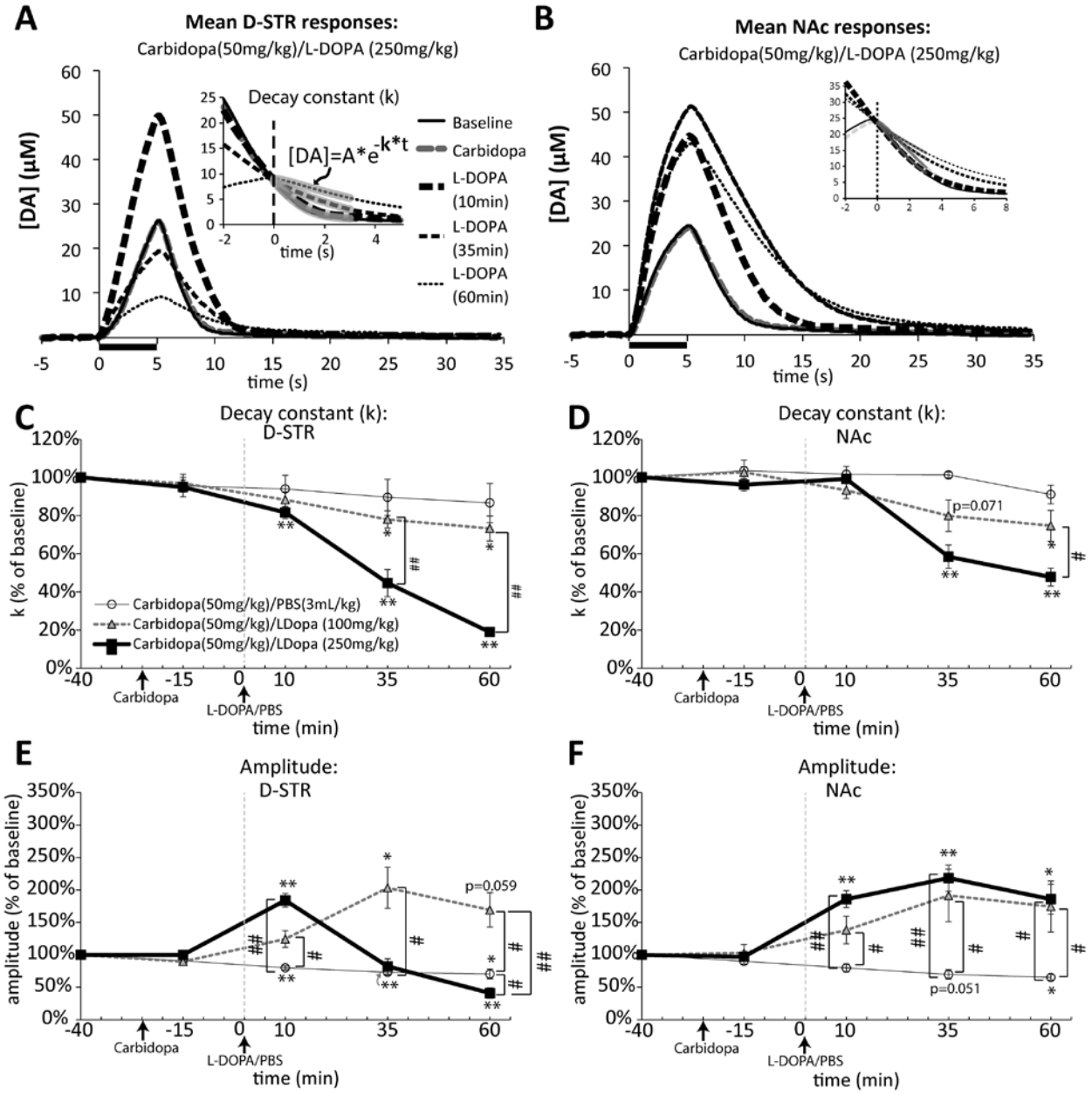

Figure 10: Changes in DA response shapes in the context of carbidopa/L-DOPA administration

Mean 5s baseline, carbidopa, and post-L-DOPA responses in the D-STR (A) and NAc (B) demonstrate effects of L-DOPA on DA responses shapes in terms of response amplitudes and the slopes of the decay phases. The insets in (A,B) demonstrate how DA responses were time shifted to obtain the exponential decay constant (k). k progressively decreased over time in the D-STR (C) and the NAc (D), with the higher dose leading to faster decreases k (rmANOVA: $p<0.005$ and $p<0.05$, respectively). E) L-DOPA caused dose dependent changes in response amplitudes ($p<0.005$), with the high dose causing significant increases in amplitude at 10min (↑83.8 ±10.0%, $p<0.005$) and significant decreases at 60min(↓58.9 ±8.0%, $p<0.005$), which contrasted from the delayed increase observed with the low dose (↑103.2 ±31.6%). F) L-DOPA caused similar increases in amplitude over time between the high ($p<0.005$) and low dose ($p<0.080$) groups. *$p<0.05$, **$p<0.005$ compared to baseline and #$p<0.05$, ##$p<0.005$ for denoted comparisons

We noted that animals treated with carbidopa/PBS tended to decrease k over time ($p=0.075$) (**Fig 10C/D**); however, these effects were small, with an overall 11.2±6.4% decrease ($p=0.141$) by 60min post-PBS administration (i.e. 85min post-carbidopa administration). A general progressive decrease in k over time was observed in all experimental groups in all regions, but k decreased over time differentially between groups, with significant differences apparent between the high-dose L-DOPA group and the carbidopa/PBS group ($p<0.005$ in the D-STR, and $p<0.05$ in the NAc). Although, k significantly decreased over time in the low dose L-DOPA group ($p<0.05$ for both regions), this effect did not reach significance when compared to the effects of carbidopa/PBS itself in either region.

L-DOPA administration caused dose-dependent decreases in k in the D-STR ($p<0.05$) and in the NAc ($p<0.05$), with the higher dose producing faster decreases in k. By 35min and 60min post-L-DOPA administration, k was significantly decreased following high dose L-DOPA compared to low-dose L-DOPA in the D-STR ($p<0.005$ for both comparisons) and in the NAc at 60min ($p<0.05$). We also observed a regional difference in the effect of L-DOPA on temporal k effects, whereby the high dose of L-DOPA decreased k faster over time in the D-STR compared to the NAc ($p<0.005$). By 60min post-L-DOPA administration, k decreased by 81.0±2.2% in the DL-STR vs. 52.2±4.7% in the NAc ($p<0.005$). As DAT is the primary mechanism of DA clearance after stimulated release, the dose, time, and region-dependent decreases in k strongly indicate that L-DOPA inhibits DAT activity.

We next examined how response amplitudes were affected over time in the experimental groups. Response amplitudes represent a balance of release minus reuptake, which dynamically change over the course of stimulated DA responses (Harun et al. 2015). Consistent with the idea that carbidopa itself inhibits DA synthesis (Jonkers et al. 2001), response amplitudes significantly

decreased over time in the carbidopa/PBS group similarly in both the D-STR and NAc ($p<0.005$ for both regions) (**Fig 10 E/F**). By 60min post-PBS administration, there was an overall 32.0±4.8% reduction in response amplitudes relative to baseline. Unpublished work in our lab suggests that a higher 100mg/kg dose of carbidopa produced even more marked inhibition of response amplitudes (>50%).

Because L-DOPA should enhance DA synthesis, it may be predicted to enhance DA release and augment response amplitudes. In the NAc, there was a significant dose ($p<0.05$), time ($p<0.005$), and dose*time interaction ($p<0.05$) on how response amplitudes were affected in the different experimental groups. Response amplitudes in the L-DOPA groups were significantly different over time compared the carbidopa/PBS group ($p<0.05$ for the both L-DOPA doses). Both doses of L-DOPA resulted in significant increases in response amplitude in the NAc at all post-L-DOPA time points compared to corresponding times in the carbidopa/PBS group (**Fig 10F**).

L-DOPA produced significant time-dependent changes in response amplitudes in the D-STR ($p<0.005$) as well, which significantly differed by dose ($p<0.05$) (**Fig 10E**). The low dose of L-DOPA enhanced response amplitudes relative to the carbidopa/PBS controls at all time points post-L-DOPA/PBS administration ($p<0.05$ for all time point comparisons). In contrast, the high dose of L-DOPA initially enhanced amplitude 10min post-L-DOPA administration (83.8±10.5% ↑ relative to baseline, $p<0.005$), which decreased drastically over the experimental time course. Surprisingly, by 60min, the D-STR amplitude *decreased* by 58.9±8.0% ($p<0.005$) relative to baseline by 60min post-L-DOPA administration. This marked attenuation of amplitude was a significantly greater than the 29.3±7.5% inhibition observed 60min post-PBS in the carbidopa/PBS challenge group ($p<0.05$).

The delayed attenuation of response amplitude in the D-STR caused by the high dose of L-DOPA was very paradoxical considering that L-DOPA is thought to enhance DA neurotransmission. The progressive impairment of DA reuptake inferred from the analysis of response decay behavior would be predicted to enhance response amplitude, but the concomitant decrease in D-STR amplitude after a delay following the high dose L-DOPA challenge suggests that L-DOPA causes profound impairments in D-STR DA release.

3.4.2 QN modeling of experimental DA responses demonstrate the effects of L-DOPA on DA release and reuptake dynamics

The application of the QN framework was used to generate simulations of the 60H, 5s experimental data as demonstrated in the representative set of D-STR responses from the carbidopa(50mg/kg)/L-DOPA (250mg/kg) group (**Fig 11A**). Overall, the fit of simulations on all experimental data resulted in a mean R^2= 0.9956±0.0003. The simulations provided estimates of release and reuptake rates over the course of the stimulated DA response that fit the assumptions of the model, which can be visualized as in **Fig 11B**. Moreover, simulation parameters were extracted to provide estimates of initial release rate (DAR_i), stimulation-induced attenuation of release described by the time constant $\Delta DAR\tau$, maximal clearance rate (Vmax), and initial Km (Km_i), all of which can contribute to the kinetics of presynaptic DA release and reuptake.

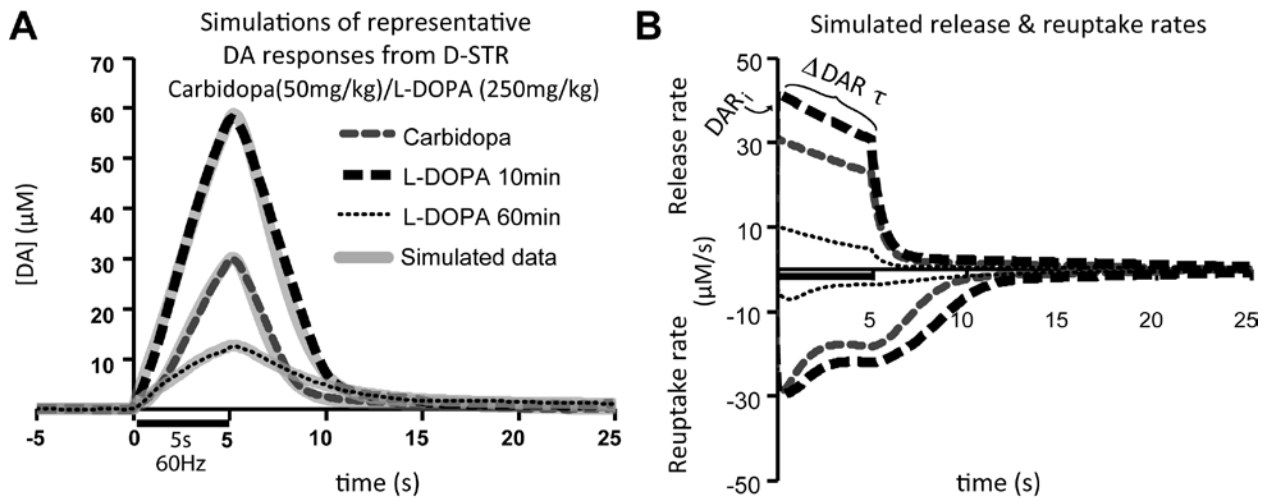

Figure 11: Representative simulations of DA responses

A) Experimental DA responses obtained from a representative D-STR (dashed lines) and their corresponding simulations (solid gray lines) demonstrates that the QN model can fit experimental data remarkably well- in this case, R^2=0.9996. B) Simulated release and reuptake rates that produced the simulations in (A) are plotted to demonstrate the dynamics of release and reuptake over the course of stimulations.

3.4.3 L-DOPA has biphasic effects on DA release and inhibitory effects on apparent RRP size

Using the QN model, we first examined how L-DOPA affected DA release by specifically examining the initial rate of DA release (DARi). DAR_i may be affected by various factors like the size of the readily releasable pool (RRP), the number of fibers being stimulated, or the local density of terminals. Interestingly, we found that DAR_i was significantly higher in the D-STR compared to the NAc (27.8±2.4 vs. 16.0 ±2.0, respectively, $p<0.005$) (**Fig 12A**). DAR_i progressively decreased in the carbidopa/PBS group similarly between regions (**Fig 12B/C**), resulting in an overall 27.0 ±4.6% decrease relative to baseline by 60min post-PBS administration ($p<0.005$). This finding is consistent with the idea that carbidopa inhibits DA synthesis (Jonkers et al. 2001).

L-DOPA produced dose-dependent changes in DAR_i in the D-STR ($p<0.005$). Interestingly, the effects of the low dose of L-DOPA on DAR_i were very small and did not reach significance

(p=0.177) despite significant effects of the low L-DOPA dose on response amplitudes which are a balance of release and reuptake (see above). In contrast, the high dose of L-DOPA tended to increase DAR_i in the D-STR at 10min (29.1 ±12.0% increase relative to baseline, p=0.073), which was significantly different from the 13.2±4.2% decrease in DAR_i 10min post-PBS administration ($p<0.05$). Thereafter, the high dose L-DOPA caused a marked reduction of DAR_i at 35 and 60min by 46.1±6.8% ($p<0.005$) and 72.3±2.5% ($p<0.005$), respectively, which was significantly greater than the decreases observed post-PBS administration at 10 and 60min ($p<0.05$ and $p<0.005$, respectively). This profound inhibition of DAR_i in the D-STR with the high dose L-DOPA challenge corroborates with the expected release inhibition predicted from the basic characterization of response amplitudes and decay rates.

L-DOPA had a significant effect on DAR_i in the NAc over time when compared to the carbidopa/PBS group ($p<0.005$) and a trend was noted between low dose and carbidopa/PBS group (p=0.096) (**Fig 12C**). Similar to the D-STR, the low dose of L-DOPA did not significantly increase DAR_i above baseline in the NAc, but DAR_i was significantly enhanced at 35min post L-DOPA administration compared to the slight decreases observed 35min post-PBS ($p<0.05$). The high dose challenge significantly enhanced DAR_i at both 10 and 35min post-L-DOPA (increases of 36.9 ±8.0%, $p<0.05$ and 30.8 ±10.1%, $p<0.05$, respectively). In contrast to the D-STR, DAR_i did not decrease below baseline following the high dose L-DOPA challenge in the NAc. These findings suggest that L-DOPA differentially affects DA release between regions, and surprisingly, the 100mg/kg L-DOPA had very modest apparent effects on DA release rate.

The QN framework accounts for DA release with an exponentially decreasing function with the time constant $\Delta DAR\tau$ to model the hypothesized depletion of the RRP by electrical stimulation. $\Delta DAR\tau$ can provide valuable information about the size of the readily releasable pool, where a

longer ΔDARτ may corroborate with a larger RRP size (Pyott & Rosenmund 2002). Interestingly, we found significant regional differences in ΔDARτ, where the ΔDARτ was longer in the D-STR compared to the NAc (21.6±1.2s vs. 11.3±1.5s, $p<0.005$, respectively) (**Fig 12D**), suggesting that the RRP size may be larger in the D-STR and may also contribute to the greater DAR_i in the D-STR noted above.

ΔDARτ was not significantly affected by carbidopa administration in either region (**Fig 12E/F**). Both doses of L-DOPA progressively decreased ΔDARτ in the D-STR, with the higher dose leading to faster decreases in ΔDARτ. At 60min post-L-DOPA administration, ΔDARτ values were significantly different between the high dose vs. the low dose challenge (20.1±3.5% vs. 69.2±10.3% of baseline, respectively, $p<0.005$) (**Fig 12E**). Similar changes in ΔDARτ were observed in the NAc, except that low dose L-DOPA did not have a significant effect on ΔDARτ over time ($p=0.137$), while the high dose did ($p<0.005$) (**Fig 12F**). 60min post-L-DOPA administration, ΔDARτ values were significantly different between the high dose vs. the low dose challenge (20.1±3.5% vs. 69.2±10.3% of baseline, respectively, $p<0.005$). This analysis of how ΔDARτ changes following L-DOPA administration suggests that L-DOPA may effectively be reducing the amount of vesicles available for stimulated release (i.e. decreasing the size of the RRP), particularly in the D-STR or when using a high dose.

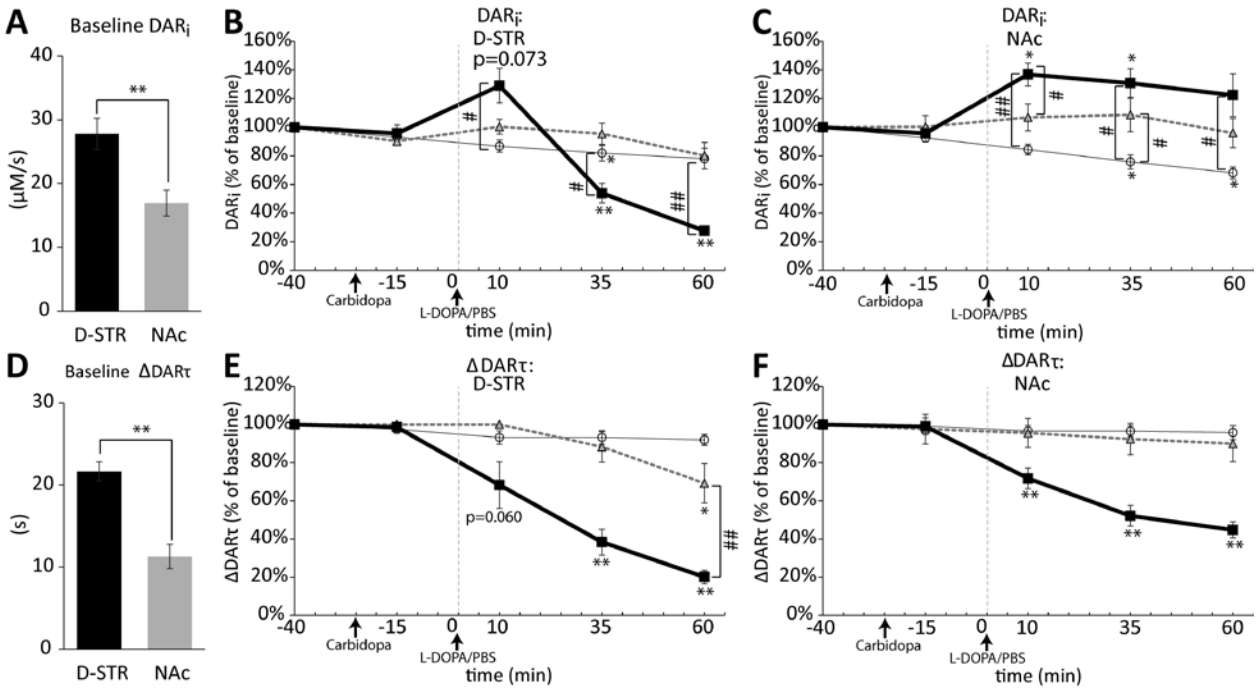

Figure 12: Effects of carbidopa and L-DOPA on DA release simulation metrics

A) Baseline DAR_i was significantly higher in the D-STR compared to the NAc (27.8±2.4 vs. 16.0 ±2.0, respectively, $p<0.005$). B) L-DOPA had non-significant effects on DAR_i in the D-STR at the low dose, while the high dose tended to cause an initial enhancement at 10min but significant reductions at 35 and 60min ($p<0.005$ for both comparisons). C) L-DOPA caused a significant enhancement of DAR_i at 10min and 35min at the high dose in the NAc, while the low dose did not have a significant effect. D) ΔDARτ was significantly higher in the D-STR compared to the NAc (21.6±1.2s vs. 11.3±1.5s, $p<0.005$, respectively). E) L-DOPA caused a progressive dose-dependent decrease in ΔDARτ in the D-STR, where the high dose produced faster decreases in ΔDARτ. F) Although ΔDARτ was not decreased by the low dose L-DOPA challenge, the high dose progressively decreased ΔDARτ over time. *$p<0.05$, **$p<0.005$ compared to baseline and #$p<0.05$, ##$p<0.005$ for denoted comparisons

3.4.4 L-DOPA inhibits DA reuptake through changes in V_{max} and K_m

Analyzing k-values above demonstrated that both doses of L-DOPA significantly prolonged the decay phase of stimulated DA responses in both regions, highly suggesting that L-DOPA inhibits DAT activity. Quantitative simulations can further clarify whether changes in reuptake could be attributed to changes in Km, which is inversely related to the efficiency of DAT, or to Vmax, which reflect both the efficiency of DAT and surface expression of functional DAT.

Simulations revealed that baseline Vmax was higher in the D-STR relative to the NAc (35.9 ± 1.4 vs. 20.2 ± 0.9 µM/s, $p<0.005$) (**Fig13 A**), which is consistent with the known higher DAT density and faster DA reuptake kinetics in the D-STR compared to the NAc (Ciliax et al. 1995, Harun et al. 2014, Jones et al. 1995a). Small decreases in Vmax were noted in the carbidopa/PBS group over time ($p<0.05$). Interestingly, both doses of L-DOPA led to robust, progressive, and dose-dependent decreases in Vmax in both regions, with higher doses causing faster decreases in Vmax. All time points post-L-DOPA administration at both doses and both regions had significantly decreased Vmax values compared to baseline (**Fig13 B/C**). The reductions in Vmax were also significantly greater compared to carbidopa/PBS effects with both doses in both regions except for in the 10min time point in the D-STR. These robust changes in Vmax suggest that L-DOPA can rapidly cause a dose-dependent inhibition of DAT activity in both regions.

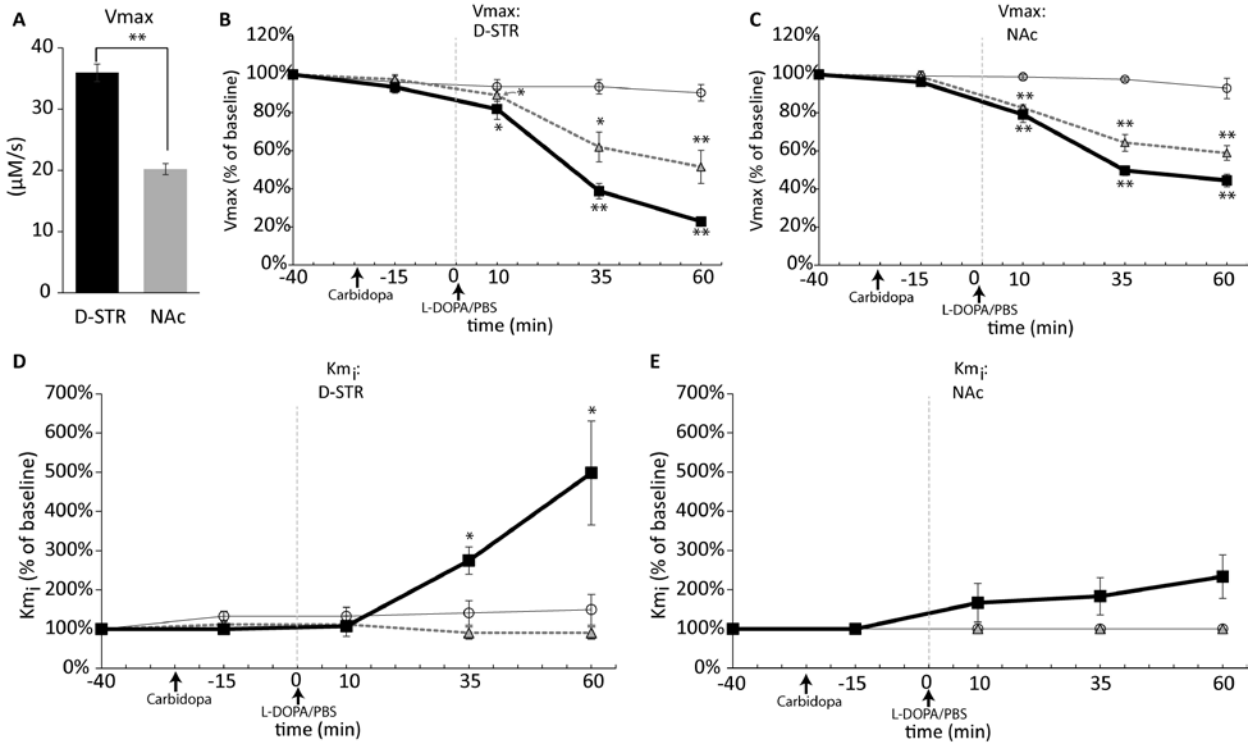

Figure 13: Effects of carbidopa and L-DOPA on DA reuptake simulation metrics

A) Vmax was significantly greater in the D-STR compared to the NAc (35.9 ± 1.4 vs. 20.2 ± 0.9 µM/s, $p<0.005$). B/C) L-DOPA dose-dependently decreased Vmax in the D-STR (B) and NAc (C). D/E) Km_i increased significantly

in the D-STR (D) and tended to increase over time in the NAc (p=0.086) following the high dose challenge, while the low-dose did not have an appreciable effect on Km_i. *p<0.05, **p<0.005 compared to baseline

In our QN model, we modeled Km as a variable term to model increases over the course of stimulation due to a stimulation-induced diminution of Na^+ electrochemical gradients that are necessary for DA reuptake. As Km changes induced by stimulation are relatively large compared to estimated physiological Km values, it is difficult to extrapolate to initial Km values (Kmi) through the modeling approach. Nevertheless, we attempted to circumvent this problem by constraining baseline Km_I values between Km_i=0.1 and 0.4μM as described in the methods. Using this approach, we examined if it was necessary to change Km_i to model subsequent DA responses after pharmacological manipulation. This method revealed that the Km_i increased over time in the D-STR following the high dose of L-DOPA (p<0.05), while Km_i tended to increase as well in response to the high dose L-DOPA challenge in the NAc (p=0.086). (**Fig13 D/E**) The L-DOPA induced increases in Km_i suggest that L-DOPA inhibits DAT efficiency; however, it is also possible that L-DOPA increases extracellular DA concentrations, which may increase the apparent Kmi values through competitive inhibition of DAT. When taken together, the increases in Kmi along with the decreases in Vmax presented above, indicate that L-DOPA inhibits DA reuptake.

3.5 DISCUSSION

Monitoring stimulated DA responses with FSCV is an effective means to elucidate mechanisms by which pharmacological agents alter DA neurotransmission. We demonstrated that L-DOPA has regionally selective effects on striatal DA neurotransmission, which could be related to the inherent regional differences in baseline DA release and reuptake kinetics demonstrated in this

report and elsewhere (Jones *et al*. 1995a, Stamford *et al.* 1988). Consistent with previous observations, both the 100 and 250mg/kg L-DOPA enhanced DA release in both the D-STR and NAc 10min after administration, but surprisingly, 250mg/kg L-DOPA caused a marked delayed inhibition of DA release in the D-STR. Moreover, L-DOPA attenuated DA reuptake kinetics in both regions by progressively and dose-dependently decreasing Vmax and also by increasing in Km with the high L-DOPA dose (250mg/kg).

The relative impact of L-DOPA-induced release inhibition in clinically relevant doses of L-DOPA in the context of disease is a matter that requires further investigation, but a recent study demonstrated that even a modest 30mg/kg dose of L-DOPA resulted in a profound inhibition of DA response amplitudes using a sustained stimulated release paradigm in a transgenic mouse model of PD (Yavich *et al.* 2004). The mechanism underlying the inhibitory effects of L-DOPA on DA release that we demonstrated in this report are unknown, but the finding may be related to the physical changes in synaptic vesicles that occur after L-DOPA administration. Recent studies have demonstrated that L-DOPA increases the volume of synaptic vesicles, which is associated with alterations in vesicle fusion dynamics that are necessary for DA release (Sombers et al. 2004, Amatore et al. 2005). It is plausible that as synaptic vesicles accumulate DA and expand following L-DOPA administration, increased tensile forces oppose the full fusion of synaptic vesicles with the plasma membrane to inhibit DA release. Overfilled synaptic vesicles may underlie the observed gradual inhibition of DA release and dose-dependent changes in the effective size of the readily releasable pool following L-DOPA. In line with the concept that DA overfills synaptic vesicles to inhibit DA release, we found release inhibition was more pronounced in the D-STR, where we would predict greater intracellular [DA] following L-DOPA administration (Mosharov *et al*. 2009).

Over-filling of synaptic vesicles is one possible mechanism of L-DOPA-induced release inhibition, but it is conceivable that there are homeostatic mechanisms to down regulate DA release in response to L-DOPA administration. There are various neurochemical differences between the D-STR and NAc that may contribute to regional differences in DA release regulation by L-DOPA such as regional differences in Ca^{2+}-coupling, cholinergic regulation, and autoregulation by D2-like autoreceptors (Stamford et al. 1991, Wu et al. 2002, Brimblecombe *et al.* 2015, Zhang *et al.* 2009, Maina & Mathews 2010). For instance, L-DOPA may augment extracellular DA levels to inhibit DA release through the activation of D2 DA autoreceptors. Although, this form of homeostatic regulation of release seems to be important in physiological contexts (Benoit-Marand *et al.* 2001), our experience suggests that D2 agonists like quinpirole do not have strong release inhibitory effects in the context of supraphysiological stimulations used in these studies (data not shown). Paradoxically, we even found release to be enhanced by D2 autoreceptor activation as reported elsewhere (Kita *et al.* 2007). Thus, if L-DOPA causes homeostatic changes to inhibit DA release, it likely involves other mediators besides D2 autoreceptors.

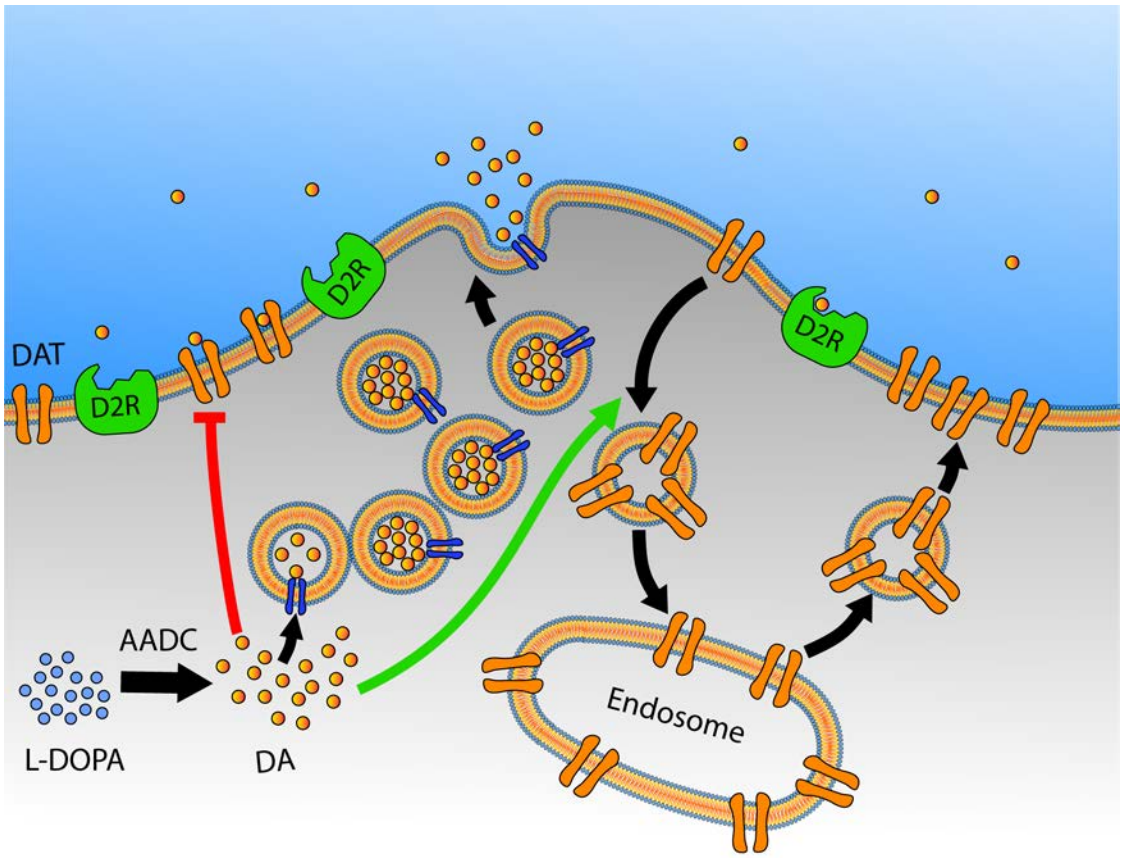

Figure 14: Conceptual schematic of presynaptic DA neurotransmission regulation by L-DOPA

L-DOPA is converted to DA in DAergic neurons, which can be sequestered into synaptic vesicles to alter DA release. Additionally, intracellular DA may inhibit DA reuptake by a functional inhibition of DAT and by a down-regulation of DAT surface expression as well.

In addition to the effects on DA release, we demonstrated that L-DOPA progressively attenuated DA reuptake kinetics (↓Vmax and ↑Km), with more marked effects in the D-STR compared to the NAc. Similarly, some studies demonstrated that repeated application of exogenous DA inhibited *in vivo* DA clearance more profoundly in the D-STR compared to the NAc (Gulley *et al.* 2002), and brief DA exposure inhibited ^{3}[H]DA uptake to a greater extent in synaptosomes from the D-STR compared to the NAc (Richards & Zahniser 2009). The uptake inhibitory effect of DA may be partly caused by a down-regulation of DAT surface expression, which involves PKC activation (Gorentla & Vaughan 2005, Gulley *et al.* 2002). Notably,

exogenous DA application decreases DAT surface expression, even in *xenopus* oocytes that do not express DA receptors (Gulley *et al.* 2002), suggesting that intracellular DA may mediate DAT down-regulation directly as demonstrated for amphetamine (Kahlig *et al.* 2006). These findings suggest that L-DOPA may elevate intracellular [DA], which could subsequently down-regulate DAT surface expression as illustrated in the conceptual **figure 14**.

While in vitro studies using heterologous expression systems and striatal synaptosomes suggest DAT surface expression can be altered by pharmacological manipulation (Johnson *et al.* 2005, Furman *et al.* 2009b, Saunders et al. 2000), some recent reports that suggest that DAT trafficking is not a prominent phenomenon observed with intact neuronal systems (Block *et al.* 2015, German *et al.* 2012), and thus, functional changes in DAT may be a major contributor to L-DOPA associated kinetic changes in DA clearance. In contrast, other *in vivo* studies demonstrate that acute high doses of L-DOPA significantly decrease striatal DAT binding in rodents, suggesting that L-DOPA induces DAT internalization (Scheffel *et al.* 1996, Dresel *et al.* 1998). Moreover, these reports also demonstrated that acute administration of the DA synthesis inhibitor α-methyl-p-tyrosine decreases DAT binding as well, perhaps as a compensatory response to decreased extracellular DA levels. These latter studies suggest that *in vivo* DAT surface expression may be manipulable by certain DAergic agents, including L-DOPA, and contribute to the changes in Vmax noted in our study.

Our data also suggests that DAT efficiency is impaired based on the Km increases in both regions following high-dose L-DOPA administration. Functionally, DAT is regulated by multiple potential mechanisms including phosphorylation, post-translational modification, and protein-protein interactions (Vaughan & Foster 2013, Garcia-Olivares *et al.* 2013, Lee *et al.* 2007, Gnegy 2003), but how L-DOPA inhibits DAT function is also currently unknown. L-DOPA could activate

PKC similar to DA and amphetamine (Gorentla & Vaughan 2005, Gulley *et al*. 2002), a signaling mechanism that not only down-regulates DAT surface expression, but also inhibits DAT function (Foster *et al.* 2008). Alternatively, L-DOPA could increase intracellular [DA], causing a thermodynamic inhibition of DAT function (Harun *et al.* 2014, Metzger *et al.* 2002) (**Figure 14**). Intracellular DA could also form reactive oxygen species, which are known to inhibit DAT function (Fleckenstein *et al.* 1997, Berman *et al.* 1996). Clearly, future studies will be pivotal for identifying the specific molecular changes underlying the observed effects of L-DOPA on DA release and reuptake kinetics.

The characterization of the effects of L-DOPA in this report utilized the use of 100mg/kg and 250mg/kg doses, which is similar to previous FSCV studies that examined the effects of L-DOPA at 200-250mg/kg doses (Peters & Michael 2000, Wightman & Zimmerman 1990). Although these doses seem very high, doses of L-DOPA that were less than 100mg/kg have been shown to have insignificant effects on extracellular [DA] in naïve rats (Rodriguez et al. 2007b). Additional FSCV studies using 25 and 75mg/kg L-DOPA did not appreciable affect response amplitudes (data not shown). Moreover, our analysis suggested that even the 100mg/kg dose of L-DOPA had very small effects on release (DAR_i) that did not reach significance compared to the carbidopa group in the D-STR. Although L-DOPA doses <100mg/kg have been reported to have therapeutic effects in Parkinson's models, where L-DOPA is noted to have large effects on DA neurotransmission (Rodriguez et al. 2007b, Yavich et al. 2004), we needed to perform our analysis using doses ≥100mg/kg in the naïve rats in order to observe significant effects of L-DOPA on DA neurotransmission. Thus, whether the observed results translate to the therapeutic actions of L-DOPA remains to be determined.

Although we examined the acute effects of L-DOPA, these effects may relate to long-term changes in the DAergic system with chronic L-DOPA therapy. Several SPECT imaging studies reported that chronic L-DOPA treatment decreases striatal DAT binding in PD subjects (Guttman *et al.* 2001, Parkinson Study 2002, Whone *et al.* 2003), which we suggest could be due to the repeated acute effects of L-DOPA on DAT down-regulation that we suggest here. Though chronic DAT down-regulation can enhance presynaptic DA neurotransmission and contribute to improved function observed in PD patients on L-DOPA therapy (Fahn *et al.* 2004), DAT down-regulation is also associated with L-DOPA induced dyskinesias (Troiano *et al.* 2009). Aside from down-regulating DAT, L-DOPA may additionally induce dyskinesia through ectopic DA release from serotonergic terminals in the striatum that lack DA autoreceptors to regulate DA release (Carta *et al.* 2007). The amount of ectopic DA release in the striatum after L-DOPA administration is expected to be limited compared to normal DA release through DAergic fibers in naïve animals because of the sparse serotonergic innervation of the striatum (Zhou *et al.* 2005); however, serotonergic fibers have been shown to hyper-innervate the striatum in the setting of PD and may significantly alter the pharmacodynamic response to L-DOPA (Gagnon *et al.* 2015, Gaspar *et al.* 1993, Bedard *et al.* 2011) and contribute to the increased susceptibility to L-DOPA-induced dyskinesias following DAergic denervation of the striatum (Di Monte *et al.* 2000).

In contrast to the chronic effects of L-DOPA on DAT regulation, very little is known about the chronic effects of L-DOPA on DA release, which can be elucidated in future FSCV studies. Moreover, both chronic and acute L-DOPA administration are known to affect DA neuronal firing patterns that should be considered in the context of the acute effects of L-DOPA on DA release and reuptake that we report here to understand the effects of L-DOPA on behavior (Harden & Grace 1995).

Using *in vivo* FSCV and the QN model, we demonstrated that L-DOPA has differential dose-dependent effects on DA release and reuptake in the D-STR vs. the NAc, which illustrates that the specific neurochemical environment greatly influences the effects of L-DOPA. Also, differences in neurochemistry may exist between individuals due to common variations in genes that regulate DA neurotransmission, as several reports suggest that polymorphisms in the DAT, DRD2, and brain-derived neurotrophic factor (BDNF) genes significantly influence the development of L-DOPA induced dyskinesias (Kaiser *et al.* 2003, Oliveri *et al.* 1999, Strong *et al.* 2006, Wang *et al.* 2001, Zappia *et al.* 2005, Foltynie *et al.* 2009). Furthermore, adjuvant treatments with other DAergic agents like D2 agonists are common in PD subjects, and they produce long-lasting changes in the DAergic system as well (Parkinson Study 2002, Marek *et al.* 2002, Ahlskog *et al.* 1999). Although L-DOPA is mostly utilized in the context of PD, it has beneficial effects in in other conditions like traumatic brain injury (Crownover 2012, Lal *et al.* 1988, Krimchansky *et al.* 2004, Haig & Ruess 1990), which has its own patterns of neurochemical alterations and genetic influences on DA neurotransmission (Wagner *et al.* 2014, Wagner et al. 2005b, Wagner et al. 2009a, Wagner et al. 2009b, Bales *et al.* 2009, Massucci *et al.* 2004, Shin *et al.* 2011, Failla *et al.* In Press). The specific region, pathology, genetic influences, and drug interactions are all important contributors to understanding how even the same agent differentially affects DA neurotransmission between individuals and in different regions of the same individual. Although this report describes general attributes of the acute effects of L-DOPA on DA release and reuptake kinetics in naïve rats, future FSCV studies combined with the QN model interpretive framework can serve to clarify the relative impact of various factors on how they modulate baseline DA neurotransmission and subsequent drug-induced effects.

4.0 CONTROLLED-CORTICAL IMPACT PRODUCES REGIOSPECIFIC DYSFUNCTION OF STIMULATED DA NEUROTRANSMISSION IN THE DORSAL STRIATUM THAT CAN BE REVERSED WITH CHRONIC METHYLPHENIDATE TREATMMENT

Rashed Harun, BS; Miranda J. Munoz; Kristin M. Hare;

M. Elizabeth Brough, Amy K. Wagner, MD

4.1 SUMMARY

Dysfunction in the dopaminergic (DAergic) system is common following traumatic brain injury (TBI), which may underlie many aspects of cognitive and behavioral impairments following TBI. Although the DAergic system has widespread projections throughout the cortex and basal ganglia to modulate diverse functions throughout the brain, little is known about the regiosepcificity of DAergic dysfunction following brain injury. We used FSCV to examine the effects of CCI on electrically stimulated DA responses in the dorsal striatum (D-STR) and nucleus accumbens (NAc). By performing simultaneous recordings in both regions, a majority of naïve rats exhibited simultaneous responses in both regions, but only 1/9 rats exhibited non-responses in the DL-STR. In contrast, 7/8 CCI rats exhibited non-responses in the DL-STR on day 15 post-CCI, indicative of severe dysfunction with DA neurotransmission in the DL-STR after CCI. Post-CCI treatment with chronic daily MPH (5mg/kg) for 2wks exerted robust neurorestorative effects leading to the observation of stimulated DA responses in 6/7 animals with response amplitudes that tended to be 74.9±37.2% higher

than naïve controls. Using our recently developed quantitative neurobiological (QN) theoretical framework to discern and characterize release and reuptake components from stimulated DA responses, we demonstrated that CCI tends to impair the amount of stimulated DA released during 60Hz, 10s stimulations in the NAc, while chronic MPH tended to restore this impairment with DA release. In the D-STR, post-CCI chronic MPH treatment not only restored estimates of initial DA release rate and DA released during stimulation, but actually exceeded naïve estimates by 42.9±14.3% ($p<0.05$) and 45.0±13.8% ($p<0.01$), respectively. This work suggests that there are widespread striatal impairments of DA neurotransmission after CCI, while certain regions like the D-STR appear to be more susceptible to injury-induced deficits. Notably, this work may have important relevance to the associations between TBI and Parkinson's disease, for which the D-STR is known to be particularly susceptible to degeneration.

4.2 INTRODUCTION

Traumatic brain injury (TBI) affects over 1.5 million individuals in the U.S. each year, with over 5 million suffering from chronic disability related to TBI (Langlois *et al*. 2006). TBI often produces cognitive and behavioral impairments that are among the most challenging symptoms to treat. However, indirect and direct dopamine (DA) agonists can be very effective for treating TBI-induced cognitive impairments, which suggest the involvement of the DAergic system in TBI pathophysiology. Various clinical and preclinical studies have demonstrated that brain injury can cause chronic alterations in the DAergic system. We have previously demonstrated that there are chronic impairments in electrically stimulated DA neurotransmission in the dorsomedial striatum

using the controlled cortical impact (CCI) model of moderate TBI in rats (Wagner et al. 2005b, Wagner et al. 2009a, Wagner et al. 2009b), with deficits observed in DA release, clearance, and responsivity to an acute challenge of the DAT inhibitor/psychostimulant methylphenidate (MPH). Several laboratories have observed changes in tissue DA content and alterations of tyrosine hydroxylase expression, phosphorylation, and activity that vary by time, regional brain location, and injury model (McIntosh *et al.* 1994, Massucci et al. 2004, Kobori *et al.* 2006, Shin et al. 2011, Yan *et al.* 2007). In contrast, other markers of the DAergic system like striatal vesicular monoamine transporters (VMAT-2) remain relatively stable, suggesting that there is limited degeneration in brain injury (Wagner et al. 2009a). However, one of the most consistent findings has been the observed decrease in DA transporter (DAT) levels in both preclinical TBI models (Wagner *et al.* 2005a, Wagner et al. 2009a, Wilson *et al.* 2005, Yan *et al.* 2002) and in clinical cases of TBI (Wagner et al. 2014, Donnemiller *et al.* 2000). These decreases in DAT following brain injury may reflect a homeostatic down-regulation of DAT to compensate for the functional hypodopaminergic state caused by brain injury.

Although brain injury often produces a hypodopaminergic state, little is known about how TBI differs from other conditions like Parkinson's disease (PD), which is characterized by the loss of DAergic neurons in the substantia nigra pars compacta (SNpc) (Fearnley & Lees 1991, McRitchie et al. 1997) and the degeneration of corresponding terminals in the dorsal striatal (D-STR) regions (Kish *et al.* 1988) with a relative sparing of ventral tegmental area DAergic neurons and ventral striatal regions like the nucleus accumbens (NAc). Some epidemiological studies support an association between prior head injury and PD (Bower *et al.* 2003, De Michele *et al.* 1996, Seidler *et al.* 1996, Taylor *et al.* 1999), with one study in twins showing the relative risk of developing PD nearly quadruples with a prior history of head injury (Goldman *et al.* 2006).

Nevertheless, a few studies have not identified any significant association between head injury and PD development (Williams *et al.* 1991, McCann *et al.* 1998, Werneck & Alvarenga 1999), which makes this relationship still controversial even today (Wong & Hazrati 2013). Two recent preclinical studies have shown that mild and moderate fluid percussion injury (FPI) are both capable of producing progressive degeneration of DAergic neurons in the SNpc, which further suggests a link between TBI and the development of PD (Hutson *et al.* 2011, van Bregt *et al.* 2012).

It is important to identify potential therapies that may mitigate PD-like DA neurodegeneration following brain injury. Interestingly, several studies in preclinical PD models demonstrate dysfunctional DA neurotransmission precedes actual neuronal loss and terminal degeneration (Janezic et al. 2013, Lam *et al.* 2011), suggesting that restoring functional deficits serve as a potential avenue to halt the progression of neurodegeneration. We have previously shown that chronic daily MPH treatment MPH (5mg/kg) has robust neurorestorative effects following CCI, which enhances stimulated DA release, clearance, and restores the responsivity to an acute MPH challenge (Wagner et al. 2009a, Wagner et al. 2009b). In this study, we used fast-scan cyclic voltammetry (FSCV) to demonstrate that CCI produces regional dysfunction with electrically stimulated DA neurotransmission the D-STR, with a relative sparing of the NAc, similar to the pattern of neurodegeneration in PD. Moreover, we demonstrate that chronic daily treatment with MPH (5mg/kg) for two weeks after CCI can restore stimulated DA neurotransmission in both regions. As stimulated DA responses reflect the complex interplay between DA release and reuptake processes that are dynamically changing over the course of a stimulated DA response, we recently developed a quantitative neurobiological (QN) framework, based on modern neurotransmission principles, to discern release from reuptake processes that

contribute to the overall stimulated DA response shapes observed (Harun et al. 2015). Using this methodology we demonstrate that the neurorestorative effects of MPH following CCI involves both enhancement of release and reuptake processes.

This work not only has implications for supporting a link between brain injury and PD, but it also suggests that MPH therapy can not only diminish TBI related symptoms and deficits, but also, mitigate DA-related pathophysiology after brain injury. These findings have very strong translational potential for individuals with clinical TBI. Future studies are needed to examine if MPH therapy produces *lasting* neurorestorative effects, the most appropriate time window for introduction of MPH therapy, and the histological changes that maybe associated with the restorative DA transmission effects of chronic MPH therapy.

4.3 METHODS

Animals:

Twenty-four (24) young-adult male Sprague Dawley rats (Hilltop Laboratories, Scottsdale, PA, USA) weighing between 325-350g were used for this study in accordance to the University of Pittsburgh's Institutional Animal Care and Use Committee. Rats were housed in a 12 h light-dark cycle, with food and water provided *ad libitum* for at least 1 week prior any surgical procedures. Animals were separated into one of three groups, naïve animals that received .1M phosphate buffered saline (PBS) (1ml/kg) chronically for 14 days (Naïve+PBS) (n=9), or CCI animals that received PBS (n=7) or MPH (5mg/kg) (n=8) daily starting the day after CCI (CCI+PBS and CCI+MPH, respectively).

Controlled cortical impact (CCI) injury

The CCI injury device (Pittsburgh Precision Instruments, Inc., Pittsburgh, PA, USA) used for this study has been described previously (Dixon et al. 1991). Under isoflurane anesthesia (4% isoflurane and a 2:1 N_2/O_2 initially, followed by 1–1.5% isoflurane), animals were placed in a stereotaxic frame. Core body temperature was maintained at 37°C during surgery using a homeothermic blanket (Harvard Apparatus, Edenbridge, UK). A midline scalp incision was made and the soft tissues reflected to perform a craniotomy over the right parietal cortex between lambda and bregma and approximately 2 mm lateral to the central suture. The exposed dura was struck to a depth of 2.8 mm with an impact velocity of 4 m/s by the CCI device as previously described (Wagner *et al.* 2005a,b, 2007a,b, 2009). The scalp was sutured, 2% lidocaine jelly was applied to the incision, and post-injury righting reflexes were monitored after completion of surgical procedures. Animals were returned to their home cages after recovery with ad libitum access to food and water.

Fast-scan cyclic voltammetry (FSCV):

Naïve or CCI animals 15d post-injury (i.e. the day after the last PBS/MPH administration) were anesthetized with urethane (1.3g/kg, i.p.), and mounted onto a stereotactic frame. Core body temperatures were maintained at 37°C with a homeothermic blanket. For stereotaxic placement of electrodes in the brain, a midline incision was made, soft-tissues reflected, and burr holes were drilled into the right parietal and frontal bones, after which dura was removed. Carbon fiber microelectrodes (7µm in diameter and 250µm long) were fabricated as previously described (Wagner et al. 2005b, Harun et al. 2014). Prior to use, electrodes were electrochemically pretreated by applying a 70Hz biphasic potential waveform to the electrodes for 2s from 0 to 2 to 0 V vs. an Ag/AgCl reference electrode to enhance electrode sensitivity. Two recording microelectrodes were simultaneously inserted using flat skull coordinates (in mm) into the D-STR [anterioposterior (AP)

+1.7, mediolateral (ML): 1.4, and dorsoventral (DV): -3.4] and into the NAc [AP: 1.0, ML: 2.1, and DV:-6.6] (Paxinos & Watson 2007). A reference electrode was placed in contact with proximal soft muscle tissue to create a salt bridge. A bipolar stimulating electrode (MS301-1, Plastics One, Roanoke, VA) was inserted over the median forebrain bundle (MFB) [AP: -4.0, ML: 1.6, DV: -7.2].

Biphasic 60Hz, 5s or 10s (280µA amplitude and 2ms pulse width) electrical stimulations were used to evoke DA overflow in the right striatum. Regional DA responses were detected using carbon fiber microelectrodes to which a triphasic cyclic voltage waveform (0→1→-0.5→0V) was applied a rate of 300V/s every 100ms using the TarHeel CV software (ESA, Chelmsford, MA). The stimulating electrode was lowered 200µm every 5 min until a clear DA signal was observed, and then lowered 100µm every 10 min, until the signal amplitudes of the two electrodes peaked. For analysis purposes, experimental DA responses were then collected using 60Hz, 10s stimulations. Subsequently, a 40Hz, 10s and 60Hz, 5s stimulation was additionally collected to aid in performing simulations of the 60Hz, 10s DA responses. Responses were converted from currents to DA concentrations ([DA]) following electrode explantation and *in vitro* microelectrode calibration using seven standard DA concentration solutions in artificial cerebrospinal fluid (pH=7.2) composed of (in mM): 1.2 $CaCl_2$, 2.0 Na_2HPO_4, 1.0 $MgCl_2$, 2.7 KCl, 145 NaCl.

Interpretation of DA responses

DA response analysis

DA response analysis was performed using two methods, by simply examining DA responses amplitudes, determining the frequency of measurable DA responses in the two simultaneously monitored regions, and by simulating stimulated DA responses to discriminate DA

release from reuptake components according to our recently developed QN framework (Harun et al. 2015).

Quantitative neurobiological model

To estimate how CCI and CCI + chronic MPH therapy affects regional DA release and reuptake kinetics, 60Hz, 10s DA responses were modeled using the QN model (Harun et al. 2014). Traditionally, stimulated DA responses can be interpreted using the Michaelis-Menten (M-M) model (Wightman & Zimmerman 1990), which assumes a constant DA release rate, and DA reuptake rate through DAT that is modeled using M-M enzyme kinetics defined by constant Vmax and Km terms. The QN model is a refinement of the M-M model that accounts for stimulation effects on DA responses by including equations to describe stimulation-induced attenuated DA release, attenuated DA reuptake efficiency (increasing Km), and incorporation of a biphasic post-stimulation DA release component.

Table 8: Equations and parameters used for simulations

DA release rate (during stimulation):		
$\boldsymbol{DAR_{stim}(t) =}$	ΔDAR	DA release rate undergoing decay
$\boldsymbol{\Delta DAR * e^{-t_{stim}/\Delta DAR\tau} + DAR_{SS}}$ **(Equation 1)**	$\Delta DAR\tau$	Exponential decay constant of release
	DAR_{ss}	Steady-state DA release rate
DA release rate (post-stimulation):		
$\boldsymbol{DAR_{post}(t_{post}) =}$	X_R	Rapid release fractional component
$\boldsymbol{X_R * DAR_{ES} * e^{-\frac{t_{post}}{\tau_R}}}$	DAR_{ES}	DA release rate at end of stimulation
$\boldsymbol{+(1 - X_R) * DAR_{ES} - m * t_{post}}$ **(Equation 2)**	τ_R	Exponential decay time constant of rapid release component
	m	Linear decay slope of prolonged release component
DA reuptake rate:		
$\boldsymbol{ReuptakeRate(t) = \frac{V_{max}}{\frac{K_m(t)}{[DA]} + 1}}$	V_{max}	Maximal reuptake rate
	$K_m(t)$	M-M constant (an inverse measure of efficiency)
where,	K_{m_i}	Initial K_m
$\boldsymbol{K_m(t) =}$	ΔK	Magnitude of change in K_m dynamics
$\boldsymbol{K_{m_i} + \Delta K_m\left(1 - \frac{1}{1 + \frac{t}{K_{m\,inf}}^{k}}\right)}$ **(Equation 3)**	$K_{m\,inf}$	Time of inflection of K_m dynamics
	k	Measure of the steepness of the inflection in K_m dynamics

The equations and terms that the QN model utilizes to describe the release and reuptake components of stimulated DA responses are reproduced in **table 8**. Briefly, DA release rate during stimulation (DAR_{stim}) is described by **equation 1** as an exponential decay function with a time constant of $\Delta DAR\tau$ and a steady-state release rate (DAR_{ss}). This parameterization of stimulated DA release rate is adopted from studies characterizing how stimulation trains exponentially decrease the rate of neurotransmitter release (i.e. pulse-train depression (PTD)) (Pyott & Rosenmund 2002). The PTD of neurotransmitter release is associated with stimulation frequency and ambient temperature. When these factors are held constant, they can reflect the effective size of the readily-releasable pool (RRP) of vesicles, with faster stimulation induced decay of release associated with a smaller size of the RRP (Pyott & Rosenmund 2002, Dobrunz & Stevens 1997). Post-stimulation DA release rate (DAR_{post}) is described in **equation 2** as release rate that decreases bi-phasically after stimulation ends, with rapid exponential and

prolonged linear decay components. The biphasic nature of post-stimulation DA release has been described previously (Atluri & Regehr 1998) and is likely related to the biphasic kinetics of intracellular Ca^{2+} clearance after stimulation (Fierro et al. 1998), which mediates neurotransmitter release through different Ca^{2+}-sensitive proteins (Groffen et al. 2010, Yao et al. 2011). Lastly, reuptake kinetics was modeled similar to the M-M model, except Km here is defined as a dynamic term that increases during stimulation according to the logistic function in **equation 3.** We incorporated the concept of stimulation-induced increases in Km to account for how stimulation frequency and duration attenuate the apparent reuptake kinetics that others and we have observed (Wang et al. 2011, Harun et al. 2014). How stimulation attenuates reuptake efficiency is not clearly understood, but it could be due to stimulation-induced depletion of energy stored in Na^{+}-gradients that are necessary for DA reuptake through DAT. The effects of stimulation on energy depletion may be particularly relevant to the stimulation-induced attenuation of reuptake efficiency concept because DAergic neurons are in a delicate energy balance state owing to their dense axonal arborizations and lack of myelination (Pissadaki & Bolam 2013).

The equations in **table 8** were combined into **equation 4**, which was used to model experimental DA responses in Matlab R2014a (The MathWorks, Inc, Natick, MA). Because multiple sets of parameterizations are able to simulate the same experimental DA response well, we performed simulations systematically across studies to minimize artifacts of simulation methods by constraining initial Km (Km_i) between 0.1-0.4μM, which is similar to the Km assumed in other voltammetry studies and to Km parameters extracted from *in vitro* studies (Wu et al. 2001, Povlock et al. 1996). Moreover, we included a prior 60Hz, 10s stimulation and 60Hz, 2s stimulations into the experimental protocol for internal validation that for the accuracy of the fit

of simulations to the 5s DA responses. Since our initial inception of the QN model, we have since updated the framework to assume the rapid post-stimulation has a time constant (τ_R) that increases with increasing stimulation duration, which may occur due to greater calcium accumulation by increased stimulation-duration to prolong post-stimulation DA release. Although these adaptations provide larger estimates of release and reuptake metrics than previously reported (Harun et al. 2015), in our experience, they have enhanced the fit of simulations to experimental data. Moreover, these adaptations furthers our goal of developing systematic rational means of constraining parameters to enhance the accuracy of the simulations to model underlying release and reuptake processes.

$$[DA](t) = \int \left(DAR_{stim}(t) + DAR_{post}\left(t_{post}\right) \right) dt - \int \frac{V_{max}}{\frac{K_m(t)}{[DA]} + 1} dt$$

Equation 4

The simulations provide estimates of DA release and reuptake rates over the time course of single DA responses that are consistent with the assumptions of the model. We examined two metrics that are particularly relevant to characterizing the effect of CCI and MPH therapy on DA neurotransmission- 1) the initial DA release rate (DAR_i), which may be related to the physiological effects of CCI and MPH therapy on DA release and readily releaseable pool size, and 2) V_{max}, which is often related to the local density of DAT and also their efficiency for DA reuptake. Moreover, we examined the total simulated amount of DA released during the 10s of stimulation ($DA_{released}$), which may relate to amount of DA available for stimulated release in the experimental contexts.

Statistical analysis

All response metrics (e.g. amplitudes, Vmax, and others) were analyzed statistically in similar ways using SPSS 2.0 for Mac (SPSS Inc., Chicago, IL). One-way ANOVAs were used to probe for differences in between groups, significant effects were followed up with post-hoc independent samples Student's T-Test. P-values ≤ 0.05 were considered to be significant in all comparisons.

4.4 RESULTS

In this study, we electrically stimulated the MFB-containing ascending DAergic projections to monitor *in vivo* striatal DA responses simultaneously in the D-STR and the NAc to characterize CCI effects and chronic daily MPH treatment after CCI on regional stimulated DA neurotransmission. We used naïve rats that underwent a 2-week chronic treatment regimen with PBS (1mg/kg/day) (n=9), and CCI rats that underwent PBS (n=7) or chronic MPH treatment (5mg/kg/day) (n=8).

4.4.1 CCI increases the frequency of non-responses in the D-STR, while post-CCI chronic MPH therapy restores responses in the D-STR

Stimulated DA responses are subject to great deal of variability that may largely be due to the imprecision between animals with stimulating a consistent population of ascending DAergic projections traversing through the MFB. Albeit an infrequent occurrence in our hands, this imprecision may have also led to the observation of non-responses in one region while detection of simultaneous responses in the other region, even among naïve rats (**Fig 15C/F**). Nevertheless,

replication of experiments circumvents some of the inherent variability in the methodology to allow for group-based comparisons.

In the NAc, DA responses were detected in all rats in all three experimental groups, with the exception of one Naïve+PBS rat (**Fig 15C**). Although the mean DA responses are different between the Naïve+PBS, CCI+PBS, and CCI+MPH groups, there was a large degree of variability as evidenced by the overlapping standard error bars between mean group DA responses (**Fig 15A**). Thus, there were no significant differences between groups in terms of response amplitudes in the NAc (**Fig 15B**).

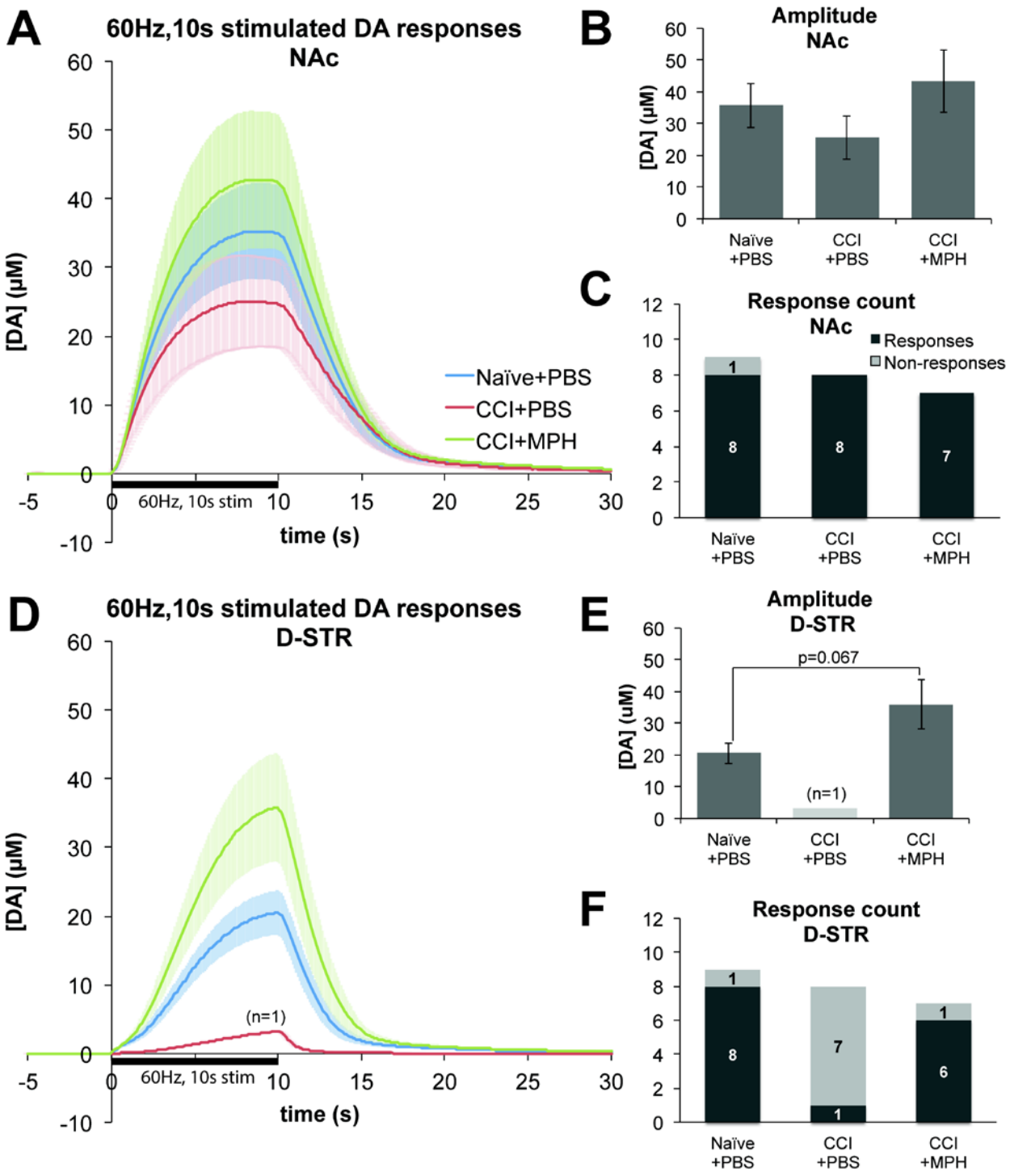

Figure 15: Regional stimulated DA responses and the frequency of their observation

A/D) Mean±SEM of 60Hz,10s stimulated DA responses of each group are represented in (A) for the NAc and (D) for the D-STR. The amplitudes did not significantly differ by group in the NAc (B), but tended to be higher in the CCI+MPH group vs. Naïve+PBS group in the D-STR (E). Responses were generally simultaneously observed in the NAc (C) and D-STR (F) of most rats except in the CCI+PBS group, where only 1/8 rats exhibited a DA response.

In contrast to the NAc, we found that were profound impairments with stimulated DA neurotransmission in the D-STR in CCI+PBS rats compared to the Naive+PBS rats, such that we only observed a response in only 1/8 CCI+PBS rats, compared to the 8/9 responses in the Naïve+PBS group (**Fig 15E**). Moreover, the 1 D-STR response in the CCI+PBS group was smaller in amplitude than any responses observed in the Naïve+PBS group (**Fig15D/E**). Because only 1 small response was observed in the D-STR of CCI+PBS animals, it precluded the ability to accurately simulate the DA response or perform statistical comparisons between the D-STR of the CCI-PBS group with the other groups.

Consistent with our previous observations (Wagner et al. 2009a, Wagner et al. 2009b), chronic MPH therapy following CCI had robust neurorestorative effects. Not only did chronic MPH treatment increase the frequency of D-STR DA responses in the CCI+MPH group to 6/7 compared to 1/8 in the CCI+PBS group, but also, response amplitudes tended to be 74.9±37.2% higher than the Naïve+PBS group (p=0.067) (**Fig 15E**).

4.4.2 Post-CCI chronic daily MPH treatment restores stimulated DA neurotransmission by enhancing DA release and reuptake

As stimulated DA responses represent a balance between DA release and reuptake processes, we used the QN framework to generate estimates of release and reuptake components that contribute to the shape of 60Hz, 10s stimulated DA responses as detailed in the methods.

Our simulations suggested there were no significant differences between groups in terms of estimated initial DA release rate (DAR_i), maximal clearance rate (Vmax), or DA released during the 10s ($DA_{released}$) (**Fig 16A-C**). Although the DAR_i and Vmax were somewhat decreased in the CCI+PBS group compared to the Naïve+PBS group, these observations were not statistically

significant (p>0.1). $DA_{released}$ tended to be 32.6±18.2% lower in the CCI+PBS group compared to the Naïve+PBS (p=0.096). Moreover, the $DA_{released}$ in the CCI+MPH group tended to be 73.4±34.2% higher compared to the CCI+PBS group (p=0.052) (**Fig 16C**). These findings suggest that there may be modest impairments in DA neurotransmission in the NAc after CCI, and chronic MPH treatments appear to have restorative effects in this region.

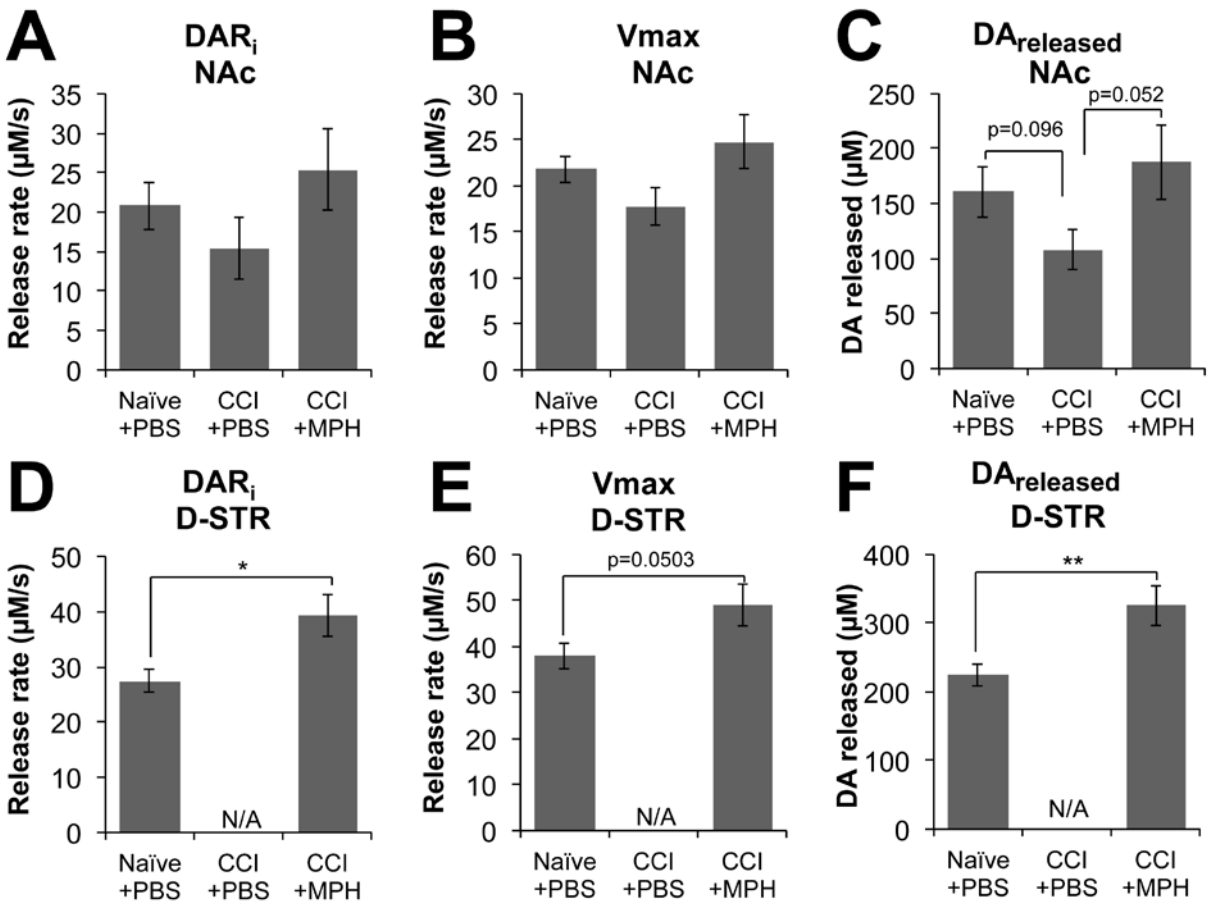

Figure 16: Simulation metrics of release and reuptake derived from experimental DA responses

Simulation metrics of release and reuptake derived from experimental 60Hz,10s stimulated DA responses. In the NAc (A-C), no significant differences were observed in DARi (A), Vmax (B), or DAreleased (C) between groups. However, DAreleased tended to be lower in the CCI+PBS group compared to both the Naïve+PBS and CCI+MPH groups. In the D-STR (D-F), we could not quantify the changes in the CCI+PBS group. However, DARi (D) and DAreleased (F) was higher in the CCI+MPH group compared to the Naïve PBS group ($p<0.05$ and $p<0.01$, respectively). Vmax also tended to be higher in the CCI+MPH group (p=0.0503). *$p<0.05$ and **$p<0.01$ for denoted comparisons

In the D-STR, although we could not quantify changes occurring in the CCI+PBS group due to the lack of responses in this region, we found notable differences between the Naïve+PBS

and CCI+MPH groups. DAR_i was significantly higher in the CCI+MPH vs. Naïve+PBS rats (39.3±3.7 vs. 27.5±2.1μM/s, respectively, $p<0.05$) (**Fig 16D**). Likewise $DA_{released}$ was also greater in the CCI+MPH rats compared to Naïve+PBS rats (325.5 ± 29.1 vs. 224.5 ± 16.1 μ M, respectively, $p<0.01$) (**Fig 16F**). Moreover, we found a tendency for Vmax to be higher the CCI+MPH group compared to Naïve+PBS group (49.1 ± 4.6 vs. 38.0 ± 2.8, respectively, $p=0.0503$) (**Fig 16E**). These findings suggest that not only does the chronic MPH (5mg/kg/day) treatment restore DA neurotransmission, but it may also enhance DA neurotransmission beyond what is observed in naïve animals.

4.5 DISCUSSION

In this report, we demonstrated that CCI produces regional DAergic dysfunction that is similar in pattern to the region-specific degeneration that occurs in PD. This pattern of neurodegeneration adds to the body of literature that supports the possible link between brain injury and subsequent development of PD (Bower et al. 2003, De Michele et al. 1996, Goldman et al. 2006, Hutson et al. 2011, Seidler et al. 1996, Taylor et al. 1999, van Bregt et al. 2012). Although, we have previously demonstrated DA neurotransmission deficits in our CCI model (Wagner et al. 2005a, Wagner et al. 2009a, Wagner et al. 2009b), this report extends previous work by demonstrating that there is a regiospecifity to the pattern of DAergic dysfunction with severe dysfunction in the D-STR and relative sparing of the NAc. As DA affects various functions like working memory, attention, motivation, and movement that are dependent upon specific brain regions that DA is acting on, regional characterization of DAergic dysfunction is important for understanding the etiology of the neuropsychiatric sequelae associated with TBI. The severe impairments of DA

neurotransmission in the D-STR may contribute to the persistent cognitive deficits, which can extend years after TBI (van Zomeren & van den Burg 1985, Oddy *et al.* 1985).

This report features several methodological advancements we have made in characterizing DAergic deficits in experimental brain injury, including the simultaneous use of two electrodes for concurrently sampling in multiple regions. Since there is inherent experimental variability in stereotaxically placing the stimulating electrode into the MFB to stimulate ascending DAergic projections, the use of two electrodes is particularly advantageous in serving as a method to ascertain that the MFB is being stimulated when responses are observed in one region and not the other. Previously, non-responses in the dorsal striatal regions could be dismissed as being due to inaccurate placement of the stimulating electrode rather than the nature of DAergic dysfunction in our CCI model. This methodology demonstrates that non-responses in the D-STR are much more frequent following moderate CCI. This same methodology may be used in future FSCV studies to examine striatal dopamine function with different experimental injury models, and it can even be implemented for characterizing DAergic dysfunction in animal models of PD, including with recent attempts to model susceptibility to PD post-TBI (refs)(Sauerbeck *et al.* 2012, Hutson et al. 2011, Zou H. 2010). Similar to the effects of MPH in CCI, this could be used to identify potential neurorestorative agents in PD.

Using our recently developed QN framework (Harun et al. 2015), we have demonstrated that MPH treatment not only restores the frequency of response observations in the D-STR following CCI, but it even enhances stimulated DA release in the CCI+MPH group greater than in the Naïve+PBS group. Moreover, Vmax tended to be higher in the CCI+MPH group as well ($p=0.0503$). Although the traditional Michaelis-Menten model of stimulated DA neurotransmission has been applied widely in the FSCV field to interpret stimulated DA responses

(May & Wightman 1989, Wightman & Zimmerman 1990), the simplicity of the model's assumptions precludes its application to the study of D-STR DA responses, which significantly differ in response shape from the NAc (**Fig 15A/D**). In contrast, the QN framework incorporates contemporary principles of stimulated DA neurotransmission that can be used to model heterogeneous stimulated DA response shapes observed throughout the striatum, including the D-STR, in order to provide estimates of DA release and reuptake rates and parameters to describe the heterogeneous release and reuptake processes that occur in in different striatal regions. As the we demonstrate here that the D-STR is particularly vulnerable to damage after brain injury and with PD (Kish et al. 1988), we demonstrate that the QN framework represents significant advancement that allows for quantitative evaluation and comparative assessment of stimulated DA neurotransmission in context of these pathological conditions.

Similar to this report, we have previously demonstrated that CCI impairs striatal DA neurotransmission and that post-CCI chronic daily MPH treatment can have robust neurorestorative effects on DA neurotransmission (Wagner et al. 2009a, Wagner et al. 2009b). However, we did not know about the regiospecific nature of the DAergic dysfunction or the generalizability of the restorative effects of MPH, which this report elucidates on. The mechanisms underlying the effects of MPH are still unknown, but may related to its effects on altering synaptic vesicle distribution and properties as demonstrated previously (Sandoval et al. 2002, Volz et al. 2008). MPH may exert its effects by altering the expression of various genes (Adriani *et al.* 2006). The simple effect of pharmacologically enhancing DA neurotransmission may itself entrain DAergic neurons to restore its function. In this way, the restorative effects of MPH may also extend to other indirect and direct DA agonists that should be explored. Along these lines, clinical reports have demonstrated functional restorative effects of various DAergic agents following head injury

such as amphetamine (Hornstein *et al.* 1996), amantadine (Zafonte *et al.* 1998, Meythaler *et al.* 2002, Whyte *et al.* 2005, Wu & Garmel 2005, Giacino *et al.* 2012), bromocriptine (Passler & Riggs 2001, Powell *et al.* 1996), and L-DOPA ((Haig & Ruess 1990, van Woerkom *et al.* 1982). Moreover, some DAergic agents have not only been shown to improve cognitive and behavioral function (Kline *et al.* 2004), but also restore DAergic dysfunction (Tan *et al.* 2015, Huang *et al.* 2014), and even enhance neuronal survival (Kline et al. 2004, Wang *et al.* 2014) in experimental TBI models.

Although we have demonstrated that MPH treatments can have neurorestorative effects on stimulated DA neurotransmission following CCI, we do not know if there is a particular therapeutic window for MPH to exert its restorative effects or whether these effects are long lasting. Previous groups have demonstrated that experimental brain injury can produce progressive degeneration of DAergic neurons (Hutson et al. 2011, van Bregt et al. 2012), suggesting that early intervention maybe more promising than late intervention. However, it is unclear whether chronic MPH therapy has an impact on DA neuronal loss, or whether the effects of chronic MPH are purely functional. Although this work highlights a potential neurorestorative therapy following brain injury that has a strong translational potential, further investigation is required to clarify the mechanism underlying this effect.

5.0 SEX AND OVARIAN HORMONES INFLUENCE STRIATAL DOPAMINERGIC FUNCTION FOLLOWING EXPERIMENTAL BRAIN INJURY

Rashed Harun, BS; Kristin M. Hare;

M. Elizabeth Brough; Amy K. Wagner, MD

5.1 SUMMARY

Traumatic brain injury (TBI) often produces cognitive and behavioral deficits that partly relate to post-traumatic dysfunction in dopaminergic (DAergic) systems that maybe secondary to the development of post-traumatic hypogonadism. Fast-scan cyclic voltammetry was used to characterize how sex and ovariectomy (OVX) affects DA neurotransmission in our controlled-cortical impact (CCI) model of moderate TBI in Sprague Dawley rats. We found that baseline striatal DA responses to 60Hz, 2s electrical stimulations were similar in amplitude between naïve male and female rats, but were increased in naïve OVX, CCI males, and CCI females ($p<0.05$ for all comparisons). These changes paralleled the decreased estimates of maximal clearance rate (Vmax), and decreased responsivity to an acute challenge of the DA transporter (DAT) inhibitor, methylphenidate (MPH) (10mg/kg, i.p.). We noted sex-based differences in the pharmacology of MPH, where the male groups had the closest association between Vmax and MPH responsivity and the shortest onset and duration of DA reuptake inhibitory effects of MPH. This work suggests that both CCI and OVX may down-regulate DAT function, which maybe a compensatory response

to impaired DA neurotransmission. This work supports that hypothesis that decreased circulating ovarian hormones could contribute to the development of post-traumatic DAergic dysfunction.

5.2 INTRODUCTION

Traumatic brain injury (TBI) is a leading cause of death and disability in the US (Langlois et al. 2006). Although TBI afflicts each individual differently depending on the location, severity, and type of injury, various factors like age, sex, and genetic make-up affect TBI prognosis (Farace & Alves 2000a, Failla *et al.* 2013, Chiang *et al.* 2003, Hukkelhoven *et al.* 2003, Davis & Cunningham 1984, Ono *et al.* 2001), some of which are sex specific (Wagner *et al.* 2007, Myrga (In Revision)). Understanding how various clinical factors affect TBI pathology can enhance individualized treatment strategies.

Many studies report sex-based differences in functional outcomes after TBI, with some investigations demonstrating that women fare worse than men (Kraus *et al.* 2000, Kirkness *et al.* 2004, Edna & Cappelen 1987, Farace & Alves 2000b), and this relationship varies by age (Davis *et al.* 2006). In a large study of 1425 subjects with mild TBI, women were more likely than men to have post-concussive symptoms three months after injury. Notably, this effect was observed primarily during childbearing ages (Bazarian *et al.* 2010). Similarly, female high school/college athletes were over 1.7 times more likely than men to be cognitively impaired following concussion (Broshek *et al.* 2005). These findings suggest that female sex hormones may affect outcomes and cognition after TBI. Indeed, hypogonadism occurs in up to 80% of patients after significant TBI, which is long-lasting in many (Behan *et al.* 2008, Wagner *et al.* 2012, Barton (in revision)). Moreover, cortisol associated luteinizing hormone suppression (Ranganathan (in review)) also

amenorrhea (Ranganathan (in review)) commonly occurs following TBI, with longer durations of amenorrhea related to worse global outcomes, health-related quality of life, and community participation measures (Ripley *et al.* 2008). These lines of evidence suggest that the sudden decline of female sex hormones, like estradiol, after TBI may exacerbate the neuropsychiatric sequelae experienced after injury. How a sudden reduction in female sex hormones relates to specific post-TBI impairments is unknown, but one intriguing hypothesis is that the drop in estradiol exacerbates dopaminergic dysfunction to a greater extent in women than men.

The DAergic system underlies functions like attention, motivation, working memory, and information processing speed, which are commonly impaired following TBI (van Zomeren & van den Burg 1985, Oddy et al. 1985) and improved by pharmacological enhancement of DA neurotransmission (Powell et al. 1996, McDowell *et al.* 1998, Patrick *et al.* 2003, Speech *et al.* 1993, Plenger *et al.* 1996, Moein *et al.* 2006, Gualtieri & Evans 1988). Moreover, both preclinical and clinical studies have demonstrated DAergic system dysfunction after TBI (Kobori et al. 2006, Massucci et al. 2004, Shin et al. 2011, Wagner et al. 2009a), including a consistent down-regulation of the DA transporter (DAT) that likely reflects a compensatory response to impaired DA neurotransmission (Donnemiller et al. 2000, Wagner et al. 2005a, Wagner et al. 2009a, Wagner et al. 2014).

There are sex-based differences in the DAergic system, notably in DAT and D2 receptor levels and affinity (Pohjalainen *et al.* 1998, Rivest *et al.* 1995) that may contribute to the varied sensitivity to dopaminergic agents between men and women. Sex hormones, of which estradiol has been the most studied, has a prominent role in mediating sexually dimorphic characteristics of the DAergic system. Estradiol has complex dose, time, target-dependent effects on pre- and post-synaptic DA neurotransmission through rapid non-genomic and delayed genomic mechanisms,

that have led to various, and sometimes contradictory, conclusions about its effects on DA neurotransmission (Thompson & Moss 1994, Watson *et al.* 2006, Disshon *et al.* 1998, Maus *et al.* 1989, Levesque & Di Paolo 1993, Mermelstein *et al.* 1996).

Most studies support the assertion that physiological estradiol concentrations acutely enhances DA neurotransmission as evidenced by estradiol mediating greater DA turnover (Di Paolo *et al.* 1985), enhanced amphetamine-stimulated DA overflow (Becker 1990a), and DA reuptake inhibition (Disshon et al. 1998). Many of the estrogen effects on DA neurotransmission may be mediated by estrogen uncoupling the interaction between $G\alpha_{i/o}$ proteins and D2 DA autoreceptors (Kelly & Wagner 1999, Thompson & Certain 2005) that modulate inhibition of DA release and enhancement of DA reuptake (Wu et al. 2002, Benoit-Marand *et al.* 2011, Gubernator *et al.* 2009). As estradiol has a general pro-DAergic effect, a sudden decline in CNS estradiol levels following TBI-induced hypogonadism may impair DA neurotransmission to a greater extent in women than men. Consistent with this working hypothesis, striatal DA concentrations were found to be lower only in gonadectomized female rats but not males compared to their sex-based controls (Xiao & Becker 1994). Moreover, as estradiol mediates sex-based differences in the pharmacology of indirect and direct DA agonists (Becker 1990a, Becker 1990b, Becker 1999, Gordon 1980, Hruska *et al.* 1982), understanding the role of estradiol in TBI-induced DAergic dysfunction is critical to tailoring treatments based on age, sex, and hormonal status.

Using the CCI model, we previously evaluated several DAergic markers and their relationship to presynaptic neurotransmission. Total striatal vesicular monoamine transporter type 2 (VMAT2) and tyrosine hydroxylase protein content is not altered 2 weeks after CCI (Wagner et al. 2009a). The DA transporter (DAT) is the primary structure in modulating DA transmission, and DAT trafficking and function are closely regulated by D2 auto-receptors. Our research

suggests total striatal DAT concentration is reduced post-CCI in the setting of increased membrane bound synaptosomal DAT (Wagner et al. 2009a). Using fast scan cyclic voltammetry (FSCV), we have shown that there are relative decreases with maximal evoked DA overflow 2 weeks following CCI proportional to striatal DAT reductions (Wagner et al. 2009a, Wagner et al. 2005b). Also, daily methylphenidate (MPH) administration restored maximal evoked DA overflow (Wagner et al. 2009a)confirming a diminished capacity for maximal striatal outflow after CCI and stimulant induced plasticity evident with presynaptic DA neurotransmission after CCI. We have also shown reductions in striatal outflow augmentation occur with MPH challenge in our CCI model (Wagner et al. 2005b, Wagner et al. 2009b). Together, these data suggest that elements of both DA release and reuptake are impaired by CCI.

In this study, we examined sex and hormonal influences on electrically stimulated DA neurotransmission using FSCV in the context of CCI. Stimulated DA neurotransmission was evaluated in male, female, and ovariectomized (OVX) rats 2wks following injury and in corresponding naïve controls. Moreover, because we previously demonstrated that CCI alters the pharmacological response to the clinically relevant psychostimulant/DAT inhibitor MPH, we monitored how MPH alters stimulated DA responses over a 60-minute time course in all rats. Baseline and post-MPH DA response amplitudes and alterations in response decay behavior were evaluated. In addition, we implemented a modified version of the quantitative neurobiological (QN) model (Harun et al. 2014) to simulate baseline DA responses in order to estimate baseline DA release rates and maximal reuptake rates (Vmax), which we then correlated to the responsivity to the MPH challenge.

5.3 METHODS

Animals and Surgery

Young adult male (279–410g), female (245–323g), and ovariectomized (OVX 295–368g) Sprague-Dawley rats (Hilltop Laboratories, Scottsdale, PA, USA) were used in accordance with the regulations of the University of Pittsburgh's Institutional Animal Care and Use Committee. Rats received controlled cortical impact injury (CCI) (male n=7, female n=5, OVX=5) or were naive (male n=7, female n=6, OVX=6) to surgery for a total of 36 animals. Rats were housed in a 12 h light-dark cycle, with food and water provided *ad libitum*. Ovariectomized rats received this procedure with the vendor approximately 3 weeks prior to CCI procedures.

Controlled cortical impact (CCI) injury

The CCI injury device (Pittsburgh Precision Instruments, Inc., Pittsburgh, PA, USA) used for this study has been described previously (Dixon et al. 1991). Under isoflurane anesthesia (4% isoflurane and a 2:1 N_2/O_2 initially, followed by 1–1.5% isoflurane), animals were placed in a stereotaxic frame. Core body temperature was maintained at 37°C during surgery using a homeothermic blanket (Harvard Apparatus, Edenbridge, UK). A midline scalp incision was made and the soft tissues reflected to perform a craniotomy over the right parietal cortex between lambda and bregma and approximately 2 mm lateral to the central suture. The exposed dura was struck to a depth of 2.8 mm with an impact velocity of 4 m/s by the CCI device as previously described (Wagner *et al.* 2005a,b, 2007a,b, 2009). The scalp was sutured, 2% lidocaine jelly was applied to the incision, and post-injury righting reflexes were monitored after completion of surgical procedures. Animals were returned to their home cages after recovery with ad libitum access to food and water.

Fast scan cyclic voltammetry (FSCV)

To fabricate working electrodes, 7µm diameter carbon fibers (T-300; Union Carbide, Danbury, CT, USA) were threaded through borosilicate glass capillaries (0.6mm o.d. and 0.4mm i.d. [Sutton Instruments, Novato, CA, USA]). The glass capillary was pulled to a tip with a micropipette puller (Narshige, East Meadow, NY, USA), and the tip was epoxy-sealed (Spurr Polysciences, Warrington, PA, USA). Electrodes were cured for at least 12 h at 70°C. The glass capillary was filled with mercury, and a nichrome wire was inserted to make an electrical connection. Exposed carbon fibers were cut to ~400µm lengths as previously described (Wagner *et al.* 2005a). Carbon fiber microelectrodes were sonicated in isopropanol/active carbon powder solution for 30 minutes to enhance electrode sensitivity before voltammetric experiments. Electrodes were post-calibrated after experiments with standard [DA] solutions (0.5µM--5µM in artificial cerebrospinal fluid (aCSF) buffer solution) to convert *in vivo* current recordings to DA concentrations.

Fast scan cyclic voltammetry (FSCV) studies were performed 14 days after CCI. At this time, rats were re-anesthetized with 5% isoflurane and O_2 initially, followed by 2.5% isoflurane and O_2 for maintenance of anesthesia. Once a surgical level of anesthesia was established, the animals were placed in a stereotaxic frame (Kopf, Tujunga, CA, USA). The skull was exposed and the soft tissues reflected. Portions of skull were removed using a drill to expose dura to allow for placement of the working, reference, and stimulating electrodes. Core body temperature was maintained at 37°C during surgery using a homeothermic blanket (Harvard Apparatus, Edenbridge, UK)

Carbon fiber microelectrodes were lowered in the right striatal hemisphere, (ipsilateral to the injury site in CCI animals) using flat-skull coordinates [1.7mm AP, 2.0mm ML, and -4.5mm

DV] (Paxinos and Watson 1998). A bipolar stimulating electrode (MS301-1, Plastics One, Roanoke, VA, USA) was lowered onto the right medial forebrain bundle (MFB) at the stereotaxic coordinates of -4.0mm AP, 1.6mm ML, and -7.6mm DV (Paxinos and Watson 1998). A salt bridge was formed by placing an Ag/AgCl reference electrode in direct contact with the dura mater in the left hemisphere.

DA detection using FSCV has been previously described (Wagner *et al*. 2005a, 2009). Briefly, FSCV was performed with a computer-controlled potentiostat (EI-400; Ensman Instruments, Bloomington, IN, U.S.A.) using TarHeel CV 1.0. A triphasic cyclic voltage waveform was applied to carbon fiber electrodes (0V→1V→-0.5V→0V vs. the Ag/AgCl reference electrode at 400V/s). Scans were repeated every 100ms during *in vivo* recordings. The presence of DA was determined by visual inspection of background-subtracted cyclic voltammograms. The maximum concentration of evoked (EO) DA overflow was taken as the maximum change in DA signal following medial forebrain bundle stimulation.

The MFB was stimulated at 60Hz for 2s (280 µA biphasic current pulse, 2ms pulse width) every 10min. The location of stimulating electrode, and also the carbon fiber microelectrode, was optimized to achieve a maximized and stable baseline DA response, where at least 3 consecutive responses had amplitudes within 10% of each other. Subsequently, 10 mg/kg MPH was administered intraperitoneally, and stimulated DA responses were collected every 10 minutes for 60 minutes after drug administration. Baseline and post-MPH stimulated DA responses from each ratl were used for kinetic analysis.

Data analysis:

Basic DA response shape analysis

DA response shapes were analyzed using two morphometric methods: decay behavior and response amplitudes. Response amplitude is simply the peak [DA] of a stimulated DA response. Decay behavior was examined similar to previous studies (Moquin & Michael 2009, Jones et al. 1995b), where responses were time-shifted to match similar [DA] in the decay phase to directly evaluate differences in decay behavior (see **Figure 18H**). The decay behavior was quantified by fitting an exponential regression to the 2s following the time point where responses were aligned. This approach yielded a decay constant (k) that corresponded to the decay behavior, with larger k-values corresponding to faster decay kinetics.

Table 9: Equations and parameters used to simulate DA responses

DA release rate (during stimulation):		
$\boldsymbol{DAR_{stim}}$ **(Equation 1)**	$\boldsymbol{DAR_{stim}}$	Estimated DA release rate during stimulation
DA release rate (post-stimulation):		
$\boldsymbol{DAR_{post}(t_{post}) =}$	X_R	Rapid release fractional component
$\boldsymbol{DAR_{stim} * X_R * e^{-\frac{t_{post}}{\tau_R}}}$	τ_R	Time constant of rapid release component (Fixed at $0.4s^{-1}$)
$\boldsymbol{+ DAR_{stim} * (1 - X_R) - m * t_{post}}$ **(Equation 2)**	m	Linear decay slope of prolonged release component
DA reuptake rate:		
$\boldsymbol{ReuptakeRate(t) = \frac{V_{max}}{\frac{K_m(t)}{[DA]} + 1}}$ **(Equation 3)**	V_{max}	Maximal reuptake rate
	$K_m(t)$	M-M constant (an inverse measure of efficiency)
	K_{m_i}	Initial K_m
where,	ΔK_m	Magnitude of change in K_m dynamics (Fixed at 20μM)
$\boldsymbol{K_m(t) = K_{m_i} + \Delta K_m \left(1 - \frac{1}{1 + \frac{t}{K_{minf}}^{k_{Hill}}}\right)}$ **(Equation 4)**	$K_{m_{inf}}$	Time of inflection of K_m dynamics
	k_{Hill}	Measure of the steepness of the inflection in K_m dynamics

Modeling stimulated DAergic responses

Baseline stimulated DA responses from each animal were modeled using a variation of the quantitative neurobiological (QN) framework that we recently developed (Harun et al. 2014).

The QN framework was used to simulate experimental DA responses to make theoretical estimates of DA release and reuptake components using equations to describe stimulation-induced attenuation of DA release, stimulation-induced attenuation of DA reuptake efficiency, and also a biphasic post-stimulation DA release component. Although estimates of DA release and reuptake can be generated from single DA responses, multiple durations of stimulation enhances the accuracy of simulations. Because our experimental DA responses only contained DA responses to 2s of electrical stimulation, we modified some QN equations and assumptions of the QN model as summarized in **Table 9**. 2s stimulated DA responses cannot accurately be used to model the dynamics of DA release during stimulation. Thus, we simplified our assumption to include a constant DA release rate (**Equation 1**), similar to the traditional Michaelis-Menten (M-M) model (May & Wightman 1989). Although the constant release assumption is a simplification of underlying DA release processes, DA response shapes are predominantly affected by changes in reuptake efficiency in the dorsal striatum and not DA release; we previously demonstrated that the majority of the DA released by 2s of stimulation in the caudate-putamen is sequestered by reuptake during the 2s of electrical stimulation (Harun et al. 2014). Post-stimulation DA release was modeled according to the equations of the QN framework (**Equation 2**), except we held the time constant for the rapid phase of post-stimulation DA release (τ_R) at $0.4s^{-1}$. This assumption allowed us to attribute differences in the DA response decay phases to differences in reuptake dynamics rather than differences in post-stimulation DA release kinetics. Stimulation-induced attenuation of reuptake efficiency was modeled as described for the QN framework (**Equation 3**), where the M-M constant, K_m, is a dynamic term that increases during stimulation according to the logistic function in **equation 4**. Previous application of the QN framework demonstrated that Km is rapidly changing at 2s when using 60Hz stimulations, usually starting at $Km_i \approx 0.05$. To model Km

dynamics during the 2s of stimulation, ΔKm was held constant at 20μM, and the inflection point (Km_{inf}) and the steepness of the inflection defined by the Hill coefficient, k_{Hill}, were modified to simulate baseline DA responses from each study. The equations in **Table 9** were combined into **equation 5**, which was used to model experimental DA responses in Matlab R2014a (The MathWorks, Inc, Natick, MA).

$$[DA](t) = \int \left(DAR_{stim} + DAR_{post}\left(t_{post}\right)\right) dt - \int \frac{V_{max}}{\frac{K_m(t)}{[DA]} + 1} dt$$

Equation 5

Because MPH alters stimulated DA release dynamics and reuptake dynamics, the simplified QN framework was not amenable for simulating post-MPH responses adequately in our dataset. Nevertheless, the modified QN framework still provided estimates of baseline DA release rate and V_{max}. Although our modified QN framework is more complex than the traditional M-M model, it provides a good fit of stimulated DA responses collected from the dorsomedial striatum that often exhibited a concave rising phase, which is not possible using the traditional M-M model that can only model DA responses with convex rising phases due to its simplified assumptions of DA release and reuptake (May & Wightman 1989).

Statistical analysis

All response metrics (e.g. amplitudes, k values, V_{max}, and others) were analyzed statistically using SPSS 2.0 for Mac (SPSS Inc., Chicago, IL). Baseline differences in metrics between groups were evaluated using one-way repeated measure analysis of variance (ANOVA) or an independent samples Student's T-Test. Time dependent changes in MPH-induced effects between experimental groups were evaluated using two-way repeated measures (rm)ANOVA. Follow-up independent

samples descriptive comparisons were performed using Fisher's least significant difference. P-values ≤0.05 were considered to be significant in all comparisons.

5.4 RESULTS

In light of the evidence demonstrating sex-based differences in the DAergic system and the potential effects of female ovarian hormones in regulating DA neurotransmission, we investigated how sex and ovariectomy influences stimulated DA neurotransmission in the context of CCI using FSCV. Moreover, because of sex-based differences in the pharmacological response to psychostimulants, we also examined how sex, hormone status, and CCI affect stimulated DA responses following a pharmacological challenge to MPH (10mg/kg i.p.) over a 60min time course.

5.4.1 DA response shape analysis reveals sex- and injury-based differences in baseline DA response amplitudes and the temporal effects of MPH

60Hz, 2s electrical stimulations of the MFB were used to elicit DA responses in the right hemisphere (ipsilateral to the CCI) dorsomedial striatum as described earlier. The mean ± SEM of baseline, post-MPH 10min, and post-60min stimulated DA responses are depicted in **Figure17A-G** to demonstrate descriptive group differences in pre- and post-MPH stimulated DA responses.

Baseline response amplitudes were significantly different between groups (ANOVA: $p<0.05$) (**Figure 17G**). Although we found no difference in response amplitudes between naïve male and female rats ($p=0.286$), naïve OVX rats had significantly higher baseline amplitudes

compared to naïve female counterparts ($p<0.05$) and naïve males ($p<0.005$). Both CCI males and females had significantly higher baseline amplitudes compared to naïve males and females, respectively ($p<0.005$ for both comparisons). In contrast, CCI OVX rats had similar baseline response amplitudes compared to the naïve OVX group, suggesting a possible ceiling effect where CCI does not enhance response amplitudes beyond the effects of ovariectomy itself. Since response amplitudes reflect a balance between DA release and reuptake, the increased response amplitudes in OVX animals and in male and female CCI animals, relative to male and female naïve rats, may be due to enhanced release and/or reduced reuptake (examined later).

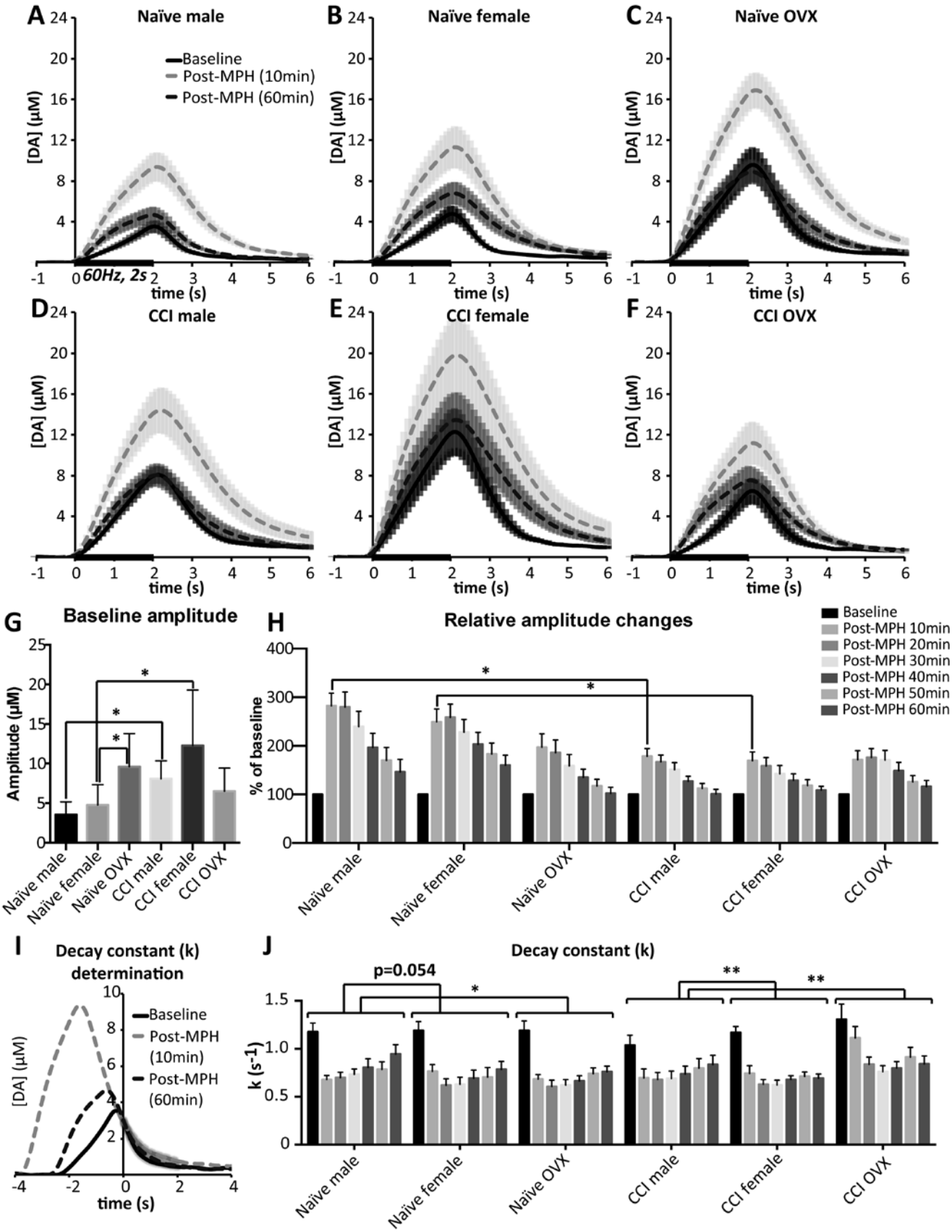
A
Naïve male
B
Naïve female
C
Naïve OVX
Baseline
Post-MPH (10min)
Post-MPH (60min)
[DA] (µM)
time (s)
60Hz, 2s
D
CCI male
E
CCI female
F
CCI OVX
G
Baseline amplitude
Amplitude (µM)
Naïve male
Naïve female
Naïve OVX
CCI male
CCI female
CCI OVX
H
Relative amplitude changes
Baseline
Post-MPH 10min
Post-MPH 20min
Post-MPH 30min
Post-MPH 40min
Post-MPH 50min
Post-MPH 60min
% of baseline
I
Decay constant (k) determination
J
Decay constant (k)
p=0.054
k (s-1)

Figure 17: Stimulated DA response shape characteristics

A-F) Mean ± SEM baseline, post-MPH 10min, and post-MPH 60min DA responses to 60Hz, 2s electrical stimulations demonstrate differential response characteristics across experimental groups pre- and post-MPH (10mg/kg) administration. G) Baseline amplitudes were significantly different between groups (ANOVA: $p<0.005$), where the amplitudes of the naïve OVX group was greater than naïve females ($p<0.05$). Additionally, CCI males and females had greater amplitudes than naïve counterparts ($p<0.05$ for both comparisons). H) MPH administration augmented DA response amplitudes differentially over time between groups (two-way repeated measures ANOVA: $p<0.001$), where CCI male and female groups exhibited attenuated post-MPH 10min responses compared to naïve male and female groups ($p<0.005$, and $p<0.05$, respectively). I) DA responses from individual studies were aligned to similar [DA] to examine relative changes in DA response decay behavior. An exponential regression was performed on the 2s following the point where responses were aligned to generate an exponential decay constant (k). H) k-values were decreased following MPH administration in all groups, but k was differentially altered over time between groups (two-way rmANOVA: $p<0.005$). The naïve male group tended to restore k faster than naïve females (two-way rmANOVA: $p=0.054$) and naïve OVX groups (two-way rmANOVA: $p<0.05$). Similarly, the CCI male group restored k values faster compared to CCI female and CCI OVX groups (2-way rmANOVA: $p<0.005$ for both comparisons).

In response to MPH administration, DA response amplitudes were augmented relative to baseline at the post-MPH 10 time point in all groups (**Figure 17H**), consistent with MPH effects on reuptake inhibition reuptake and enhanced release (Harun et al. 2014, Volz et al. 2008). Response amplitudes subsequently decreased over the 60min assessment window in all groups. However, MPH had differential effects on response amplitudes between groups ($p<0.005$) and between groups across time ($p<0.005$). Although MPH responsivity at post-MPH 10min was similar between naïve groups, the naïve OVX animals had the lowest responsivity to MPH (197.27±28%) compared to naïve males and females (282.40±26%, 249.65±26%, respectively). CCI male and female rats exhibited an attenuated response to MPH in terms of amplitude enhancement compared to respective naïve groups (10min post-MPH amplitude relative to baseline for naive male: 282.40±26% vs. CCI male: 178.50±16%, $p<0.05$; naive female: 249.65±26% vs. CCI female: 169.35 ±18%, $p<0.05$). This finding is similar to our previous study demonstrating male CCI rats exhibited an attenuated amplitude enhancement to an MPH (5mg/kg) challenge compared to naïve male rats (Wagner et al. 2009b). Interestingly, the CCI OVX rats did not exhibit a significantly attenuated response to MPH compared to naïve OVX rats (171.50±19%

vs. 197.27±28%, p=0.479, respectively). We speculate that the modest effects of CCI on the OVX animals in terms of attenuating MPH-responsivity can be explained by a floor effect, where CCI cannot robustly diminish the response to MPH more than the effect of ovariectomy itself. This speculation suggests that hypogonadism maybe contributing to the deficits in MPH responsivity observed after CCI.

We next examined how MPH alters DA response decay behavior, which is sensitive to changes in DAT mediated DA reuptake. Decay behavior was examined by aligning all stimulated DA response from each study to similar DA concentrations and comparing the decay phase of pre- and post-MPH responses as illustrated in **Figure 17I**. Decay behavior was quantified by a mono-exponential decay constant, k, where decreases in k correspond to prolonged DA clearance that can result from DA reuptake inhibition. MPH significantly attenuated k at all time points in all groups except at post-MPH 10min in the CCI OVX group. Notably, we found a significant group*time interaction for how MPH affected k values ($p<0.005$). Post-hoc comparisons demonstrated that naïve males tended to have a differential time course of MPH effects on decay behavior compared to naïve females ($p=0.054$) and naïve OVX ($p<0.05$) rats (**Figure 17H**). Similarly, CCI male rats had a differential time course of MPH effects on decay behavior compared to CCI females and CCI OVX rats ($p<0.01$ both comparisons) (**Figure 17H**). The effects of MPH on response decay behavior had a faster onset in male rats, with a maximal inhibition of k-values at 10min post-MPH in male groups, as opposed to 20-30min in the non-male groups. Moreover, male groups exhibited a shorter duration of MPH effects whereby k-values tended normalize more quickly in naïve and CCI male groups. In contrast, we noted that CCI female rats had the most persistent inhibition of decay with k=59.3±2.4% of baseline k-values at 60min post-MPH administration, which was significantly lower than male naïve and CCI groups (80.75±6.4% and

80.1 ±3.0%, respectively, $p<0.005$ for both comparisons). Taken together, the time course effects of MPH on DA response decay behavior suggests that MPH has more rapid onset and a shorter time course of effects on DA reuptake in males compared to females and OVX groups, an effect which persists even among CCI animals, and which may provide some insight into sex differences with MPH behavioral effects after CCI (Wagner et al., 2007).

5.4.2 Data modeling demonstrates reduced V_{max} in CCI and OVX animals

DA response amplitude and decay behavior are simple methods to examine effects of pharmacological manipulation, but both of these quantitative parameters reflect a balance of DA release and DA reuptake dynamics that can only be estimated from modeling DA responses with a theoretical model of stimulated DA neurotransmission. As described in the methods, we applied a modified version of our QN model (Harun et al. 2014) to evaluate DA release and reuptake dynamics from baseline DA responses from each animal. We implemented the simplified assumption that DA release rate was constant, reuptake efficiency could be modeled by dynamic M-M enzyme kinetics, where the M-M constant, K_m, increases over the course of stimulation, and post-stimulation DA release decays with a the time constant $\tau_R=0.4s^{-1}$ in all groups. Using these assumptions, baseline DA responses were well simulated, with a mean $R^2=0.983\pm0.005$ for all simulations performed. Estimated baseline DA release rates were highly variable, and no significant differences between groups were observed (**Figure 18A**). The lack of significant differences in DA release rate may, in part, be due electrode sampling bias necessary to optimize electrode placement to obtain feasible 60Hz, 2s stimulated DA responses for monitoring pre- and post-MPH effects. In contrast, we found significant differences in V_{max} between groups ($p<0.05$), where naïve OVX rats had lower V_{max} values compared to naïve female rats ($p<0.005$), consistent

with a decreased DAT expression following ovariectomy reported by others (Bosse *et al.* 1997, Chavez *et al.* 2010). Moreover, CCI female rats tended to have lower V_{max} values compared to naïve females ($p=0.0528$), and CCI males had lower V_{max} values compared to naïve males ($p<0.05$). This finding is consistent with our previous characterization of stimulated DA neurotransmission in male rats (Wagner et al. 2009a) and the differential effects of sex on CCI-induced DAT down-regulation (Wagner et al. 2005a). In contrast, V_{max} was not significantly different between CCI OVX and naïve OVX groups.

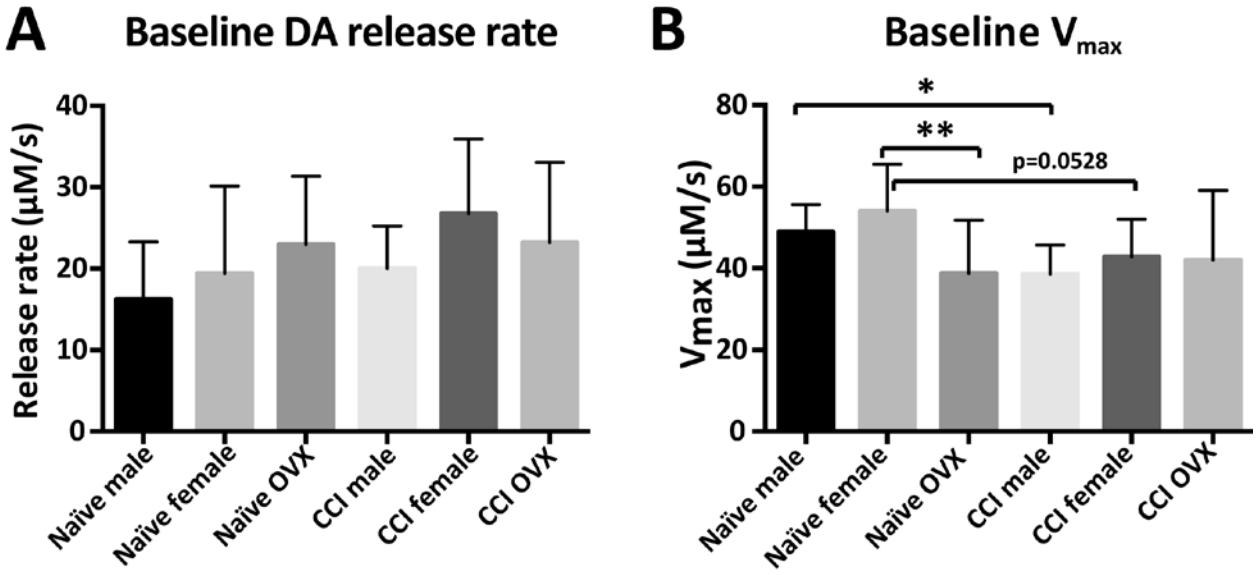

Figure 18: Estimates of DA release rate and V_{max} from modeling baseline experimental DA responses

A) DA release rates were highly variable and no significant differences were found between groups. B) Estimated V_{max} differed between groups (one-way ANOVA: $p<0.05$), where naïve OVX animals had lower Vmax compared to naïve females. V_{max} was lower in CCI male animals compared to naïve males ($p<0.05$), and tended to be lower in CCI females compared to naïve counterparts ($p=0.058$).

5.4.3 MPH responsivity is partly explained by baseline V_{max} and sex-differences

Because V_{max} is an estimate of the functional capacity of DAT, and MPH primarily acts by competitively inhibiting DAT, we postulated that the MPH-induced DA responses amplitude

augmentation would be directly related to V_{max}. To test this hypothesis, we examined the relationship between the relative enhancements of stimulated DA response amplitudes by MPH 10min post-injection vs. baseline V_{max} values from each individual study (**Figure 19**). Overall, there was a significant association between MPH-induced response amplitude augmentation and V_{max} ($p<0.005$) (**Figure 19A**), with a particularly marked association in the male naïve and CCI groups ($R^2=0.559$, $p<0.005$) (**Figure 19B**). Although there was a modest association among female groups ($R^2=0.153$, $p=0.054$) (**Figure 19C**), this association was even less apparent in the OVX groups ($R^2=0.127$, $p=0.156$) (**Figure 19D**). The association between MPH responsivity and Vmax that we demonstrate here suggests that decreases in DAT density in male and female rats after CCI may, in part, underlie the reduced responsivity to MPH that we demonstrate here and previously (Wagner et al. 2009b).

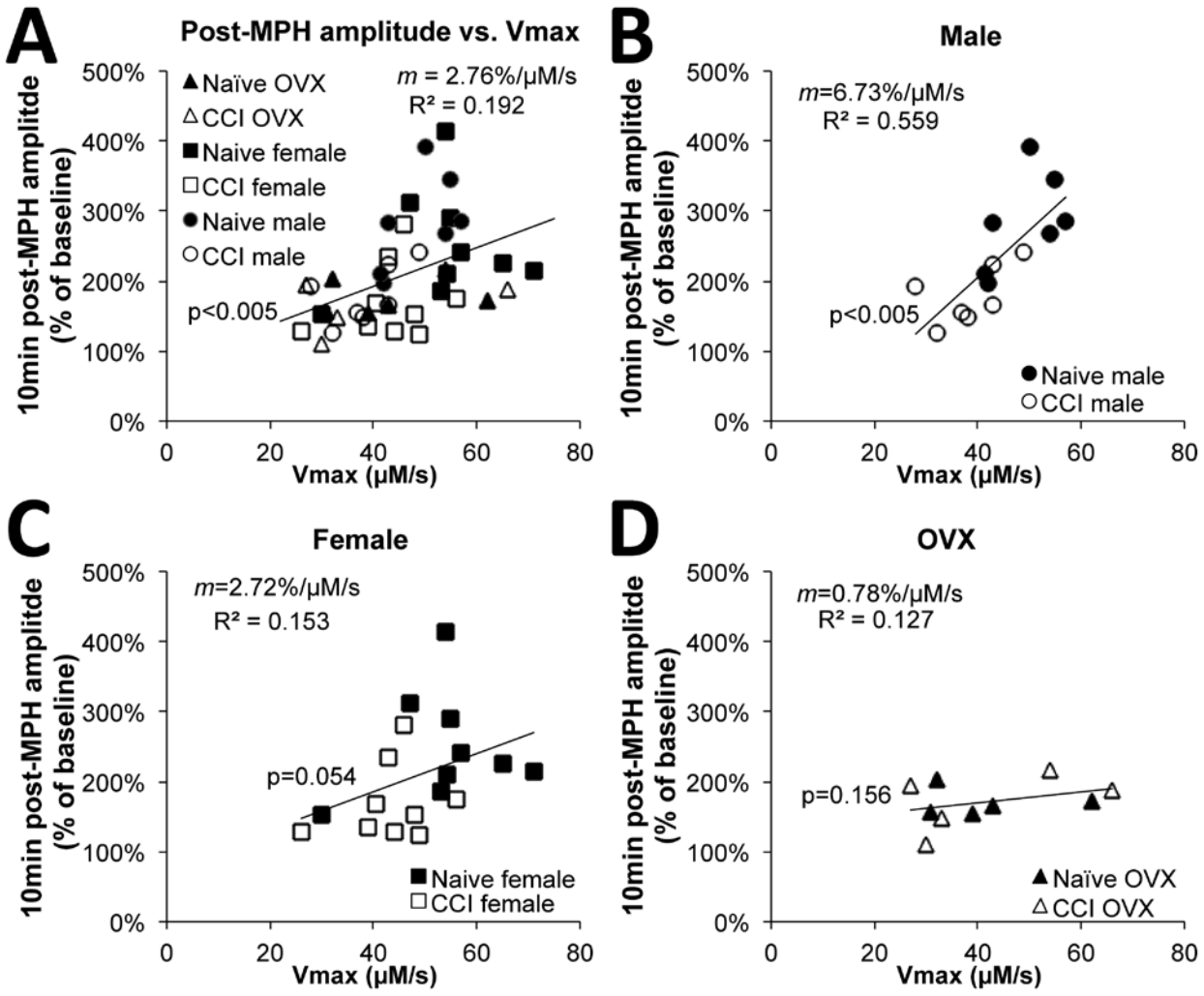

Figure 19: Sex-based associations between MPH-induced response enhancement at 10min post-MPH (10mg/kg) and baseline V_{max}

A) A plot of post-MPH (10min) amplitude enhancement vs. baseline Vmax values demonstrates an overall positive relationship when examining individual studies in all groups (R^2=0.192, p<0.005). B) The amplitude enhancement vs. baseline Vmax correlation was strongest in the male groups (R^2=0.559, p<0.005). In contrast, the female (C) and OVX (D) groups had non-significant positive relationships between post-MPH (10min) amplitude enhancement and Vmax (p=0.054 and p=0.127, respectively).

The positive correlation between MPH responsivity and V_{max} is consistent with the expected relationship between baseline V_{max} and MPH responsivity. However, the smaller associations between V_{max} and MPH responsivity among female and OVX groups suggests sex and hormone-dependent variation in DAT functional states may mediate differential MPH

pharmacodynamics. Contributors to variation could perhaps be due to estrous cycle variation (Czoty *et al.* 2009, Morissette & Di Paolo 1993) or non-DAT dependent mechanisms of MPH action (Volz et al. 2008, Sandoval et al. 2002).

5.5 DISCUSSION

In this study, we explored how sex and hormone status affects DA neurotransmission in the context of experimental brain injury. Unlike previous electrochemical DA monitoring studies (Walker *et al.* 2000, Walker *et al.* 2006), we did not find significant sex-based differences in baseline DA response amplitudes, V_{max}, nor did we see a differential effect of a DAT inhibitor on DA response amplitude augmentation. Although this was somewhat surprising, there is a large degree of variability in DAT function over the rat estrous cycle that may contribute to non-significant sex-based differences (Morissette & Di Paolo 1993, Thompson & Moss 1997). We found that male and female CCI animals had similar alterations in DA neurotransmission compared to their naïve counterparts, such that male/female CCI animals had increased response amplitude, decreased V_{max}, and decreased the responsivity to an acute MPH challenge, consistent with our previous reports (Wagner et al. 2009a, Wagner et al. 2009b). While our current study does not fully support a "double hit hypothesis" for further increasing DA transmission deficits for OVX rats and females after TBI relative to males, the findings do suggest novel alterations in DA transmission with hormone status that are similar in nature to those observed with CCI. In addition, DA clearance patterns, and their relationship to DAT concentration with MPH challenge, appear to be both sex and hormone specific.

In this report, male/female CCI animals had increased DA response amplitudes to 60Hz,2s stimulation compared to naïve counterparts, which contrasts from a previous study demonstrating attenuated response amplitudes to maximal 60Hz, 10s stimulations in male CCI animals (Wagner et al. 2009a). This discrepancy may be explained by the use of a submaximal stimulation paradigm used in this report, while utilizing a maximal stimulation paradigm previously. It is likely that if we prolonged the stimulation duration, male/female CCI animals would have exhibited attenuated response amplitudes compared to their naïve counterparts, as both release and reuptake dynamics vary over time. Moreover, the optimization of the working electrode placement in this report to obtain robust 60Hz, 2s responses to compare pre- and post-MPH pharmacodynamics may have introduced a bias towards sampling more intact responses from injured animals in this report. Our previous study using unbiased stereotaxic methods demonstrated profound deficits in stimulated DA neurotransmission in the dorsomedial striatum that implicated deficits in DA release and reuptake (Wagner et al. 2009a).

As response amplitudes reflect a balance between DA release and reuptake, and we saw no significant changes in DA release between groups (**Figure 18A**), the decreases in V_{max} in male/female CCI animals may, in part, explain the increased amplitudes in male/female CCI animals. The decreases in V_{max} following CCI may reflect a compensatory down-regulation of DAT to a functional hypodopaminergic state after brain injury, similar to the findings of down-regulated DAT expression following a prolonged DA synthesis inhibition with α-methyl-p-tyrosine (Han *et al.* 1999). Interestingly, injury-induced down-regulation of DAT is a consistent finding in the clinical and preclinical TBI literature (Donnemiller et al. 2000, Wagner et al. 2009a, Wagner et al. 2005a, Wagner et al. 2014). Although we did not observe significant sex-based differences in injury-induced effects on baseline DA neurotransmission in this report, it is possible

that differences may be observed in a mild injury paradigm where it may be possible to model the clinically observed sex-based differences in functional outcome after mild TBI (Bazarian et al. 2010, Broshek et al. 2005).

We observed significant differences in baseline DA responses in ovariectomized rats compared to naïve female rats, such that OVX rats had increased response amplitudes and decreased Vmax, similar to the effects of CCI itself. Although, the naïve OVX group had an attenuated response to MPH compared to the naïve female group, this effect was not significant (10min. post-MPH amplitude as a % of baseline: 249.6±26% vs. 197.3±28%, respectively, p=0.204) (**Figure 17H**). Others have demonstrated that ovariectomy decreases striatal DAT expression in rats (Bosse et al. 1997, Chavez et al. 2010), which is consistent with the reduction in V_{max} that we demonstrate in this study. The decreases in V_{max} may be due to a compensatory response to impaired DA neurotransmission following ovariectomy. Interestingly, V_{max} was not further down-regulated in the CCI OVX group compared to the naïve OVX group, as we observed in male/female groups. This finding suggests that ovariectomy either produces a floor effect, where CCI cannot further down-regulate DAT function or that CCI precipitates hypogonadism that partly mediates decreases in DAT function after CCI according to our working model. The link between hypogonadism and DA dysfunction after brain injury requires further study. Because ovariectomy was performed by our vendor approximately 3 weeks prior to CCI, our injured OVX animals did not precisely model post-traumatic hypogonadism. Nevertheless, it is interesting to note that ovariectomy mimics some of the effects of CCI on stimulated DA neurotransmission, which may underlie the clinical finding that post-injury functional outcomes are exacerbated in females of childbearing ages that would be expected to be particularly affected by the effects of post-traumatic hypogonadism (Bazarian et al. 2010, Broshek et al. 2005).

Clinically, post-traumatic hypogonadism occurs in both males and females (Behan et al. 2008, Barton (in revision), Wagner et al. 2012, Ranganathan (in review)), but little is known about how a lack of testosterone itself affects DA neurotransmission in males. Although androgen receptors exist on midbrain DAergic neurons (Purves-Tyson *et al.* 2012), castration of male rats has no apparent effect on nigral mRNA levels for DAergic markers like tyrosine hydroxylase, DAT, vesicular monoamine transporter, and various DA receptors (Purves-Tyson et al. 2012, Purves-Tyson *et al.* 2014), nor does castration affect striatal DA levels like the decreases in DA levels observed after ovariectomy (Xiao & Becker 1994). Thus, although both sexes frequently exhibit post-traumatic hypogonadism, females are more likely to have DAergic impairments resulting from it.

Clinical and experimental data show efficacy with DA enhancing agents in reducing cognitive dysfunction after CCI (Bales et al. 2009). Our experimental work evaluating sex differences with daily MPH treatment suggests that females are more sensitive than males to stimulant treatment (Wagner et al. 2007). The findings in our current study are consistent with this behavioral study and suggest sex-specific pharmacodynamics and mechanisms of action where DAT inhibition is longer lasting in female rats compared to male rats. Although, this post-hoc contrast should be validated and further understood in order to further inform if/how treatment with stimulants like MPH might be tailored based on sex.

Clinically, DA dysfunction post-injury, and its effects on cognition, clinically can be mediated by genetic variants that influence DA levels. In addition, studies indicate a sex-based dimorphism, or a difference in outcomes or phenotype related to biological differences between the sexes, within the DA system (Munro *et al.* 2006, Becker 1999). Recent clinical work suggests that interactions with DA genetics and sex could affect cognitive performance (Gurvich & Rossell

2015, Jacobs & D'Esposito 2011, Glatt *et al.* 2006, Harrison & Tunbridge 2008, Soeiro-De-Souza *et al.* 2013). Our own clinical work demonstrates significant interactions between sex and DA genotype in moderating DA neurotransmission effects on cognition after severe TBI (Myrga (In Revision)), findings that may be due to post-injury hypogonadotropic hypogonadism and sensitivity of DA systems to sex hormone dysfunction as well as injury specific effects.

While this animal study did not fully illustrate a double hit hypothesis for DA transmission, our investigation suggests that hypogonadism may produce similar alterations in stimulated DA neurotransmission as CCI such as increased response amplitude and decreased V_{max} as we observed among ovariectomized rats. These findings are consistent with the idea that post-traumatic hypogonadism can contribute to post-traumatic DAergic alterations. However, a detailed investigation of how CCI influences female gonadal hormone and gonadotropin levels and how hormone replacement strategies affects DAergic alterations would be important next steps to test this causal relationship. In addition, these data show distinct DA stimulant response patterns that are sex specific. These animal data, taken together with our findings of sex-specific DA gene effects on cognition after TBI, support further study into the mechanisms underlying possible sex-specific differences in DA neurotransmission and neurostimulant response after TBI. In particular, future work should focus on the timing of ovariectomy in relationship to TBI. Also, future work could further characterize mechanisms underlying possible enhanced vulnerability to cognitive and behavioral dysfunction for women after TBI.

With our recent advancements in FSCV interpretative framework and methodology (Harun et al. 2014), future studies using multiple stimulation durations and unbiased carbon fiber electrode placement would be expected to enhance our ability to extract multiple parameters relating to DA release and reuptake dynamics that we might expect to show significant group-based differences

in DA release that we failed to observe in this report. Although we demonstrated that CCI and OVX induce decreases in V_{max} that imply DAergic impairments in these contexts, V_{max} is an indirect measure of impaired DA neurotransmission that could be corroborated with future *in vivo* microdialysis measurements of basal DA levels and electrophysiology to monitor DA neuron firing activity.

ACKNOWLEDGEMENTS: Ying Liu, PhD for data collection

6.0 DISCUSSION

As the (neuro)science fiction author William Gibson said, “the future is here, it’s just not evenly distributed yet.” Our work on developing the QN model does not reflect so much on groundbreaking observations on the kinetics of neurotransmission that have been made, but rather, it reflects a synthesis of wide-ranging principles of neurotransmission that is supported by the research of others in various neuroscience sub-fields. Although the QN model incorporates concepts gleaned from electrochemical investigations of DA neurotransmission (Wang et al. 2011, May & Wightman 1989), it is largely supplemented by neurotransmission research on GABAergic, glutamatergic, and cholinergic neurotransmission using electrophysiology, false-fluorescent neurotransmitters, calcium imaging, and various molecular and genetic techniques (Atluri & Regehr 1998, Fierro et al. 1998, Goda & Stevens 1994, Liley & North 1953, Pan & Ryan 2012, Pyott & Rosenmund 2002). These principles have largely guided the development of the QN model that defines the expected patterns of release and reuptake during the course a stimulated DA response. As we ourselves have experienced, without this theoretical framework, it is quite challenging to estimate effectively how DA release and reuptake are balanced to produce a stimulated DA response.

Although the MFB-stimulated DA response paradigm has been around since the mid-1980s, there is still intense current interest in understanding how to properly interpret MFB stimulated DA responses. Recent studies have demonstrated again that stimulated DA responses do not follow simple M-M model kinetics (Moquin & Michael 2009, Taylor et al. 2012, Wang et al. 2011, Taylor *et al.* 2013). To explain observed DA response patterns, a recent model was even published this year shortly after the publication of our QN model (Taylor *et al.* 2015). The

assumptions of the QN model are grounded and supported by what is known about contemporary principles of neurotransmission as discussed in chapter 2. Briefly, we introduce the concept that stimulated DA release rate monotonically decreases over the course of stimulation to the FSCV field, which is similar to the concept of pulse train depression that electrophysiologists have known and studied for years (Pyott & Rosenmund 2002, Hagler & Goda 2001). This contrasts from the constant or region-dependent increasing/decreasing DA release patterns suggested by the other available quantitative models of stimulated DA neurotransmission (Taylor et al. 2015, May & Wightman 1989). We also introduced the concept of post-stimulation DA release that is supported by research on in various neurotransmitter systems (Goda & Stevens 1994, Medrihan *et al.* 2013, Barrett & Stevens 1972, Dodge et al. 1969, Neves & Lagnado 1999), and attenuation of reuptake efficiency during stimulation that has been vetted through our own investigations and supported by the observations made by others in the voltammetry field (Harun et al. 2015, Wang et al. 2011). The QN model has been tested using various stimulation frequencies, stimulation durations, examining DA responses in different regions, and in the context of various pharmacological manipulations. All of this testing has led to findings that might be expected in these various contexts from what is known about the effects of stimulation on neurotransmitter release patterns, the known neurochemical differences between regions, and the known pharmacology of the agents we tested.

6.1.1 Limitations of the QN model and the stimulated DA neurotransmission paradigm

The QN model has been vetted through various experimental manipulations, which has demonstrated that it can be a very powerful tool to study DA neurotransmission. However, the model is only slightly less than a year old. Already, we have five publications that have either been

accepted, submitted, or in progress using the QN model. However, what our experimental work has suggested thus far is that the model is still a work in progress, with more experimentation leading to modest adaptions of the model, resulting in improved consistency with our approach to simulating FSCV data.

The application of the QN model to interpret FSCV data of stimulated DA neurotransmission is admittedly complex, but reflects the fact that DA response signals are a complex interplay of DA release and reuptake. As we developed the QN model, we took the principle that a good model should be as simple as possible, but just simple enough to generally capture the complexity of release and reuptake processes that we hypothesize underlie stimulated DA responses. Nevertheless, systematically applying the equations of the QN model to simulate DA responses is a process that can involve a long learning curve when done without appropriate bearings in mathematics and computer programing in Matlab, and this, in and of itself is likely a barrier for those interested in utilizing these methods. To address this issue, we are actively working on freely disseminating software and publishing an instructional video that may make using these techniques more practical and accessible for interested parties through a software program we have developed.

Although the QN model has advanced our quantitative analysis of MFB-stimulated DA neurotransmission data, like all quantitative models, it is limited by the conditions in which the assumptions are valid. For instance, one of the assumptions of the model is that DA clearance is mediated by DAT. This assumption is supported by work in DAT knockout mice that demonstrates DAT is by and large, the predominant mechanism of DA clearance in the striatum (Budygin et al. 2002); however, clearance by diffusion and neighboring norepinephrine transporters are likely more prominent factors in other regions like the amygdala or prefrontal cortex (Garris &

Wightman 1994b, Jones et al. 1995a, Garris & Wightman 1994a). Although the current version of the QN model does not incorporate other clearance components that may be more relevant in extra-striatal regions, the modular nature of the QN model is such that other quantifiable assumptions can be incorporated and modified as necessary for other regions or as more is learned about the processes underlying stimulated DA neurotransmission.

6.1.2 QN model to characterize DAergic pharmacology

The benefits of a quantitative framework that suitably disentangles release from reuptake components to study DAergic pharmacology cannot be emphasized fully. FSCV generates data of *in vivo* DA concentration fluctuations at sub-second resolution that contains within it rich information about the kinetics of DA release and reuptake, but this information is largely lost without a biologically applicable framework. For example, in *chapter 3*, it was possible to demonstrate the effects of L-DOPA on response amplitudes and the decay phase of DA responses without the use of the QN model. This finding highly suggested that L-DOPA produces changes in DA release and reuptake kinetics. However, QN model introduced additional quantitative analysis that demonstrated L-DOPA decreased Vmax, increased Km, enhanced initial DA release rate, but also showed how DA release rate decays over the course of stimulation. Moreover, the QN model allowed us to quantify to what extent all of these parameters changed over time, between different regions, and by different doses. As such, this body of work demonstrates that this QN model can perform flexibility, and with a high degree of accuracy, to characterize how pharmacological agents affect the kinetics of DA neurotransmission; thus, our work has perhaps the greatest implications for those interested in DA pharmacology.

6.1.3 QN model to characterize regiospecific DAergic dysfunction in disease-states

The use of FSCV to study *in vivo* stimulated neurotransmission is a very remarkable technique. It allows us to monitor neurotransmission with the temporal and spatial resolution that cannot be achieved with any other method. Moreover, this technique is best for detecting DA, which has implications for many functions, diseases, and drugs. Although the M-M model had been developed over 25 years ago to interpret FSCV data of stimulated DA neurotransmission, it was known that DA response patterns can be very heterogeneous and not all DA responses appear to follow the M-M model. This has been the focus of FSCV research early on (May & Wightman 1989), but there has also been a resurgence of this topic lately (Wang et al. 2011, Taylor et al. 2013, Moquin & Michael 2009). Groups have differed in their hypotheses and suppositions about the underlying reasons for the DA response heterogeneity, citing cytoarchitectural differences between regions that may produce diffusional mass-transport barriers for DA (May & Wightman 1989), differences in the size of synaptic vesicle pools (Wang et al. 2011), or nuance conceptualizations similar to the original assertion that there are regional differences in DA diffusion (Taylor et al. 2013, Taylor et al. 2015). As I saw the value in the type of information that FSCV research could provide us with for so many research questions, understanding and properly explaining the underlying neurobiological processes of stimulated DA responses was the impetus for me to continue my graduate studies under the mentorship of Dr. Amy Wagner. We toiled with many theories over the years, and we have repeatedly proven ourselves wrong until we developed the QN model. This theory is supported by contemporary neurotransmission principles, and it can quantifiably explain the regional heterogeneity of the stimulated DA response shapes remarkably well. For us, this body of work represents an extensive endeavor immersed in theory and experimentation that ultimately led to a fruitful outcome where we are now better able to interpret

stimulated DA responses to answer many research questions, including our original questions that focused on determining how DA neurotransmission is altered in the context of traumatic brain injury and how can these dysfunctional neurotransmission patterns be manipulated by drug treatment paradigms.

In the chapter 3, we demonstrated that CCI produced DAergic deficits that were much more pronounced in the D-STR compared to the NAc. In the end, the QN model served simply to corroborate data generated using conventional response shape analysis that demonstrate this effect; importantly, this work benefited from the use of our simultaneous recording electrodes so that we could better demonstrate this effect. Nevertheless, the QN model was helpful in demonstrating that post-CCI chronic MPH treatment enhanced both release and reuptake in the D-STR relative to naïve animals.

Because this experimental paradigm was able to demonstrate the striking regiospecific dysfunction in DA neurotransmission after CCI, we became interested in other neuropathological conditions. To our surprise, very little has been published on the use of the MFB-stimulated DA neurotransmission in contemporary Parkinson's disease models that are known to produce regiospecific degeneration of DAergic neurons and terminals (Cannon *et al.* 2009). Similarly, little research using FSCV has been published characterizing and comparatively assessing DA transmission in other disease states including attention deficit hyperactivity disorder, schizophrenia or Huntington's Disease. In our own research center, there are on-going investigations using various disease models that produce neurodegeneration. One such model that we have begun to examine was a 5-minute asphyxial cardiac arrest (CA) model in rats. At similar a 2-week time point post-injury to what we have studied with experimental TBI (CCI), we found the CA model produced a very different pattern of regiospecific DAergic alterations, where

stimulated DA responses are greatly augmented after CA as opposed to decreased in CCI (**Figure 20**).

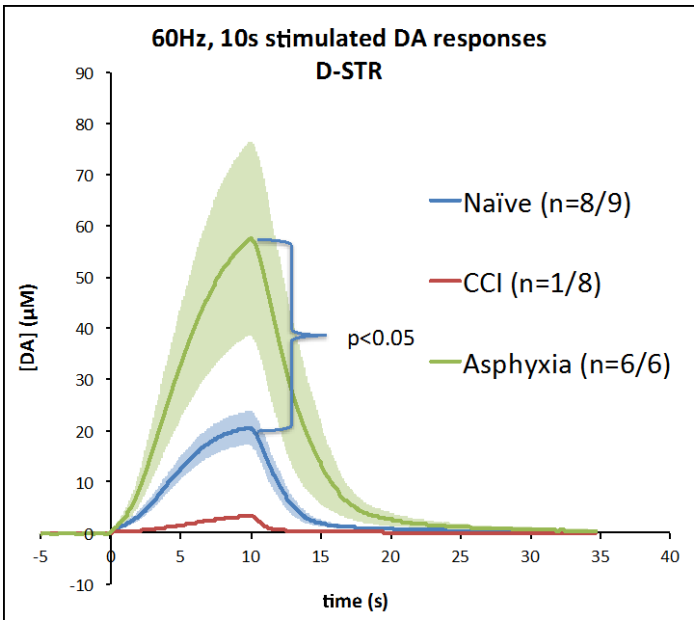

Figure 20: Comparison of stimulated DA responses in CCI and cardiac arrest models

One working hypothesis we have is that the spontaneous spiking of DAergic neurons is impaired after TBI and results in hypotonic DA state that contributes to the alterations, but other points of dysfunction (e.g. with vesicular release and docking proteins) may also exist. However, our early evidence suggests that other clinical conditions like CA alter DA status in ways that are vastly different than anything we have observed with TBI; if corroborated, the findings will have significant impact in guiding specific treatment approaches for an emerging CA survivor population that only exists through other advancements in acute care and resuscitation research forged by some of my colleagues and mentors at the Safar Center for Resuscitation Research, the research center which I have embraced as my dissertation home here at the University of Pittsburgh. Although we evaluated the 2-week time point in both conditions, future work will extend investigations to earlier and later time points, and examine relevant behavioral correlates to these changes.

6.2 CONCLUSION

Our body of work has focused on how to maximize our understanding and use of data generated by the MFB-stimulated DA neurotransmission experimental paradigm primarily through the development of the QN model. There are, however, clear limitations on what kind of DA neurotransmission-relevant information this methodology can provide us with- problems that have always been present with the use of the MFB-stimulated DA neurotransmission paradigm. The experimental paradigm uses artificial electrical stimulations, but we cannot say what changes are occurring in spontaneous DA neural firing; that line of inquiry falls in the realm of electrophysiology research. We can probe for alterations in DA release and reuptake machinery, but we cannot say what changes are actually occurring to spontaneous DA neurotransmission per se; that line of inquiry falls in the realm of more recent advancements being made in the FSCV field to monitor spontaneous DA neurotransmission in awake freely-moving animals. Although we may gain insight into the presynaptic mechanisms that alter basal DA levels, measurements of basal DA levels are best performed by microdialysis or informed by clinical PET imaging. Moving forward, the comprehensive understanding of how drugs and disease affect DA neurotransmission will clearly require the use of complementary research methodologies. This body of work demonstrates the advancements we have made to just one methodology that can be used to extract a unique and information-rich perspective on presynaptic DA neuronal function in the context of drugs and disease.

BIBLIOGRAPHY

(1996) Guide for the Care and Use of Laboratory Animals. National Research Council, Washington, DC.

Adriani, W., Leo, D., Greco, D., Rea, M., di Porzio, U., Laviola, G. and Perrone-Capano, C. (2006) Methylphenidate administration to adolescent rats determines plastic changes on reward-related behavior and striatal gene expression. *Neuropsychopharmacology : official publication of the American College of Neuropsychopharmacology,* **31,** 1946-1956.

Ahlskog, J. E., Uitti, R. J., O'Connor, M. K., Maraganore, D. M., Matsumoto, J. Y., Stark, K. F., Turk, M. F. and Burnett, O. L. (1999) The effect of dopamine agonist therapy on dopamine transporter imaging in Parkinson's disease. *Movement disorders : official journal of the Movement Disorder Society,* **14,** 940-946.

Amatore, C., Arbault, S., Bonifas, I., Bouret, Y., Erard, M., Ewing, A. G. and Sombers, L. A. (2005) Correlation between vesicle quantal size and fusion pore release in chromaffin cell exocytosis. *Biophysical journal,* **88,** 4411-4420.

Armstrong-James, M., Millar, J. and Kruk, Z. L. (1980) Quantification of noradrenaline iontophoresis. *Nature,* **288,** 181-183.

Atluri, P. P. and Regehr, W. G. (1998) Delayed release of neurotransmitter from cerebellar granule cells. *The Journal of neuroscience : the official journal of the Society for Neuroscience,* **18,** 8214-8227.

Bales, J. W., Wagner, A. K., Kline, A. E. and Dixon, C. E. (2009) Persistent cognitive dysfunction after traumatic brain injury: A dopamine hypothesis. *Neuroscience and biobehavioral reviews,* **33,** 981-1003.

Barrett, E. F. and Stevens, C. F. (1972) The kinetics of transmitter release at the frog neuromuscular junction. *The Journal of physiology,* **227,** 691-708.

Barton, D. J., Kumar, R.G., Arenth, P.M., Galang, G., Berga, S. Wagner, A.K. ((in revision)) Persistent hypogonadotropic hypogonadism in men after severe traumatic brain injury: Temporal Hormone Profiles and Outcome Prediction. *Journal of Head Trauma Rehabilitation*.

Bazarian, J. J., Blyth, B., Mookerjee, S., He, H. and McDermott, M. P. (2010) Sex differences in outcome after mild traumatic brain injury. *Journal of neurotrauma,* **27,** 527-539.

Becker, J. B. (1990a) Direct effect of 17 beta-estradiol on striatum: sex differences in dopamine release. *Synapse,* **5,** 157-164.

Becker, J. B. (1990b) Estrogen rapidly potentiates amphetamine-induced striatal dopamine release and rotational behavior during microdialysis. *Neuroscience letters,* **118,** 169-171.

Becker, J. B. (1999) Gender differences in dopaminergic function in striatum and nucleus accumbens. *Pharmacology, biochemistry, and behavior,* **64,** 803-812.

Bedard, C., Wallman, M. J., Pourcher, E., Gould, P. V., Parent, A. and Parent, M. (2011) Serotonin and dopamine striatal innervation in Parkinson's disease and Huntington's chorea. *Parkinsonism & related disorders,* **17,** 593-598.

Behan, L. A., Phillips, J., Thompson, C. J. and Agha, A. (2008) Neuroendocrine disorders after traumatic brain injury. *Journal of neurology, neurosurgery, and psychiatry,* **79,** 753-759.

Benoit-Marand, M., Ballion, B., Borrelli, E., Boraud, T. and Gonon, F. (2011) Inhibition of dopamine uptake by D2 antagonists: an in vivo study. *Journal of neurochemistry,* **116,** 449-458.

Benoit-Marand, M., Borrelli, E. and Gonon, F. (2001) Inhibition of dopamine release via presynaptic D2 receptors: time course and functional characteristics in vivo. *The Journal of neuroscience : the official journal of the Society for Neuroscience,* **21,** 9134-9141.

Berman, S. B., Zigmond, M. J. and Hastings, T. G. (1996) Modification of dopamine transporter function: effect of reactive oxygen species and dopamine. *Journal of neurochemistry,* **67,** 593-600.

Block, E. R., Nuttle, J., Balcita-Pedicino, J. J., Caltagarone, J., Watkins, S. C., Sesack, S. R. and Sorkin, A. (2015) Brain Region-Specific Trafficking of the Dopamine Transporter. *The Journal of neuroscience : the official journal of the Society for Neuroscience,* **35,** 12845-12858.

Borges, S., Gleason, E., Turelli, M. and Wilson, M. (1995) The kinetics of quantal transmitter release from retinal amacrine cells. *Proceedings of the National Academy of Sciences of the United States of America,* **92,** 6896-6900.

Borisovska, M., Bensen, A. L., Chong, G. and Westbrook, G. L. (2013) Distinct modes of dopamine and GABA release in a dual transmitter neuron. *The Journal of neuroscience : the official journal of the Society for Neuroscience,* **33,** 1790-1796.

Bosse, R., Rivest, R. and Di Paolo, T. (1997) Ovariectomy and estradiol treatment affect the dopamine transporter and its gene expression in the rat brain. *Brain research. Molecular brain research,* **46,** 343-346.

Bower, J. H., Maraganore, D. M., Peterson, B. J., McDonnell, S. K., Ahlskog, J. E. and Rocca, W. A. (2003) Head trauma preceding PD: a case-control study. *Neurology,* **60,** 1610-1615.

Brimblecombe, K. R., Gracie, C. J., Platt, N. J. and Cragg, S. J. (2015) Gating of dopamine transmission by calcium and axonal N-, Q-, T- and L-type voltage-gated calcium channels differs between striatal domains. *The Journal of physiology,* **593,** 929-946.

Broshek, D. K., Kaushik, T., Freeman, J. R., Erlanger, D., Webbe, F. and Barth, J. T. (2005) Sex differences in outcome following sports-related concussion. *Journal of neurosurgery,* **102,** 856-863.

Budygin, E. A., John, C. E., Mateo, Y. and Jones, S. R. (2002) Lack of cocaine effect on dopamine clearance in the core and shell of the nucleus accumbens of dopamine transporter knock-out mice. *The Journal of neuroscience : the official journal of the Society for Neuroscience,* **22,** RC222.

Cameron, C. M., Wightman, R. M. and Carelli, R. M. (2014) Dynamics of rapid dopamine release in the nucleus accumbens during goal-directed behaviors for cocaine versus natural rewards. *Neuropharmacology,* **86,** 319-328.

Camicioli, R., Lea, E., Nutt, J. G., Sexton, G. and Oken, B. S. (2001) Methylphenidate increases the motor effects of L-Dopa in Parkinson's disease: a pilot study. *Clinical neuropharmacology,* **24,** 208-213.

Cannon, J. R., Tapias, V., Na, H. M., Honick, A. S., Drolet, R. E. and Greenamyre, J. T. (2009) A highly reproducible rotenone model of Parkinson's disease. *Neurobiology of disease,* **34,** 279-290.

Cardozo, D. L. and Bean, B. P. (1995) Voltage-dependent calcium channels in rat midbrain dopamine neurons: modulation by dopamine and GABAB receptors. *Journal of neurophysiology,* **74,** 1137-1148.

Carta, M., Carlsson, T., Kirik, D. and Bjorklund, A. (2007) Dopamine released from 5-HT terminals is the cause of L-DOPA-induced dyskinesia in parkinsonian rats. *Brain : a journal of neurology,* **130,** 1819-1833.

Cechova, S. and Venton, B. J. (2008) Transient adenosine efflux in the rat caudate-putamen. *Journal of neurochemistry,* **105,** 1253-1263.

Chadchankar, H., Ihalainen, J., Tanila, H. and Yavich, L. (2011) Decreased reuptake of dopamine in the dorsal striatum in the absence of alpha-synuclein. *Brain research,* **1382,** 37-44.

Chavez, C., Hollaus, M., Scarr, E., Pavey, G., Gogos, A. and van den Buuse, M. (2010) The effect of estrogen on dopamine and serotonin receptor and transporter levels in the brain: an autoradiography study. *Brain research,* **1321,** 51-59.

Chiang, M. F., Chang, J. G. and Hu, C. J. (2003) Association between apolipoprotein E genotype and outcome of traumatic brain injury. *Acta neurochirurgica,* **145,** 649-653; discussion 653-644.

Ciliax, B. J., Heilman, C., Demchyshyn, L. L., Pristupa, Z. B., Ince, E., Hersch, S. M., Niznik, H. B. and Levey, A. I. (1995) The dopamine transporter: immunochemical characterization and localization in brain. *The Journal of neuroscience : the official journal of the Society for Neuroscience,* **15,** 1714-1723.

Crownover, J. G., G.N.F.; Wagner, A.K. (2012) Rehabilitation Considerations for Traumatic Brain Injury in the Geriatric Population: Epidemiology, Neurobiology, Prognosis, and Management. *Current Translational Geriatrics and Experimental Gerontology Reports,* **1,** 149-158.

Czoty, P. W., Riddick, N. V., Gage, H. D., Sandridge, M., Nader, S. H., Garg, S., Bounds, M., Garg, P. K. and Nader, M. A. (2009) Effect of menstrual cycle phase on dopamine D2 receptor availability in female cynomolgus monkeys. *Neuropsychopharmacology : official publication of the American College of Neuropsychopharmacology,* **34,** 548-554.

Dahlstroem, A. and Fuxe, K. (1964) Evidence for the Existence of Monoamine-Containing Neurons in the Central Nervous System. I. Demonstration of Monoamines in the Cell Bodies of Brain Stem Neurons. *Acta Physiol Scand Suppl,* SUPPL 232:231-255.

Davis, D. P., Douglas, D. J., Smith, W. et al. (2006) Traumatic brain injury outcomes in pre- and post- menopausal females versus age-matched males. *Journal of neurotrauma,* **23,** 140-148.

Davis, R. A. and Cunningham, P. S. (1984) Prognostic factors in severe head injury. *Surgery, gynecology & obstetrics,* **159,** 597-604.

Daws, L. C., Callaghan, P. D., Moron, J. A., Kahlig, K. M., Shippenberg, T. S., Javitch, J. A. and Galli, A. (2002) Cocaine increases dopamine uptake and cell surface expression of dopamine transporters. *Biochemical and biophysical research communications,* **290,** 1545-1550.

De Michele, G., Filla, A., Volpe, G., De Marco, V., Gogliettino, A., Ambrosio, G., Marconi, R., Castellano, A. E. and Campanella, G. (1996) Environmental and genetic risk factors in Parkinson's disease: a case-control study in southern Italy. *Movement disorders : official journal of the Movement Disorder Society,* **11,** 17-23.

Delaney, K. R. and Tank, D. W. (1994) A quantitative measurement of the dependence of short-term synaptic enhancement on presynaptic residual calcium. *The Journal of neuroscience : the official journal of the Society for Neuroscience,* **14,** 5885-5902.

Di Monte, D. A., McCormack, A., Petzinger, G., Janson, A. M., Quik, M. and Langston, W. J. (2000) Relationship among nigrostriatal denervation, parkinsonism, and dyskinesias in the MPTP primate model. *Movement disorders : official journal of the Movement Disorder Society,* **15,** 459-466.

Di Paolo, T., Rouillard, C. and Bedard, P. (1985) 17 beta-Estradiol at a physiological dose acutely increases dopamine turnover in rat brain. *European journal of pharmacology,* **117,** 197-203.

Disshon, K. A., Boja, J. W. and Dluzen, D. E. (1998) Inhibition of striatal dopamine transporter activity by 17beta-estradiol. *European journal of pharmacology,* **345,** 207-211.

Dobrunz, L. E. and Stevens, C. F. (1997) Heterogeneity of release probability, facilitation, and depletion at central synapses. *Neuron,* **18,** 995-1008.

Dodge, F. A., Jr., Miledi, R. and Rahamimoff, R. (1969) Strontium and quantal release of transmitter at the neuromuscular junction. *The Journal of physiology,* **200,** 267-283.

Donnemiller, E., Brenneis, C., Wissel, J., Scherfler, C., Poewe, W., Riccabona, G. and Wenning, G. K. (2000) Impaired dopaminergic neurotransmission in patients with traumatic brain injury: a SPECT study using 123I-beta-CIT and 123I-IBZM. *European journal of nuclear medicine,* **27,** 1410-1414.

Dresel, S. H., Kung, M. P., Plossl, K., Meegalla, S. K. and Kung, H. F. (1998) Pharmacological effects of dopaminergic drugs on in vivo binding of [99mTc]TRODAT-1 to the central dopamine transporters in rats. *Eur J Nucl Med,* **25,** 31-39.

Edna, T. H. and Cappelen, J. (1987) Late post-concussional symptoms in traumatic head injury. An analysis of frequency and risk factors. *Acta neurochirurgica,* **86,** 12-17.

Ewing, A. G., Bigelow, J. C. and Wightman, R. M. (1983) Direct in vivo monitoring of dopamine released from two striatal compartments in the rat. *Science,* **221,** 169-171.

Fahn, S., Oakes, D., Shoulson, I. et al. (2004) Levodopa and the progression of Parkinson's disease. *The New England journal of medicine,* **351,** 2498-2508.

Failla, M. D., Burkhardt, J. N., Miller, M. A., Scanlon, J. M., Conley, Y. P., Ferrell, R. E. and Wagner, A. K. (2013) Variants of SLC6A4 in depression risk following severe TBI. *Brain injury,* **27,** 696-706.

Failla, M. D., Scanlon, J. M., Ricker, J. E., Conley, Y. P. and Wagner, A. K. (In Press) Dopamine Type 2 Receptor Gene Functional Variant Associations with Cognition, after Severe TBI. *Journal of Head Trauma Rehabilitation.*

Farace, E. and Alves, W. M. (2000a) Do women fare worse: a metaanalysis of gender differences in traumatic brain injury outcome. *Journal of neurosurgery,* **93,** 539-545.

Farace, E. and Alves, W. M. (2000b) Do women fare worse? A metaanalysis of gender differences in outcome after traumatic brain injury. *Neurosurgical focus,* **8,** e6.

Fearnley, J. M. and Lees, A. J. (1991) Ageing and Parkinson's disease: substantia nigra regional selectivity. *Brain : a journal of neurology,* **114 (Pt 5),** 2283-2301.

Fierro, L., DiPolo, R. and Llano, I. (1998) Intracellular calcium clearance in Purkinje cell somata from rat cerebellar slices. *The Journal of physiology,* **510 (Pt 2),** 499-512.

Fleckenstein, A. E., Metzger, R. R., Beyeler, M. L., Gibb, J. W. and Hanson, G. R. (1997) Oxygen radicals diminish dopamine transporter function in rat striatum. *European journal of pharmacology,* **334,** 111-114.

Foltynie, T., Cheeran, B., Williams-Gray, C. H., Edwards, M. J., Schneider, S. A., Weinberger, D., Rothwell, J. C., Barker, R. A. and Bhatia, K. P. (2009) BDNF val66met influences time to onset of levodopa induced dyskinesia in Parkinson's disease. *Journal of neurology, neurosurgery, and psychiatry,* **80,** 141-144.

Foster, J. D., Adkins, S. D., Lever, J. R. and Vaughan, R. A. (2008) Phorbol ester induced trafficking-independent regulation and enhanced phosphorylation of the dopamine transporter associated with membrane rafts and cholesterol. *Journal of neurochemistry,* **105,** 1683-1699.

Furman, C. A., Chen, R., Guptaroy, B., Zhang, M., Holz, R. W. and Gnegy, M. (2009a) Dopamine and amphetamine rapidly increase dopamine transporter trafficking to the surface: live-cell imaging using total internal reflection fluorescence microscopy. *The Journal of neuroscience : the official journal of the Society for Neuroscience,* **29,** 3328-3336.

Furman, C. A., Chen, R., Guptaroy, B., Zhang, M., Holz, R. W. and Gnegy, M. (2009b) Dopamine and amphetamine rapidly increase dopamine transporter trafficking to the surface: live-cell imaging using total internal reflection fluorescence microscopy. *The Journal of neuroscience : the official journal of the Society for Neuroscience,* **29,** 3328-3336.

Gagnon, D., Gregoire, L., Di Paolo, T. and Parent, M. (2015) Serotonin hyperinnervation of the striatum with high synaptic incidence in parkinsonian monkeys. *Brain Struct Funct*.

Garcia-Olivares, J., Torres-Salazar, D., Owens, W. A., Baust, T., Siderovski, D. P., Amara, S. G., Zhu, J., Daws, L. C. and Torres, G. E. (2013) Inhibition of dopamine transporter activity by G protein betagamma subunits. *PloS one,* **8,** e59788.

Garris, P. A. and Wightman, R. M. (1994a) Different kinetics govern dopaminergic transmission in the amygdala, prefrontal cortex, and striatum: an in vivo voltammetric study. *The Journal of neuroscience : the official journal of the Society for Neuroscience,* **14,** 442-450.

Garris, P. A. and Wightman, R. M. (1994b) In vivo voltammetric measurement of evoked extracellular dopamine in the rat basolateral amygdaloid nucleus. *The Journal of physiology,* **478 (Pt 2),** 239-249.

Gaspar, P., Febvret, A. and Colombo, J. (1993) Serotonergic sprouting in primate MTP-induced hemiparkinsonism. *Exp Brain Res,* **96,** 100-106.

Geerlings, A., Nunez, E., Lopez-Corcuera, B. and Aragon, C. (2001) Calcium- and syntaxin 1-mediated trafficking of the neuronal glycine transporter GLYT2. *The Journal of biological chemistry,* **276,** 17584-17590.

Geppert, M., Goda, Y., Hammer, R. E., Li, C., Rosahl, T. W., Stevens, C. F. and Sudhof, T. C. (1994) Synaptotagmin I: a major Ca2+ sensor for transmitter release at a central synapse. *Cell,* **79,** 717-727.

German, C. L., Hanson, G. R. and Fleckenstein, A. E. (2012) Amphetamine and methamphetamine reduce striatal dopamine transporter function without concurrent dopamine transporter relocalization. *Journal of neurochemistry,* **123,** 288-297.

Giacino, J. T., Whyte, J., Bagiella, E. et al. (2012) Placebo-controlled trial of amantadine for severe traumatic brain injury. *The New England journal of medicine,* **366,** 819-826.

Glatt, C. E., Wahner, A. D., White, D. J., Ruiz-Linares, A. and Ritz, B. (2006) Gain-of-function haplotypes in the vesicular monoamine transporter promoter are protective for Parkinson disease in women. *Human molecular genetics,* **15,** 299-305.

Gnegy, M. E. (2003) The effect of phosphorylation on amphetamine-mediated outward transport. *European journal of pharmacology,* **479,** 83-91.

Goda, Y. and Stevens, C. F. (1994) Two components of transmitter release at a central synapse. *Proceedings of the National Academy of Sciences of the United States of America,* **91,** 12942-12946.

Goldman, S. M., Tanner, C. M., Oakes, D., Bhudhikanok, G. S., Gupta, A. and Langston, J. W. (2006) Head injury and Parkinson's disease risk in twins. *Annals of neurology,* **60,** 65-72.

Gonon, F., Cespuglio, R., Ponchon, J. L., Buda, M., Jouvet, M., Adams, R. N. and Pujol, J. F. (1978) [In vivo continuous electrochemical determination of dopamine release in rat neostriatum]. *C R Acad Sci Hebd Seances Acad Sci D,* **286,** 1203-1206.

Gordon, J. H. (1980) Modulation of apomorphine-induced stereotypy by estrogen: time course and dose response. *Brain research bulletin,* **5,** 679-682.

Gorentla, B. K. and Vaughan, R. A. (2005) Differential effects of dopamine and psychoactive drugs on dopamine transporter phosphorylation and regulation. *Neuropharmacology,* **49,** 759-768.

Groffen, A. J., Friedrich, R., Brian, E. C., Ashery, U. and Verhage, M. (2006) DOC2A and DOC2B are sensors for neuronal activity with unique calcium-dependent and kinetic properties. *Journal of neurochemistry,* **97,** 818-833.

Groffen, A. J., Martens, S., Diez Arazola, R. et al. (2010) Doc2b is a high-affinity Ca2+ sensor for spontaneous neurotransmitter release. *Science,* **327,** 1614-1618.

Gu, H., Wall, S. C. and Rudnick, G. (1994) Stable expression of biogenic amine transporters reveals differences in inhibitor sensitivity, kinetics, and ion dependence. *The Journal of biological chemistry,* **269,** 7124-7130.

Gualtieri, C. T. and Evans, R. W. (1988) Stimulant treatment for the neurobehavioural sequelae of traumatic brain injury. *Brain injury : [BI],* **2,** 273-290.

Gubernator, N. G., Zhang, H., Staal, R. G. et al. (2009) Fluorescent false neurotransmitters visualize dopamine release from individual presynaptic terminals. *Science,* **324,** 1441-1444.

Gulley, J. M., Doolen, S. and Zahniser, N. R. (2002) Brief, repeated exposure to substrates down-regulates dopamine transporter function in Xenopus oocytes in vitro and rat dorsal striatum in vivo. *Journal of neurochemistry,* **83,** 400-411.

Gurvich, C. and Rossell, S. L. (2015) Dopamine and cognitive control: sex-by-genotype interactions influence the capacity to switch attention. *Behavioural brain research,* **281,** 96-101.

Guttman, M. (1997) Double-blind comparison of pramipexole and bromocriptine treatment with placebo in advanced Parkinson's disease. International Pramipexole-Bromocriptine Study Group. *Neurology,* **49,** 1060-1065.

Guttman, M., Stewart, D., Hussey, D., Wilson, A., Houle, S. and Kish, S. (2001) Influence of L-dopa and pramipexole on striatal dopamine transporter in early PD. *Neurology,* **56,** 1559-1564.

Hagler, D. J., Jr. and Goda, Y. (2001) Properties of synchronous and asynchronous release during pulse train depression in cultured hippocampal neurons. *Journal of neurophysiology,* **85,** 2324-2334.

Haig, A. J. and Ruess, J. M. (1990) Recovery from vegetative state of six months' duration associated with Sinemet (levodopa/carbidopa). *Archives of physical medicine and rehabilitation,* **71,** 1081-1083.

Han, S., Rowell, P. P. and Carr, L. A. (1999) D2 autoreceptors are not involved in the down-regulation of the striatal dopamine transporter caused by alpha-methyl-p-tyrosine. *Research communications in molecular pathology and pharmacology,* **104,** 331-338.

Harden, D. G. and Grace, A. A. (1995) Activation of dopamine cell firing by repeated L-DOPA administration to dopamine-depleted rats: its potential role in mediating the therapeutic response to L-DOPA treatment. *The Journal of neuroscience : the official journal of the Society for Neuroscience,* **15,** 6157-6166.

Harrison, P. J. and Tunbridge, E. M. (2008) Catechol-O-methyltransferase (COMT): a gene contributing to sex differences in brain function, and to sexual dimorphism in the predisposition to psychiatric disorders. *Neuropsychopharmacology : official publication of the American College of Neuropsychopharmacology,* **33,** 3037-3045.

Harun, R., Grassi, C. M., Munoz, M. J., Torres, G. E. and Wagner, A. K. (2014) Neurobiological model of stimulated dopamine neurotransmission to interpret fast-scan cyclic voltammetry data. *Brain research,* **1599,** 67-84.

Harun, R., Grassi, C. M., Munoz, M. J., Torres, G. E. and Wagner, A. K. (2015) Neurobiological model of stimulated dopamine neurotransmission to interpret fast-scan cyclic voltammetry data. *Brain research,* **1599,** 67-84.

Hornstein, A., Lennihan, L., Seliger, G., Lichtman, S. and Schroeder, K. (1996) Amphetamine in recovery from brain injury. *Brain injury,* **10,** 145-148.

Hruska, R. E., Ludmer, L. M., Pitman, K. T., De Ryck, M. and Silbergeld, E. K. (1982) Effects of Estrogen on Striatal Dopamine receptor function in male and female rats. *Pharmacology, biochemistry, and behavior,* **16,** 285-291.

Huang, E. Y., Tsui, P. F., Kuo, T. T., Tsai, J. J., Chou, Y. C., Ma, H. I., Chiang, Y. H. and Chen, Y. H. (2014) Amantadine ameliorates dopamine-releasing deficits and behavioral deficits in rats after fluid percussion injury. *PloS one,* **9,** e86354.

Hubbard, J. I. (1963) Repetitive Stimulation at the Mammalian Neuromuscular Junction, and the Mobilization of Transmitter. *The Journal of physiology,* **169,** 641-662.

Hukkelhoven, C. W., Steyerberg, E. W., Rampen, A. J., Farace, E., Habbema, J. D., Marshall, L. F., Murray, G. D. and Maas, A. I. (2003) Patient age and outcome following severe traumatic brain injury: an analysis of 5600 patients. *Journal of neurosurgery,* **99,** 666-673.

Hutson, C. B., Lazo, C. R., Mortazavi, F., Giza, C. C., Hovda, D. and Chesselet, M. F. (2011) Traumatic brain injury in adult rats causes progressive nigrostriatal dopaminergic cell loss and enhanced vulnerability to the pesticide paraquat. *Journal of neurotrauma,* **28,** 1783-1801.

Jacobs, E. and D'Esposito, M. (2011) Estrogen shapes dopamine-dependent cognitive processes: implications for women's health. *The Journal of neuroscience : the official journal of the Society for Neuroscience,* **31,** 5286-5293.

Janezic, S., Threlfell, S., Dodson, P. D. et al. (2013) Deficits in dopaminergic transmission precede neuron loss and dysfunction in a new Parkinson model. *Proceedings of the National Academy of Sciences of the United States of America,* **110,** E4016-4025.

Johnson, L. A., Furman, C. A., Zhang, M., Guptaroy, B. and Gnegy, M. E. (2005) Rapid delivery of the dopamine transporter to the plasmalemmal membrane upon amphetamine stimulation. *Neuropharmacology,* **49,** 750-758.

Jomphe, C., Tiberi, M. and Trudeau, L. E. (2006) Expression of D2 receptor isoforms in cultured neurons reveals equipotent autoreceptor function. *Neuropharmacology,* **50,** 595-605.

Jones, S. R., Gainetdinov, R. R., Hu, X. T., Cooper, D. C., Wightman, R. M., White, F. J. and Caron, M. G. (1999a) Loss of autoreceptor functions in mice lacking the dopamine transporter. *Nature neuroscience,* **2,** 649-655.

Jones, S. R., Garris, P. A., Kilts, C. D. and Wightman, R. M. (1995a) Comparison of dopamine uptake in the basolateral amygdaloid nucleus, caudate-putamen, and nucleus accumbens of the rat. *Journal of neurochemistry,* **64,** 2581-2589.

Jones, S. R., Garris, P. A. and Wightman, R. M. (1995b) Different effects of cocaine and nomifensine on dopamine uptake in the caudate-putamen and nucleus accumbens. *The Journal of pharmacology and experimental therapeutics,* **274,** 396-403.

Jones, S. R., Joseph, J. D., Barak, L. S., Caron, M. G. and Wightman, R. M. (1999b) Dopamine neuronal transport kinetics and effects of amphetamine. *Journal of neurochemistry,* **73,** 2406-2414.

Jonkers, N., Sarre, S., Ebinger, G. and Michotte, Y. (2001) Benserazide decreases central AADC activity, extracellular dopamine levels and levodopa decarboxylation in striatum of the rat. *Journal of neural transmission,* **108,** 559-570.

Justice, J. B., Jr., Nicolaysen, L. C. and Michael, A. C. (1988) Modeling the dopaminergic nerve terminal. *Journal of neuroscience methods,* **22,** 239-252.

Kahlig, K. M., Lute, B. J., Wei, Y., Loland, C. J., Gether, U., Javitch, J. A. and Galli, A. (2006) Regulation of dopamine transporter trafficking by intracellular amphetamine. *Molecular pharmacology,* **70,** 542-548.

Kaiser, R., Hofer, A., Grapengiesser, A., Gasser, T., Kupsch, A., Roots, I. and Brockmoller, J. (2003) L -dopa-induced adverse effects in PD and dopamine transporter gene polymorphism. *Neurology,* **60,** 1750-1755.

Katz, B. and Miledi, R. (1968) The role of calcium in neuromuscular facilitation. *The Journal of physiology,* **195,** 481-492.

Kawagoe, K. T. and Wightman, R. M. (1994) Characterization of amperometry for in vivo measurement of dopamine dynamics in the rat brain. *Talanta,* **41,** 865-874.

Kawagoe, K. T., Zimmerman J. B., Wightman R. M. (1993) Principles of voltammetry and microelectrode surface states. *Journal of Neuroscience Methonds,* **48,** 225-240.

Kelly, M. J. and Wagner, E. J. (1999) Estrogen Modulation of G-protein-coupled Receptors. *Trends in endocrinology and metabolism: TEM,* **10,** 369-374.

Kennedy, R. T., Jones, S. R. and Wightman, R. M. (1992) Simultaneous measurement of oxygen and dopamine: coupling of oxygen consumption and neurotransmission. *Neuroscience,* **47,** 603-612.

Kirkness, C. J., Burr, R. L., Mitchell, P. H. and Newell, D. W. (2004) Is there a sex difference in the course following traumatic brain injury? *Biological research for nursing,* **5,** 299-310.

Kish, S. J., Shannak, K. and Hornykiewicz, O. (1988) Uneven pattern of dopamine loss in the striatum of patients with idiopathic Parkinson's disease. Pathophysiologic and clinical implications. *The New England journal of medicine,* **318,** 876-880.

Kissinger, P. T., Hart, J. B. and Adams, R. N. (1973) Voltammetry in brain tissue--a new neurophysiological measurement. *Brain research,* **55,** 209-213.

Kita, J. M., Parker, L. E., Phillips, P. E., Garris, P. A. and Wightman, R. M. (2007) Paradoxical modulation of short-term facilitation of dopamine release by dopamine autoreceptors. *Journal of neurochemistry,* **102,** 1115-1124.

Kline, A. E., Massucci, J. L., Ma, X., Zafonte, R. D. and Dixon, C. E. (2004) Bromocriptine reduces lipid peroxidation and enhances spatial learning and hippocampal neuron survival in a rodent model of focal brain trauma. *Journal of neurotrauma,* **21,** 1712-1722.

Kobori, N., Clifton, G. L. and Dash, P. K. (2006) Enhanced catecholamine synthesis in the prefrontal cortex after traumatic brain injury: implications for prefrontal dysfunction. *Journal of neurotrauma,* **23,** 1094-1102.

Kraus, J. F., Peek-Asa, C. and McArthur, D. (2000) The independent effect of gender on outcomes following traumatic brain injury: a preliminary investigation. *Neurosurgical focus,* **8,** e5.

Krimchansky, B. Z., Keren, O., Sazbon, L. and Groswasser, Z. (2004) Differential time and related appearance of signs, indicating improvement in the state of consciousness in vegetative state traumatic brain injury (VS-TBI) patients after initiation of dopamine treatment. *Brain injury,* **18,** 1099-1105.

Kuhr, W. G., Wightman, R. M. and Rebec, G. V. (1987) Dopaminergic neurons: simultaneous measurements of dopamine release and single-unit activity during stimulation of the medial forebrain bundle. *Brain research,* **418,** 122-128.

Lal, S., Merbtiz, C. P. and Grip, J. C. (1988) Modification of function in head-injured patients with Sinemet. *Brain injury,* **2,** 225-233.

Lam, H. A., Wu, N., Cely, I. et al. (2011) Elevated tonic extracellular dopamine concentration and altered dopamine modulation of synaptic activity precede dopamine loss in the striatum of mice overexpressing human alpha-synuclein. *Journal of neuroscience research,* **89,** 1091-1102.

Langlois, J. A., Rutland-Brown, W. and Wald, M. M. (2006) The epidemiology and impact of traumatic brain injury: a brief overview. *The Journal of head trauma rehabilitation,* **21,** 375-378.

Lee, F. J., Pei, L., Moszczynska, A., Vukusic, B., Fletcher, P. J. and Liu, F. (2007) Dopamine transporter cell surface localization facilitated by a direct interaction with the dopamine D2 receptor. *The EMBO journal,* **26,** 2127-2136.

Levesque, D. and Di Paolo, T. (1993) Modulation by estradiol and progesterone of the GTP effect on striatal D-2 dopamine receptors. *Biochemical pharmacology,* **45,** 723-733.

Liley, A. W. and North, K. A. (1953) An electrical investigation of effects of repetitive stimulation on mammalian neuromuscular junction. *Journal of neurophysiology,* **16,** 509-527.

Little, K. Y., Elmer, L. W., Zhong, H., Scheys, J. O. and Zhang, L. (2002) Cocaine induction of dopamine transporter trafficking to the plasma membrane. *Molecular pharmacology,* **61,** 436-445.

Macdonald, P. A. and Monchi, O. (2011) Differential effects of dopaminergic therapies on dorsal and ventral striatum in Parkinson's disease: implications for cognitive function. *Parkinson's disease,* **2011,** 572743.

Maina, F. K. and Mathews, T. A. (2010) A functional fast scan cyclic voltammetry assay to characterize dopamine D2 and D3 autoreceptors in the mouse striatum. *ACS chemical neuroscience,* **1,** 450-462.

Marek, K., Jennings, D. and Seibyl, J. (2002) Do dopamine agonists or levodopa modify Parkinson's disease progression? *European journal of neurology : the official journal of the European Federation of Neurological Societies,* **9 Suppl 3,** 15-22.

Massucci, J. L., Kline, A. E., Ma, X., Zafonte, R. D. and Dixon, C. E. (2004) Time dependent alterations in dopamine tissue levels and metabolism after experimental traumatic brain injury in rats. *Neuroscience letters,* **372,** 127-131.

Matsuda, W., Furuta, T., Nakamura, K. C., Hioki, H., Fujiyama, F., Arai, R. and Kaneko, T. (2009) Single nigrostriatal dopaminergic neurons form widely spread and highly dense axonal arborizations in the neostriatum. *The Journal of neuroscience : the official journal of the Society for Neuroscience,* **29,** 444-453.

Maus, M., Bertrand, P., Drouva, S., Rasolonjanahary, R., Kordon, C., Glowinski, J., Premont, J. and Enjalbert, A. (1989) Differential modulation of D1 and D2 dopamine-sensitive adenylate cyclases by 17 beta-estradiol in cultured striatal neurons and anterior pituitary cells. *Journal of neurochemistry,* **52,** 410-418.

May, L. J. and Wightman, R. M. (1989) Heterogeneity of stimulated dopamine overflow within rat striatum as observed with in vivo voltammetry. *Brain research,* **487,** 311-320.

McCann, S. J., LeCouteur, D. G., Green, A. C., Brayne, C., Johnson, A. G., Chan, D., McManus, M. E. and Pond, S. M. (1998) The epidemiology of Parkinson's disease in an Australian population. *Neuroepidemiology,* **17,** 310-317.

McDowell, S., Whyte, J. and D'Esposito, M. (1998) Differential effect of a dopaminergic agonist on prefrontal function in traumatic brain injury patients. *Brain : a journal of neurology,* **121 (Pt 6),** 1155-1164.

McIntosh, T. K., Yu, T. and Gennarelli, T. A. (1994) Alterations in regional brain catecholamine concentrations after experimental brain injury in the rat. *Journal of neurochemistry,* **63,** 1426-1433.

McRitchie, D. A., Cartwright, H. R. and Halliday, G. M. (1997) Specific A10 dopaminergic nuclei in the midbrain degenerate in Parkinson's disease. *Experimental neurology,* **144,** 202-213.

Medrihan, L., Cesca, F., Raimondi, A., Lignani, G., Baldelli, P. and Benfenati, F. (2013) Synapsin II desynchronizes neurotransmitter release at inhibitory synapses by interacting with presynaptic calcium channels. *Nat Commun,* **4,** 1512.

Mermelstein, P. G., Becker, J. B. and Surmeier, D. J. (1996) Estradiol reduces calcium currents in rat neostriatal neurons via a membrane receptor. *The Journal of neuroscience : the official journal of the Society for Neuroscience,* **16,** 595-604.

Metzger, R. R., Brown, J. M., Sandoval, V., Rau, K. S., Elwan, M. A., Miller, G. W., Hanson, G. R. and Fleckenstein, A. E. (2002) Inhibitory effect of reserpine on dopamine transporter function. *European journal of pharmacology,* **456,** 39-43.

Meythaler, J. M., Brunner, R. C., Johnson, A. and Novack, T. A. (2002) Amantadine to improve neurorecovery in traumatic brain injury-associated diffuse axonal injury: a pilot double-blind randomized trial. *The Journal of head trauma rehabilitation,* **17,** 300-313.

Millar, J., Stamford, J. A., Kruk, Z. L. and Wightman, R. M. (1985) Electrochemical, pharmacological and electrophysiological evidence of rapid dopamine release and removal in the rat caudate nucleus following electrical stimulation of the median forebrain bundle. *European journal of pharmacology,* **109,** 341-348.

Miller, G. M. (2011) The emerging role of trace amine-associated receptor 1 in the functional regulation of monoamine transporters and dopaminergic activity. *Journal of neurochemistry,* **116,** 164-176.

Moein, H., Khalili, H. A. and Keramatian, K. (2006) Effect of methylphenidate on ICU and hospital length of stay in patients with severe and moderate traumatic brain injury. *Clinical neurology and neurosurgery,* **108,** 539-542.

Moquin, K. F. and Michael, A. C. (2009) Tonic autoinhibition contributes to the heterogeneity of evoked dopamine release in the rat striatum. *Journal of neurochemistry,* **110,** 1491-1501.

Morissette, M. and Di Paolo, T. (1993) Sex and estrous cycle variations of rat striatal dopamine uptake sites. *Neuroendocrinology,* **58,** 16-22.

Mosharov, E. V., Larsen, K. E., Kanter, E. et al. (2009) Interplay between cytosolic dopamine, calcium, and alpha-synuclein causes selective death of substantia nigra neurons. *Neuron,* **62,** 218-229.

Munro, C. A., McCaul, M. E., Wong, D. F. et al. (2006) Sex differences in striatal dopamine release in healthy adults. *Biological psychiatry,* **59,** 966-974.

Myrga, J., Failla, M.D., Ricker, J.H., Conley, Y.P., Arenth, P.M., Wagner, A.K. ((In Revision)) Dopamine system genetics and sex Interact to affect cognitive dysfunction after TBI. *Journal of Head Trauma Rehabilitation.*

Neher, E. and Sakaba, T. (2008) Multiple roles of calcium ions in the regulation of neurotransmitter release. *Neuron,* **59,** 861-872.

Neves, G. and Lagnado, L. (1999) The kinetics of exocytosis and endocytosis in the synaptic terminal of goldfish retinal bipolar cells. *The Journal of physiology,* **515 (Pt 1),** 181-202.

Oddy, M., Coughlan, T., Tyerman, A. and Jenkins, D. (1985) Social adjustment after closed head injury: a further follow-up seven years after injury. *Journal of neurology, neurosurgery, and psychiatry,* **48,** 564-568.

Oliveri, R. L., Annesi, G., Zappia, M. et al. (1999) Dopamine D2 receptor gene polymorphism and the risk of levodopa-induced dyskinesias in PD. *Neurology,* **53,** 1425-1430.

Ono, J., Yamaura, A., Kubota, M., Okimura, Y. and Isobe, K. (2001) Outcome prediction in severe head injury: analyses of clinical prognostic factors. *Journal of clinical neuroscience : official journal of the Neurosurgical Society of Australasia,* **8,** 120-123.

Pan, P. Y. and Ryan, T. A. (2012) Calbindin controls release probability in ventral tegmental area dopamine neurons. *Nature neuroscience,* **15,** 813-815.

Pang, Z. P., Bacaj, T., Yang, X., Zhou, P., Xu, W. and Sudhof, T. C. (2011) Doc2 supports spontaneous synaptic transmission by a Ca(2+)-independent mechanism. *Neuron,* **70,** 244-251.

Parkinson Study, G. (2002) Dopamine transporter brain imaging to assess the effects of pramipexole vs levodopa on Parkinson disease progression. *Jama,* **287,** 1653-1661.

Passler, M. A. and Riggs, R. V. (2001) Positive outcomes in traumatic brain injury-vegetative state: patients treated with bromocriptine. *Archives of physical medicine and rehabilitation,* **82,** 311-315.

Patel, J., Trout, S. J. and Kruk, Z. L. (1992) Regional differences in evoked dopamine efflux in brain slices of rat anterior and posterior caudate putamen. *Naunyn-Schmiedeberg's archives of pharmacology,* **346,** 267-276.

Patrick, P. D., Buck, M. L., Conaway, M. R. and Blackman, J. A. (2003) The use of dopamine enhancing medications with children in low response states following brain injury. *Brain injury : [BI],* **17,** 497-506.

Paxinos, G. and Watson, C. (2007) *The rat brain in stereotaxic coordinates*. Elsevier, Amsterdam.

Peters, J. L. and Michael, A. C. (2000) Changes in the kinetics of dopamine release and uptake have differential effects on the spatial distribution of extracellular dopamine concentration in rat striatum. *Journal of neurochemistry,* **74,** 1563-1573.

Phillips, P. E., Stuber, G. D., Heien, M. L., Wightman, R. M. and Carelli, R. M. (2003) Subsecond dopamine release promotes cocaine seeking. *Nature,* **422,** 614-618.

Pissadaki, E. K. and Bolam, J. P. (2013) The energy cost of action potential propagation in dopamine neurons: clues to susceptibility in Parkinson's disease. *Frontiers in computational neuroscience,* **7,** 13.

Plenger, P. M., Dixon, C. E., Castillo, R. M., Frankowski, R. F., Yablon, S. A. and Levin, H. S. (1996) Subacute methylphenidate treatment for moderate to moderately severe traumatic brain injury: a preliminary double-blind placebo-controlled study. *Archives of physical medicine and rehabilitation,* **77,** 536-540.

Pohjalainen, T., Rinne, J. O., Nagren, K., Syvalahti, E. and Hietala, J. (1998) Sex differences in the striatal dopamine D2 receptor binding characteristics in vivo. *The American journal of psychiatry,* **155,** 768-773.

Povlock, S. L., Meiergerd, S. M. and Schenk, J. O. (1996) Kinetic mechanisms of the dopamine transporter: a comparison with other biogenic amine transporters. *CNS Neurotransmitters and Neuromodulators of Dopamine, CRC Press, Boca Raton, FL***,** 21-40.

Powell, J. H., al-Adawi, S., Morgan, J. and Greenwood, R. J. (1996) Motivational deficits after brain injury: effects of bromocriptine in 11 patients. *Journal of neurology, neurosurgery, and psychiatry,* **60,** 416-421.

Purves-Tyson, T. D., Handelsman, D. J., Double, K. L., Owens, S. J., Bustamante, S. and Weickert, C. S. (2012) Testosterone regulation of sex steroid-related mRNAs and dopamine-related mRNAs in adolescent male rat substantia nigra. *BMC neuroscience,* **13,** 95.

Purves-Tyson, T. D., Owens, S. J., Double, K. L., Desai, R., Handelsman, D. J. and Weickert, C. S. (2014) Testosterone induces molecular changes in dopamine signaling pathway molecules in the adolescent male rat nigrostriatal pathway. *PloS one,* **9,** e91151.

Pyott, S. J. and Rosenmund, C. (2002) The effects of temperature on vesicular supply and release in autaptic cultures of rat and mouse hippocampal neurons. *The Journal of physiology,* **539,** 523-535.

Ranganathan, R., Kumar, R., Davis, K., McCullough, E.M., Berga, S., Wagner, A.K. ((in review)) Longitudinal Sex Hormone Profiles Among Reproductive Age and Post-menopausal Women after Severe TBI a Case Series Analysis. *Brain injury,* **2015**.

Richards, T. L. and Zahniser, N. R. (2009) Rapid substrate-induced down-regulation in function and surface localization of dopamine transporters: rat dorsal striatum versus nucleus accumbens. *Journal of neurochemistry,* **108,** 1575-1584.

Ripley, D. L., Harrison-Felix, C., Sendroy-Terrill, M., Cusick, C. P., Dannels-McClure, A. and Morey, C. (2008) The impact of female reproductive function on outcomes after traumatic brain injury. *Archives of physical medicine and rehabilitation,* **89,** 1090-1096.

Rivest, R., Falardeau, P. and Di Paolo, T. (1995) Brain dopamine transporter: gender differences and effect of chronic haloperidol. *Brain research,* **692,** 269-272.

Robinson, D. L., Heien, M. L. and Wightman, R. M. (2002) Frequency of dopamine concentration transients increases in dorsal and ventral striatum of male rats during introduction of conspecifics. *The Journal of neuroscience : the official journal of the Society for Neuroscience,* **22,** 10477-10486.

Rodriguez, M., Gonzalez, S., Morales, I., Sabate, M., Gonzalez-Hernandez, T. and Gonzalez-Mora, J. L. (2007a) Nigrostriatal cell firing action on the dopamine transporter. *The European journal of neuroscience,* **25,** 2755-2765.

Rodriguez, M., Morales, I., Gomez, I., Gonzalez, S., Gonzalez-Hernandez, T. and Gonzalez-Mora, J. L. (2006) Heterogeneous dopamine neurochemistry in the striatum: the fountain-drain matrix. *The Journal of pharmacology and experimental therapeutics,* **319,** 31-43.

Rodriguez, M., Morales, I., Gonzalez-Mora, J. L., Gomez, I., Sabate, M., Dopico, J. G., Rodriguez-Oroz, M. C. and Obeso, J. A. (2007b) Different levodopa actions on the extracellular dopamine pools in the rat striatum. *Synapse,* **61,** 61-71.

Saddoris, M. P., Cacciapaglia, F., Wightman, R. M. and Carelli, R. M. (2015) Differential Dopamine Release Dynamics in the Nucleus Accumbens Core and Shell Reveal Complementary Signals for Error Prediction and Incentive Motivation. *The Journal of neuroscience : the official journal of the Society for Neuroscience,* **35,** 11572-11582.

Sandoval, V., Riddle, E. L., Hanson, G. R. and Fleckenstein, A. E. (2002) Methylphenidate redistributes vesicular monoamine transporter-2: role of dopamine receptors. *The Journal of neuroscience : the official journal of the Society for Neuroscience,* **22,** 8705-8710.

Sauerbeck, A., Hunter, R., Bing, G. and Sullivan, P. G. (2012) Traumatic brain injury and trichloroethylene exposure interact and produce functional, histological, and mitochondrial deficits. *Experimental neurology,* **234,** 85-94.

Saunders, C., Ferrer, J. V., Shi, L. et al. (2000) Amphetamine-induced loss of human dopamine transporter activity: an internalization-dependent and cocaine-sensitive mechanism. *Proceedings of the National Academy of Sciences of the United States of America,* **97,** 6850-6855.

Scheffel, U., Steinert, C., Kim, S. E., Ehlers, M. D., Boja, J. W. and Kuhar, M. J. (1996) Effect of dopaminergic drugs on the in vivo binding of [3H]WIN 35,428 to central dopamine transporters. *Synapse,* **23,** 61-69.

Seidler, A., Hellenbrand, W., Robra, B. P., Vieregge, P., Nischan, P., Joerg, J., Oertel, W. H., Ulm, G. and Schneider, E. (1996) Possible environmental, occupational, and other etiologic factors for Parkinson's disease: a case-control study in Germany. *Neurology,* **46,** 1275-1284.

Shin, S. S., Bray, E. R., Zhang, C. Q. and Dixon, C. E. (2011) Traumatic brain injury reduces striatal tyrosine hydroxylase activity and potassium-evoked dopamine release in rats. *Brain research,* **1369,** 208-215.

Soeiro-De-Souza, M. G., Bio, D. S., David, D. P., Missio, G., Lima, B., Fernandes, F., Machado-Vieira, R. and Moreno, R. A. (2013) Gender effects of the COMT Val 158 Met genotype on verbal fluency in healthy adults. *Molecular medicine reports,* **8,** 837-844.

Sombers, L. A., Hanchar, H. J., Colliver, T. L., Wittenberg, N., Cans, A., Arbault, S., Amatore, C. and Ewing, A. G. (2004) The effects of vesicular volume on secretion through the fusion pore in exocytotic release from PC12 cells. *The Journal of neuroscience : the official journal of the Society for Neuroscience,* **24,** 303-309.

Speech, T. J., Rao, S. M., Osmon, D. C. and Sperry, L. T. (1993) A double-blind controlled study of methylphenidate treatment in closed head injury. *Brain injury : [BI],* **7,** 333-338.

Stamford, J. A., Kruk, Z. L. and Millar, J. (1991) Differential effects of dopamine agonists upon stimulated limbic and striatal dopamine release: in vivo voltammetric data. *British journal of pharmacology,* **102,** 45-50.

Stamford, J. A., Kruk, Z. L., Palij, P. and Millar, J. (1988) Diffusion and uptake of dopamine in rat caudate and nucleus accumbens compared using fast cyclic voltammetry. *Brain research,* **448,** 381-385.

Strong, J. A., Dalvi, A., Revilla, F. J. et al. (2006) Genotype and smoking history affect risk of levodopa-induced dyskinesias in Parkinson's disease. *Movement disorders : official journal of the Movement Disorder Society,* **21,** 654-659.

Takmakov, P., Zachek, M. K., Keithley, R. B., Bucher, E. S., McCarty, G. S. and Wightman, R. M. (2010) Characterization of local pH changes in brain using fast-scan cyclic voltammetry with carbon microelectrodes. *Analytical chemistry,* **82,** 9892-9900.

Tan, L., Ge, H., Tang, J. et al. (2015) Amantadine preserves dopamine level and attenuates depression-like behavior induced by traumatic brain injury in rats. *Behavioural brain research,* **279,** 274-282.

Taschenberger, H. and von Gersdorff, H. (2000) Fine-tuning an auditory synapse for speed and fidelity: developmental changes in presynaptic waveform, EPSC kinetics, and synaptic plasticity. *The Journal of neuroscience : the official journal of the Society for Neuroscience,* **20,** 9162-9173.

Taylor, C. A., Saint-Hilaire, M. H., Cupples, L. A., Thomas, C. A., Burchard, A. E., Feldman, R. G. and Myers, R. H. (1999) Environmental, medical, and family history risk factors for Parkinson's disease: a New England-based case control study. *Am J Med Genet,* **88,** 742-749.

Taylor, I. M., Ilitchev, A. I. and Michael, A. C. (2013) Restricted diffusion of dopamine in the rat dorsal striatum. *ACS Chem Neurosci,* **4,** 870-878.

Taylor, I. M., Jaquins-Gerstl, A., Sesack, S. R. and Michael, A. C. (2012) Domain-dependent effects of DAT inhibition in the rat dorsal striatum. *Journal of neurochemistry,* **122,** 283-294.

Taylor, I. M., Nesbitt, K. M., Walters, S. H., Varner, E. L., Shu, Z., Bartlow, K. M., Jaquins-Gerstl, A. S. and Michael, A. C. (2015) Kinetic diversity of dopamine transmission in the dorsal striatum. *Journal of neurochemistry,* **133,** 522-531.

Thanvi, B. R. and Lo, T. C. (2004) Long term motor complications of levodopa: clinical features, mechanisms, and management strategies. *Postgraduate medical journal,* **80,** 452-458.

Thompson, T. L. and Certain, M. E. (2005) Estrogen mediated inhibition of dopamine transport in the striatum: regulation by G alpha i/o. *European journal of pharmacology,* **511,** 121-126.

Thompson, T. L. and Moss, R. L. (1994) Estrogen regulation of dopamine release in the nucleus accumbens: genomic- and nongenomic-mediated effects. *Journal of neurochemistry,* **62,** 1750-1756.

Thompson, T. L. and Moss, R. L. (1997) Modulation of mesolimbic dopaminergic activity over the rat estrous cycle. *Neuroscience letters,* **229,** 145-148.

Troiano, A. R., de la Fuente-Fernandez, R., Sossi, V., Schulzer, M., Mak, E., Ruth, T. J. and Stoessl, A. J. (2009) PET demonstrates reduced dopamine transporter expression in PD with dyskinesias. *Neurology,* **72,** 1211-1216.

van Bregt, D. R., Thomas, T. C., Hinzman, J. M., Cao, T., Liu, M., Bing, G., Gerhardt, G. A., Pauly, J. R. and Lifshitz, J. (2012) Substantia nigra vulnerability after a single moderate diffuse brain injury in the rat. *Experimental neurology,* **234,** 8-19.

van Woerkom, T. C., Minderhoud, J. M., Gottschal, T. and Nicolai, G. (1982) Neurotransmitters in the treatment of patients with severe head injuries. *Eur Neurol,* **21,** 227-234.

van Zomeren, A. H. and van den Burg, W. (1985) Residual complaints of patients two years after severe head injury. *Journal of neurology, neurosurgery, and psychiatry,* **48,** 21-28.

Vaughan, R. A. and Foster, J. D. (2013) Mechanisms of dopamine transporter regulation in normal and disease states. *Trends in pharmacological sciences,* **34,** 489-496.

Venton, B. J., Seipel, A. T., Phillips, P. E., Wetsel, W. C., Gitler, D., Greengard, P., Augustine, G. J. and Wightman, R. M. (2006) Cocaine increases dopamine release by mobilization of a synapsin-dependent reserve pool. *The Journal of neuroscience : the official journal of the Society for Neuroscience,* **26,** 3206-3209.

Volz, T. J., Farnsworth, S. J., Rowley, S. D., Hanson, G. R. and Fleckenstein, A. E. (2008) Methylphenidate-induced increases in vesicular dopamine sequestration and dopamine release in the striatum: the role of muscarinic and dopamine D2 receptors. *The Journal of pharmacology and experimental therapeutics,* **327,** 161-167.

Wagner, A. K., Brett, C. A., McCullough, E. H., Niyonkuru, C., Loucks, T. L., Dixon, C. E., Ricker, J., Arenth, P. and Berga, S. L. (2012) Persistent hypogonadism influences estradiol synthesis, cognition and outcome in males after severe TBI. *Brain injury,* **26,** 1226-1242.

Wagner, A. K., Chen, X., Kline, A. E., Li, Y., Zafonte, R. D. and Dixon, C. E. (2005a) Gender and environmental enrichment impact dopamine transporter expression after experimental traumatic brain injury. *Experimental neurology,* **195,** 475-483.

Wagner, A. K., Drewencki, L. L., Chen, X., Santos, F. R., Khan, A. S., Harun, R., Torres, G. E., Michael, A. C. and Dixon, C. E. (2009a) Chronic methylphenidate treatment enhances striatal dopamine neurotransmission after experimental traumatic brain injury. *Journal of neurochemistry,* **108,** 986-997.

Wagner, A. K., Kline, A. E., Ren, D., Willard, L. A., Wenger, M. K., Zafonte, R. D. and Dixon, C. E. (2007) Gender associations with chronic methylphenidate treatment and behavioral performance following experimental traumatic brain injury. *Behavioural brain research,* **181,** 200-209.

Wagner, A. K., Scanlon, J. M., Becker, C. R., Ritter, A. C., Niyonkuru, C., Dixon, C. E., Conley, Y. P. and Price, J. C. (2014) The influence of genetic variants on striatal dopamine transporter and D2 receptor binding after TBI. *Journal of cerebral blood flow and metabolism : official journal of the International Society of Cerebral Blood Flow and Metabolism,* **34,** 1328-1339.

Wagner, A. K., Sokoloski, J. E., Chen, X., Harun, R., Clossin, D. P., Khan, A. S., Andes-Koback, M., Michael, A. C. and Dixon, C. E. (2009b) Controlled cortical impact injury influences methylphenidate-induced changes in striatal dopamine neurotransmission. *Journal of neurochemistry,* **110,** 801-810.

Wagner, A. K., Sokoloski, J. E., Ren, D., Chen, X., Khan, A. S., Zafonte, R. D., Michael, A. C. and Dixon, C. E. (2005b) Controlled cortical impact injury affects dopaminergic transmission in the rat striatum. *Journal of neurochemistry,* **95,** 457-465.

Walker, Q. D., Ray, R. and Kuhn, C. M. (2006) Sex differences in neurochemical effects of dopaminergic drugs in rat striatum. *Neuropsychopharmacology : official publication of the American College of Neuropsychopharmacology,* **31,** 1193-1202.

Walker, Q. D., Rooney, M. B., Wightman, R. M. and Kuhn, C. M. (2000) Dopamine release and uptake are greater in female than male rat striatum as measured by fast cyclic voltammetry. *Neuroscience,* **95,** 1061-1070.

Wang, J., Liu, Z. L. and Chen, B. (2001) Association study of dopamine D2, D3 receptor gene polymorphisms with motor fluctuations in PD. *Neurology,* **56,** 1757-1759.

Wang, S. R., Yao, W., Huang, H. P. et al. (2011) Role of vesicle pools in action potential pattern-dependent dopamine overflow in rat striatum in vivo. *Journal of neurochemistry,* **119,** 342-353.

Wang, T., Huang, X. J., Van, K. C., Went, G. T., Nguyen, J. T. and Lyeth, B. G. (2014) Amantadine improves cognitive outcome and increases neuronal survival after fluid percussion traumatic brain injury in rats. *Journal of neurotrauma,* **31,** 370-377.

Watson, C. S., Alyea, R. A., Hawkins, B. E., Thomas, M. L., Cunningham, K. A. and Jakubas, A. A. (2006) Estradiol effects on the dopamine transporter - protein levels, subcellular location, and function. *Journal of molecular signaling,* **1,** 5.

Werneck, A. L. and Alvarenga, H. (1999) Genetics, drugs and environmental factors in Parkinson's disease. A case-control study. *Arquivos de neuro-psiquiatria,* **57,** 347-355.

Whone, A. L., Watts, R. L., Stoessl, A. J. et al. (2003) Slower progression of Parkinson's disease with ropinirole versus levodopa: The REAL-PET study. *Annals of neurology,* **54,** 93-101.

Whyte, J., Katz, D., Long, D. et al. (2005) Predictors of outcome in prolonged posttraumatic disorders of consciousness and assessment of medication effects: A multicenter study. *Archives of physical medicine and rehabilitation,* **86,** 453-462.

Wightman, R. M., Amatore, C., Engstrom, R. C., Hale, P. D., Kristensen, E. W., Kuhr, W. G. and May, L. J. (1988) Real-time characterization of dopamine overflow and uptake in the rat striatum. *Neuroscience,* **25,** 513-523.

Wightman, R. M. and Zimmerman, J. B. (1990) Control of dopamine extracellular concentration in rat striatum by impulse flow and uptake. *Brain research. Brain research reviews,* **15,** 135-144.

Williams, D. B., Annegers, J. F., Kokmen, E., O'Brien, P. C. and Kurland, L. T. (1991) Brain injury and neurologic sequelae: a cohort study of dementia, parkinsonism, and amyotrophic lateral sclerosis. *Neurology,* **41,** 1554-1557.

Wilson, M. S., Chen, X., Ma, X., Ren, D., Wagner, A. K., Reynolds, I. J. and Dixon, C. E. (2005) Synaptosomal dopamine uptake in rat striatum following controlled cortical impact. *Journal of neuroscience research,* **80,** 85-91.

Wong, J. C. and Hazrati, L. N. (2013) Parkinson's disease, parkinsonism, and traumatic brain injury. *Crit Rev Clin Lab Sci,* **50,** 103-106.

Wu, Q., Reith, M. E., Walker, Q. D., Kuhn, C. M., Carroll, F. I. and Garris, P. A. (2002) Concurrent autoreceptor-mediated control of dopamine release and uptake during neurotransmission: an in vivo voltammetric study. *The Journal of neuroscience : the official journal of the Society for Neuroscience,* **22,** 6272-6281.

Wu, Q., Reith, M. E., Wightman, R. M., Kawagoe, K. T. and Garris, P. A. (2001) Determination of release and uptake parameters from electrically evoked dopamine dynamics measured by real-time voltammetry. *Journal of neuroscience methods,* **112,** 119-133.

Wu, T. S. and Garmel, G. M. (2005) Improved neurological function after Amantadine treatment in two patients with brain injury. *J Emerg Med,* **28,** 289-292.

Xiao, L. and Becker, J. B. (1994) Quantitative microdialysis determination of extracellular striatal dopamine concentration in male and female rats: effects of estrous cycle and gonadectomy. *Neuroscience letters,* **180,** 155-158.

Yan, H. Q., Kline, A. E., Ma, X., Li, Y. and Dixon, C. E. (2002) Traumatic brain injury reduces dopamine transporter protein expression in the rat frontal cortex. *Neuroreport,* **13,** 1899-1901.

Yan, H. Q., Ma, X., Chen, X., Li, Y., Shao, L. and Dixon, C. E. (2007) Delayed increase of tyrosine hydroxylase expression in rat nigrostriatal system after traumatic brain injury. *Brain research,* **1134,** 171-179.

Yao, J., Gaffaney, J. D., Kwon, S. E. and Chapman, E. R. (2011) Doc2 is a Ca2+ sensor required for asynchronous neurotransmitter release. *Cell,* **147,** 666-677.

Yavich, L., Tanila, H., Vepsalainen, S. and Jakala, P. (2004) Role of alpha-synuclein in presynaptic dopamine recruitment. *The Journal of neuroscience : the official journal of the Society for Neuroscience,* **24,** 11165-11170.

Zafonte, R. D., Watanabe, T. and Mann, N. R. (1998) Amantadine: a potential treatment for the minimally conscious state. *Brain injury,* **12,** 617-621.

Zappia, M., Annesi, G., Nicoletti, G. et al. (2005) Sex differences in clinical and genetic determinants of levodopa peak-dose dyskinesias in Parkinson disease: an exploratory study. *Archives of neurology,* **62,** 601-605.

Zhang, T., Zhang, L., Liang, Y., Siapas, A. G., Zhou, F. M. and Dani, J. A. (2009) Dopamine signaling differences in the nucleus accumbens and dorsal striatum exploited by nicotine. *The Journal of neuroscience : the official journal of the Society for Neuroscience,* **29,** 4035-4043.

Zhou, F. M., Liang, Y., Salas, R., Zhang, L., De Biasi, M. and Dani, J. A. (2005) Corelease of dopamine and serotonin from striatal dopamine terminals. *Neuron,* **46,** 65-74.

Zou H., S. A., Hurwitz M., Leak R., Fowler L., Jones K., Zigmond, MJ. (2010) Modeling TBI Enhanced Susceptibility to Parkinson's Disease: An Initial Characterization. *Neurotrauma,* **27,** A-52 Online.

Zucker, R. S. (1999) Calcium- and activity-dependent synaptic plasticity. *Current opinion in neurobiology,* **9,** 305-313.